CATALYTIC MECHANISM OF A FLAVIN-DEPENDENT ALKANESULFONATE

MONOXYGENASE FROM ESCHERICHIA COLI

Except where reference is made to the work of others, the work described in this
dissertation is my own or was done in collaboration with my advisory committee.
This dissertation does not include proprietary or classified information.

_____
Xuanzhi Zhan

Certificate of Approval:

_____   _____
Douglas C. Goodwin   Holly R. Ellis, Chair
Associate Professor   Associate Professor
Chemistry and Biochemistry   Chemistry and Biochemistry

_____   _____
Evert C. Duin   Susanne Striegler
Assistant Professor   Assistant Professor
Chemistry and Biochemistry   Chemistry and Biochemistry

_____
George T. Flowers
Interim Dean
Graduate School

CATALYTIC MECHANISM OF A FLAVIN-DEPENDENT ALKANESULFONATE

MONOXYGENASE FROM ESCHERICHIA COLI

Xuanzhi Zhan

A Dissertation

Submitted to

the Graduate Faculty of

Auburn University

in Partial Fulfillment of the

Requirements for the

Degree of

Doctor of Philosophy

Auburn, Alabama
August 9, 2008

CATALYTIC MECHANISM OF A FLAVIN-DEPENDENT ALKANESULFONATE

MONOXYGENASE FROM ESCHERICHIA COLI

Xuanzhi Zhan

_____
Signature of Author

_____
Date of Graduation

VITA

Xuanzhi Zhan, Son of Chengqi Zhan and Ying Huang, was born on June 4, 1977, in Xingzi, Jingxi Province, The People's Republic of China. He graduated with a Bachelor of Science degree in biochemistry in 1998 from East China Normal University. He completed his Master of Science degree in 2001 under the guidance of Dr. Zhenqi Zhu from East China Normal University. From 2001 to 2003, He worked as a project manager in Shanghai Xinxing Medicine Co., Ltd. He married Jing Yu in the year of 2002. They have one son, Jason J. Zhan. In fall 2003, he entered the Graduate School at Auburn University in the Department of Chemistry and Biochemistry where he joined Dr. Holly R. Ellis laboratory for his research project towards the completion of his PhD degree.

DISSERTATION ABSTRACT

CATALYTIC MECHANISM OF A FLAVIN-DEPENDENT ALKANESULFONATE

MONOXYGENASE FROM ESCHERICHIA COLI

Xuanzhi Zhan

Doctor of Philosophy, August 9, 2008
(M.S., East China Normal University, 2001)
(B.S., East China Normal University, 1998)

185 Typed pages

Directed by Holly R. Ellis

The flavin-dependent alkanesulfonate monooxygenase (SsuD) catalyzes the oxidation of alkanesulfonate to aldehyde and sulfite in the presence of O_2 and $FMNH_2$ provided by an FMN reductase (SsuE). The goal of these studies was to investigate the kinetic mechanism of SsuD through rapid reaction kinetics, steady-state kinetics, and substrate binding studies. The SsuD enzyme shows a clear preference for $FMNH_2$ compared to FMN. The kinetic trace of premixed SsuD and $FMNH_2$ mixed with oxygenated buffer was best fit to a double exponential with no observed formation of the C4a-(hydro)peroxyflavin. However, when $FMNH_2$ was mixed with SsuD and oxygenated buffer an initial fast phase (k_{obs}, 12.9 s^{-1}) was observed, suggesting that the mixing order is critical for the accumulation of the C4a-(hydro)peroxyflavin. Results from fluorimetric

titrations with octanesulfonate imply that reduced flavin must bind first to promote octanesulfonate binding. There was a clear hyperbolic dependence on octanesulfonate binding, indicating that octanesulfonate binds in rapid equilibrium, and further results indicated there was a second isomerization step following binding. These results suggest that an ordered substrate binding mechanism is important in the desulfonation reaction by SsuD with reduced flavin binding first followed by either O_2 or octanesulfonate.

The conserved putative active site His228 residue was proposed as a catalytic base in the desulfonation reaction by SsuD. In this study, this conserved residue was replaced by alanine, asparatate and lysine (H228A, H228D, and H228K). The catalytic efficiencies (k_{cat}/K_m) of His228A, H228D, and H228K SsuD with octanesulfonate as substrate were 50-200 fold lower than wild-type, suggesting the involvement of His228 in the desulfonation reaction by SsuD. Stopped-flow kinetic analyses indicated that the His228 residue is not directly involved in the reaction between the C4a-(hydro)peroxyflavin and alkanesulfonate substrate. The pH dependence on the k_{cat} and k_{cat}/K_m values of wild-type and H228A SsuD were similar, suggesting His228 is not a catalytic base in catalytic steps involving the octanesulfonate substrate. The activity for H228A SsuD could be partially rescued with exogenous imidazole at increasing pH, indicating the deprotonated form of histidine exerts a functional role. Further analyses indicates that this residue is more likely indirectly participating in the catalysis by stabilizing and properly orienting another amino acid, that is directly involved in the desulfonation reaction.

ACKNOWLEDGEMENTS

I would like to express my appreciation and sincere thanks to my advisor, Dr. Holly R. Ellis, who guided and encouraged me throughout my studies. Her advice and research attitude have provided me with a model for my entire future career. I also wish to thank my advisory committee members, Dr. Douglas C. Goodwin, Dr. Evert C. Duin and Dr. Susanne Striegler for their constructive suggestions to my dissertation. I would love to show my appreciation to Dr. Goodwin for letting me use his stopped-flow instrument, Dr. Duin for letting me use his anaerobic glove box and Tom Carrington for helping me to use the gas-chromatography. I also want to thank my former and current lab members, Dr. Benlian Gao, Dr. Abdurachim Kholis, Russell Carpenter, Honglei Sun, Erin Imsand, Mary Millwood, John M Robbins and "Bear" Xiong, for their meaningful discussions and help. I also want to extend my appreciation to my many friends in Auburn for their kindly help to my family during my study here. I want to express my gratitude to my parents, my wife, my lovely son and my sister for the most valuable supports and understanding during my study in Auburn.

Style manual used: Biochemistry

Computer software used: Microsoft Word, ChemDraw, Microsoft Excel, KaleidaGraph

TABLE OF CONTENTS

LIST OF SCHEMES

xiv

LIST OF FIGURES

LIST OF TABLES

CHAPTER ONE

LITERATURE REVIEW

Flavoproteins play important roles in diverse metabolic reactions. This review will focus on the reactions of reduced flavin and flavoproteins with dioxygen. The mechanistic and structural studies of flavin-containing monooxygenases (FMOs), which is one of the most extensively characterized flavoprotein groups, will be summarized and discussed in detail. Mechanistic and structural properties of flavin-dependent oxygenase enzymes, in which flavin is present as a co-substrate rather than a prosthetic group, will also be discussed. Previous structural, functional, and mechanistic studies on the alkanesulfonate monooxygenase system, which belongs to a flavin-dependent two-component monooxygenase family, will be reviewed.

1.1 Activation of dioxygen by flavins and flavoproteins

Flavins, discovered and characterized in the 1930s, have been recognized as being capable of both one- and two-electron transfer processes [1]. They are also known as versatile compounds that can function as electrophiles and nucleophiles, with covalent intermediates of flavin and substrate frequently being involved in catalysis [2]. Flavin is a tricyclic heteronuclear organic ring based on pteridine whose biochemical source is the vitamin riboflavin (Vitamin B2). The flavin moiety is often attached with a phosphate

Ribityl Chain

OH   OH

O∕X

OH

Riboflavin, X= H

FMN, X= PO_3^{2-}

FAD, X=

Isoalloxazine Ring System
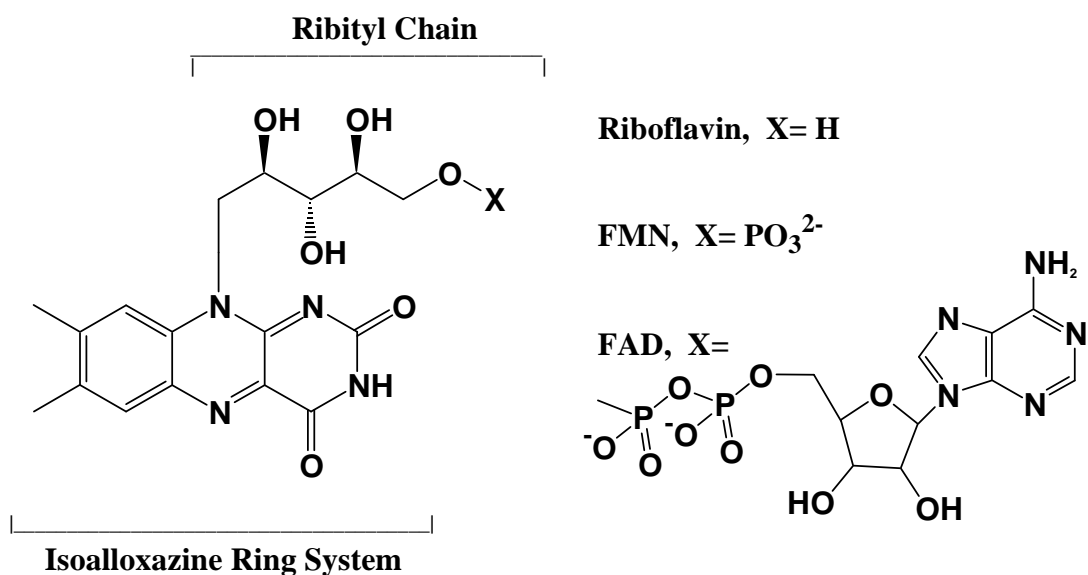
Figure 1.1 Structure of riboflavin, FMN and FAD

group to form a flavin mononucleotide (FMN). FMN can be further converted to flavin adenine dinucleotide (FAD) by is the condensation of FMN with an adenosine monophosphate (Figure 1.1).

The FMN or FAD forms are typically present as prosthetic groups or substrates in flavoproteins. In most flavoproteins, flavin cofactors are tightly but noncovalently bound to the apoprotein. A small number of flavins are covalently attached to the protein at the C(8α) or C(6) position of the isoalloxazine ring. The covalent linkage between the flavin and polypeptide is usually bridged by the 8α-methyl group of FMN or FAD linked to Tyr, His, or Cys [3]. The linkage to the C6 position of the flavin is restricted to Cys and FMN [4]. More recently, flavin has also been identified as a substrate in some enzymes [2]. The typical examples are the flavin-dependent monooxygenases from the two-component monooxygenase systems and some corresponding flavin reductases [1, 2]. Most of the

information about these two-component monooxygenases has been obtained in the last decade. This flavin-dependent monooxygenase family has only been found in bacteria, and has the ability to catalyze a wide range of metabolic reactions that include detoxification, biodegradation, and biosynthesis [2, 5, 6]. Their substrates are usually aromatic compounds or compounds containing a nitrogen, sulfur, phosphorous, selenium, or other nucleophilic heteroatoms [7].

Either as a prosthetic group or substrate, flavin is involved in a wide range of redox reactions in flavoproteins. In some instances, dioxygen is one of the substrates involved in the reaction. The protein-bound flavin always activates dioxygen first; then further oxidizes other substrates. With flavoproteins, the rate of the reaction with O_2 may differ by orders of magnitude, depending on the specific flavoprotein or the class of flavoproteins to which it belongs. Hence, the reactivity of the reduced flavin with O_2 is modulated by the protein environment where it is located. In the following sections, we will discuss the reaction routes of both free flavin and flavoproteins with dioxygen.

1.1.2 Reaction of free reduced flavin with oxygen

The reactions involved in the oxidation of free reduced flavin by dioxygen are shown in Scheme 1.1. After a relative slow oxidation of reduced flavin (FIH^-) to oxidized flavin (Fl_{ox}) through hydroperoxyflavin ($FlHOOH$), FIH^- can react with Fl_{ox} and a proton to produce a highly reactive radical $FlH^.$. The radical $FlH^.$ initiates a series of reactions to generate other active radicals such as the one electron reduced form of oxygen ($O_2^{.-}$), water radicals ($HO_2^.$), and flavin radicals ($FlH^.$). The oxidation of reduced flavin by $O_2^{.-}$

is an extremely rapid reaction. Due to the formation and accumulation of this reactive species, the reaction of reduced flavins with dioxygen is an autocatalytic process [2]. One key intermediate generated in these reactions is the C4a-(hydro)peroxyflavin. The initial reaction of reduced flavin and O_2 generates the C4a-(hydro)peroxyflavin intermediate by two spin inversion steps [8]. As shown in Scheme 1.2, an electron is transferred from singlet reduced flavin to triplet O_2 to form a radical pair, which converts to the C4a-(hydro)peroxyflavin after spin inversion. The latter is unstable in aqueous environments, dissociating heterolytically to H_2O_2 and oxidized flavin. Evidence supporting the sequences of Scheme 1.2 come from radiolysis experiments [2]: The neutral flavin radical and O_2^- were produced in an aerated solution of riboflavin by radiolysis and the flavin radical was converted to the C4a-(hydro)peroxyflavin

$$FlH^- + O_2 + H^+ \xrightarrow{k_1} FlHOOH \qquad k_1 \sim 250 \ M^{-1}s^{-1}$$

$$FlHOOH \xrightarrow{k_2} Fl_{ox} + H_2O_2 \qquad k_2 \sim 260 \ s^{-1}$$

$$FlH^- + Fl_{ox} + H^+ \underset{k_{-3}}{\overset{k_3}{\rightleftharpoons}} 2 \ FlH^\bullet \qquad \begin{array}{l} k_3 \sim 1 \times 10^6 \ M^{-1}s^{-1} \\ k_{-3} \sim 5 \times 10^8 \ M^{-1}s^{-1} \end{array}$$

$$FlH^\bullet + O_2 \xrightarrow{k_4} Fl_{ox} + O_2^- \qquad k_4 \sim 1 \times 10^8 \ M^{-1}s^{-1}$$

$$FlH^\bullet + O_2^- + H^+ \xrightarrow{k_5} Fl_{ox} + H_2O_2 \qquad k_5 \sim 1 \times 10^8 \ M^{-1}s^{-1}$$

$$FlH^- + O_2^- + 2H^+ \xrightarrow{k_6} FlH^\bullet + H_2O_2$$
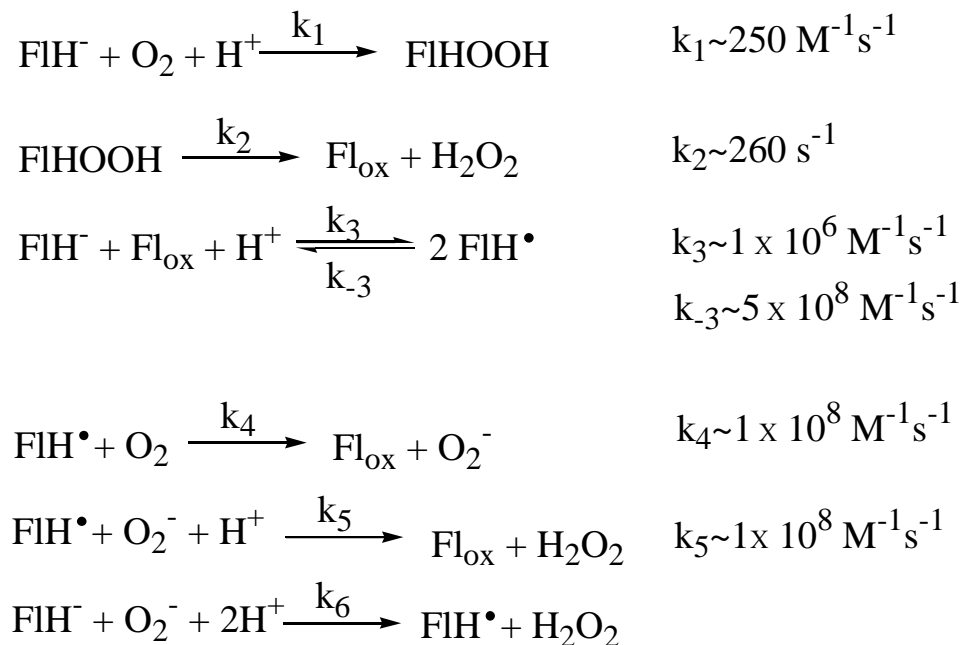
Scheme 1.1 Reactions in the oxidation of reduced flavin by dioxygen

4

intermediate at a fast second order rate, which subsequently decayed to oxidized flavin. This result is consistent with the pathways shown in Scheme 1.2. After the initial binding of the neutral flavin radical and O_2^-, this complex can be further converted to C4a-(hydro)peroxyflavin.

$$Fl_{red}H^- \; (\uparrow\downarrow) + O_2(\uparrow\uparrow) \longrightarrow [FlH^\bullet \; \uparrow\uparrow \; O_2^-] \longrightarrow [FlH^\bullet \; \uparrow\downarrow \; O_2^-]$$

$$FlHOOH \rightleftharpoons FlHOO^-$$
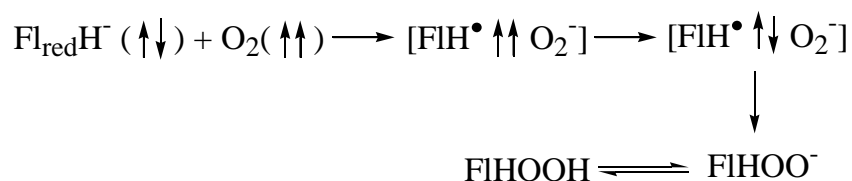
Scheme 1.2 Activation of oxygen by reduced flavin: the formation of

C4a-(hydro)peroxyflavin

1.1.2 Oxygen activation by flavoproteins.

Because of their chemical versatility, flavins are involved in a wide range of biological reactions. All flavoprotein reactions involve two separate half-reactions, which usually can be monitored separately by rapid reaction techniques [*5, 9*]. The flavoprotein-reducing substrate (AH_2) is dehydrogenated in a two-electron reduction, and the resulting reduced flavin is re-oxidized by the oxidizing substrate (B), as shown in Scheme 1.3.

In some flavoenzymes, dioxygen is the physiological oxidizing substrate. Due to different protein environments, the molecular activation of flavoproteins can

$$AH_2 \quad Fl_{ox} \quad BH_2$$

$$A \quad Fl_{red} \quad B$$
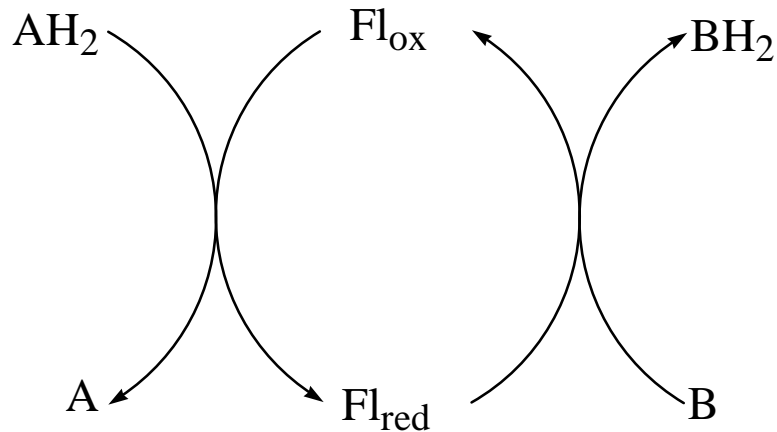
Scheme 1.3 Reductive and oxidative half-reactions of flavoproteins

Fl, flavin; ox, oxidized; red, reduced.

follow various pathways. Flavoproteins can be classified into four different groups based on the rate of the reaction of the flavin with O_2 and the nature of products formed [*1,2*]. The first group, dehydrogenases, react very slowly with dioxygen and generate mainly H_2O_2 but also some O_2^-. Acyl-CoA dehydrogenase in fatty acid metabolism is a typical example in this group. The acyl-CoA dehydrogenase oxidizes acyl-CoA thioesters to the corresponding enoyl-CoA esters, and the flavin cofactor is reduced. The reduced flavin cofactor is reoxidized by a one-electron transfer reaction, and the reoxidized flavin participates in the next cycle of fatty acid dehydrogenation [*10*]. The second group, the electron transferases, often reacts with oxygen very fast to yield mainly O_2^- and the neutral flavin semiquinone. An example of an e^- transferase is flavodoxin, which plays a direct role in nitrogen fixation by transferring an electron from the flavin semiquinone to the iron-containing subunit of the nitrogenase complex [*11*]. The third group are the

6

oxidases, which react rapidly with dioxygen and yield oxidized flavoprotein and H_2O_2. A well characterized example is glucose oxidase which catalyzes the oxidation of β-D-glucose to D-glucono-1, 5-lactone with the formation of hydrogen peroxide using dioxygen as the final electron acceptor. The production of hydrogen peroxide in peroxisomes has a protective effect against microorganisms [12]. The fourth group are the monooxygenases, which inserts one oxygen atom into a substrate and reduce the other oxygen atom to H_2O. Bacterial luciferase, which catalyzes the light-emitting reaction in the presence of reduced flavin, long-chain aldehyde, and dioxygen, is a typical example from this group. A distinguishing feature of this group of enzymes is that a stabilized flavin-oxygen intermediate, C4a-(hydro)peroxyflavin, is generated during the catalytic reaction [1, 2, 5].

As mentioned, the oxidation of free flavins proceeds via the C4a-(hydro)peroxyflavin intermediate. Therefore, generation of this flavin-oxygen intermediate is widely accepted as a common route for the reaction of all flavoproteins with dioxygen. The C4a-(hydro)peroxyflavin intermediate has been identified primarily in monooxygenases, and the stability of this intermediate varies depending on the enzyme under investigation. Some experimental data support the identification of this intermediate in flavin oxidases, including glucose oxidase, nitroalkane oxidase, and NADPH oxidase reactions, however, the C4a-(hydro)peroxyflavin intermediate is generally less stable than in monooxygenases [2].

Several possible pathways have been proposed in the reaction of reduced flavoproteins with dioxygen as shown in scheme 1.4. All flavoproteins have a common initial step: the initial 1-electron transfer reaction [1, 2]. Different flavoproteins may

7

undergo different routes to the initial electron transfer reaction. In electron transferases, the initial 1-electron transfer is very fast and would simply be followed by the dissociation of the radical pair to form the neutral flavoprotein radical ($FlH^{\cdot}$ in Scheme 1.4) and $O_2^{\cdot -}$. There is no other intermediate detected in flavin dehydrogenases, so it might be a safe assumption that the rate-limiting step is the initial 1-electron transfer. The overall reaction of these flavoproteins with dioxygen is extremely slow. The routes that follow the 1-electron transfer step are still unclear and remain an interesting challenge in this field. Studies from monooxygenases and oxidases indicated that the C4a-(hydro)peroxyflavin (Intermediate IV or V in Scheme 1.4) is the common route in the activation of dioxygen by these two groups. In oxidases, the half-lives of the C4a-(hydro)peroxyflavin intermediates are very short, which implies that the decay of C4a-(hydro)peroxyflavin must be extremely fast to oxidized flavin and H_2O_2. In monooxygenases, the enzyme-bound C4a-(hydro)peroxyflavin intermediate is protected from breakdown by the microenvironment of the enzymes. The C4a-(hydro)peroxyflavin could undergo further productive oxygen atom transfer or eliminate hydrogen peroxide to oxidized flavin. The detailed mechanism of flavin-containing monooxygenases (FMO) will be discussed later.

Although C4a-(hydro)peroxyflavin might be not the common intermediate generated in the dioxygen activation of all flavoproteins, it is still an essential intermediate in many known flavoproteins such as flavin containing/dependent monooxygenases (FMO). The actual role of the oxygenated-flavin intermediates in different flavoproteins often becomes a critical question in the mechanistic studies of these flavoproteins. The

half-lives of these intermediates bound by different active sites vary significantly among different flavoproteins. Mechanistic, structural, and functional studies on these enzymatic C4a-(hydro)peroxyflavin intermediates show that the microenvironments of active sites, substrate binding, and conformational changes may together affect the stability and activity of these intermediates.

Monooxygenases are enzymes which catalyze the incorporation of one atom of oxygen from O_2 into their substrates, while the other oxygen is reduced to water. The reducing agent works as either an external electron donor or a substrate. A number of monooxygenases have been shown to be flavoproteins with flavin as cofactor or substrate. The reactions of flavin-containing/dependent monooxygenases (FMO) usually include a NAD(P)H, dioxygen, and a substrate with the ability to be further oxidized. The C4a-(hydro)peroxyflavin intermediate is commonly generated in the activation of dioxygen by reduced flavin. The C4a-(hydro)peroxyflavin is usually directly involved in inserting one oxygen atom into the substrate by either a nucleophilic or electrophilic attack. The overall reaction catalyzed by flavoprotein monooxygenase is a complicated process including flavin reduction, dioxygen activation via reduced flavin, and oxidation of the substrate. Two different strategies have been used in nature to modulate the different requirements of this complicated process: single-component monooxygenases and two-component monooxygenases. The biological functions, catalytic mechanism, and structural studies of FMOs will be discussed in detail.
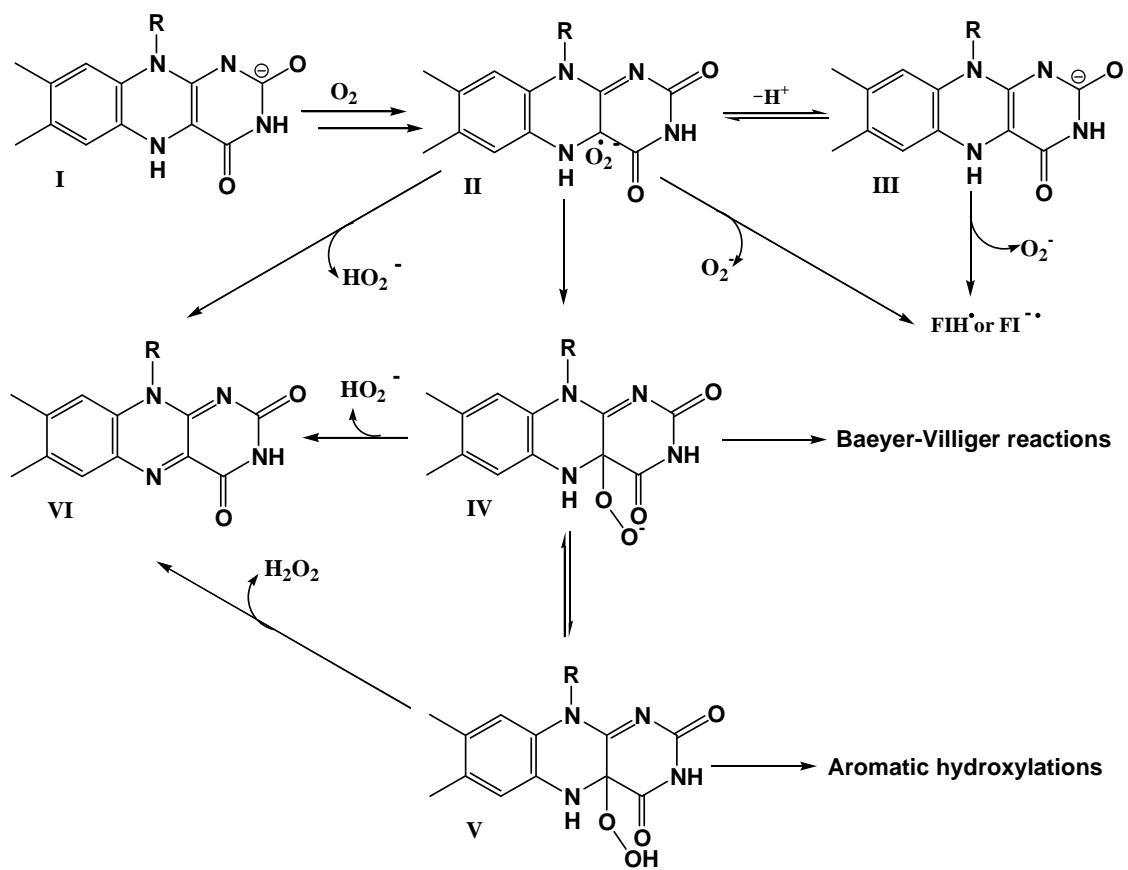
Scheme 1.4 Possible reactions of reduced flavoprotein with dioxygen

1.2 Flavin-containing/dependent monooxygenase

Flavin-containing/dependent monooxygenases (FMO) have been identified in bacteria, yeast, plants, and mammals where they perform essential biological functions by catalyzing diverse metabolic reactions [5, 13]. FMOs were first discovered during the 1960s in hepatic microsomes as NADPH- and O_2-requiring activity that converted N, N'-imethylaniline to N-oxide [14]. In animals, there are five functionally expressed FMO genes (e.g. human FMO1–FMO5) [13,14]; FMOs have also been found in bacteria and unicellular eukaryotic organisms, for example, there is a single FMO gene in yeast [13]. FMO had not been identified in plants until 2001, however, there are now many FMO-like genes found in plants [15]. FMOs can transfer hydroxyl groups to a variety of small, nucleophilic, heteroatom-containing (e.g. nitrogen, sulfur, selenium or iodine) substrates, thus rendering them more polar and readily excretive.

1.2.1 Mechanism

The mechanism by which FMOs insert a single oxygen atom into the substrates has been elucidated in detail [*16-18*]. The major characteristic steps, which are based on kinetic and spectral studies with FMOs from different sources, are summarized in Figure 1.2. In the absence of substrate, the FMO enzyme forms a complex with NADPH resulting in a rapid reduction of the enzyme-bound single flavin molecule (step 4). The reduced flavin–enzyme complex binds O_2 at the C4a position of the flavin molecule, resulting in a C4a-(hydro)peroxyflavin (Fl-OOH or Fl-OO$^-$) (step 5). In this highly

reactive conformation, the enzyme awaits the heteroatom-containing substrate, which needs a free electron pair (such as N or S) or aromatic substrate. Access to the active site is thus a crucial determinant of substrate specificity. Once the substrate is in place, one of the two oxygen atoms is transferred to the substrate (step 1), whereas the other oxygen atom reacts to form water (step 4). $NADP^+$ is released and the binding of NADPH starts a new cycle (step 3).

As stated above, the (hydro)peroxyflavin intermediate can be formed in the absence of the substrate. This means that just "a single point contact" is all that is required for product formation. This unique property is responsible for the extraordinary broad substrate ranges of these enzymes [13]. Because the energy required to drive the reaction is present in the enzyme before it encounters substrate, a precise fit (usually required to lower the energy of activation of an enzyme catalyzed reaction) is not required. FMOs catalyze the oxidation of compounds as dissimilar as iodide, boronic acids, phosphines, most functional groups bearing sulfur or selenium, as well as a host of synthetic and naturally occurring amines and hydrazines [19-22]. While a single point of contact between the substrate and the enzyme-bound flavin oxidant will often suffice, this does not preclude more complex interactions with certain substrates. For example, it is very probable that substrate binding lowers the energy of activation for the oxidation of cyclohexanone by the bacterial cyclohexanone monooxygenase [23], but the oxidation of organic sulfur compounds and boronic acids catalyzed by this flavoprotein probably requires only a single point of contact between the enzyme and substrate for catalysis [24].

12
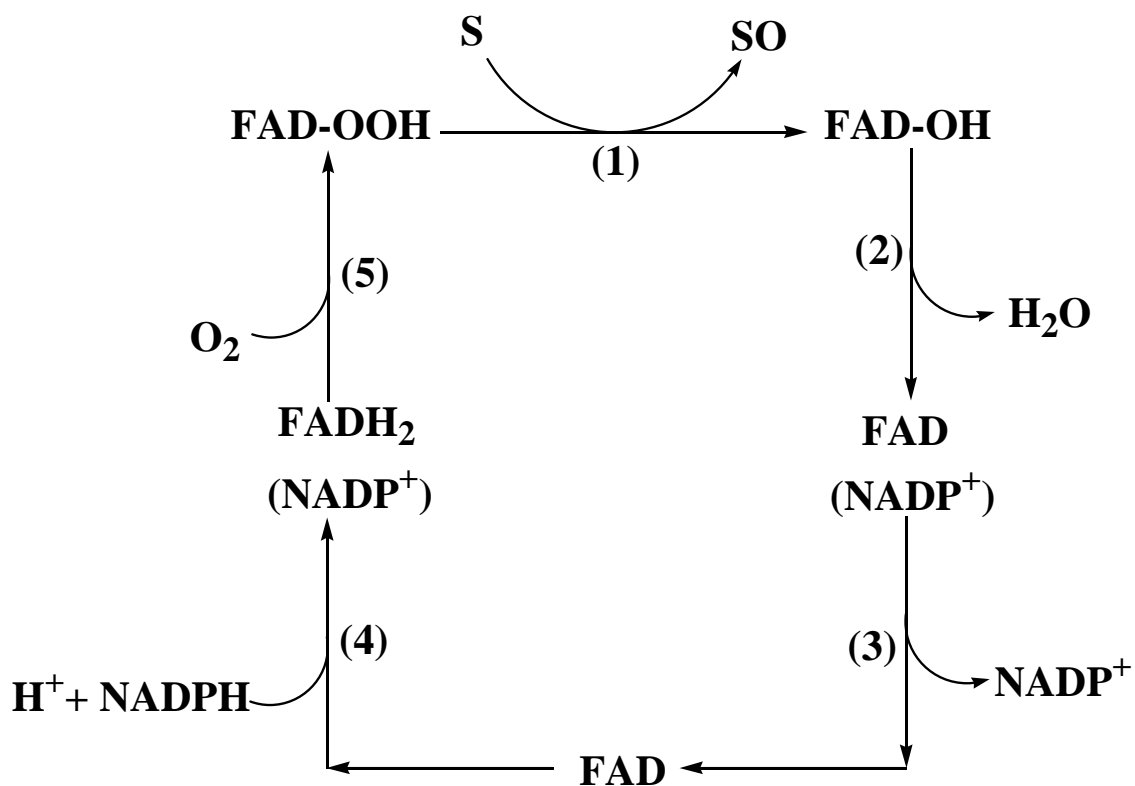
Figure 1.2 General mechanism of flavin-containing monooxygenases (FMO)

1.2.2 Hydroperoxyflavin: a nucleophile or electrophile

All FMO have three substrates, NAD(P)H to reduce the enzyme flavin, the substrate to be oxygenated, and dioxygen. The overall reaction catalyzed by flavoprotein monooxygenases involves three general chemical processes: (A) Reduction of the flavin by NAD(P)H, (B) reaction of the reduced flavin with dioxygen to generate a C4a-(hydro)peroxyflavin, which is the oxygenating agent, and (C) binding,

orienting, and activating the substrate for its oxygenation by the flavin C4a-(hydro)peroxyflavin [*1*]. C4a-(hydro)peroxyflavin is an essential intermediate and directly inserts one oxygen atom into the substrate; however, it functions in different ways depending on the type of oxygenation reaction accomplished. The C4a-(hydro)peroxyflavin intermediate are capable of oxidizing substrates through either a nucleophilic or electrophilic reaction.

The C4a-(hydro)peroxyflavin is known as a common intermediate in the reactions when free or protein-bound reduced flavin reacts with dioxygen [1, 2, 8, 13]. The C4a-(hydro)peroxyflavin has a distinguished absorption spectrum from oxidized and reduced flavin with a peak between 350-400 nm. Figure 1.3 shows the absorption spectra of the microsomal FAD-containing monooxygenase in the oxidized, reduced, and peroxyflavin forms. Label A is the spectrum of the oxidized FAD with two absorbance peaks between 350-400 nm and 420-480 nm; Label B is the spectrum of the hydroperoxyflavin with only one peak between 350-400 nm; the spectrum of reduced FAD (Label C) has no absorbance peak in both areas [*13*]. More interestingly, although the spectra of protonated and deprotonated states of the peroxyflavin intermediate (FlOOH and FlOO⁻) are quite similar to each other, there are some slight differences between these two forms. The absorbance peak of FlOOH is located at approximately 370 nm, while FlOO⁻ has a maximum absorbance at around 380 nm. These spectral differences among the three different states of flavin make it possible to trace the change of the flavin states during the catalytic reaction.
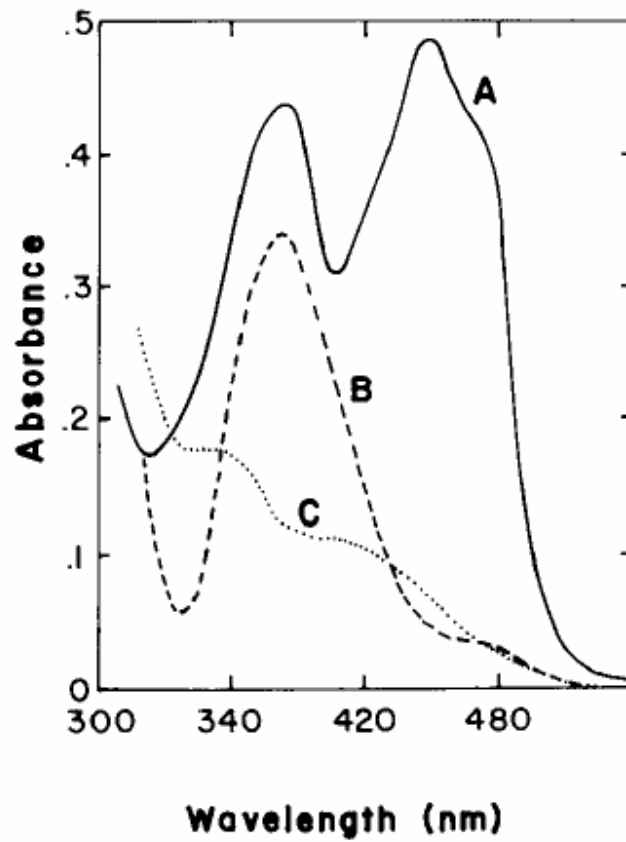
Figure 1.3 Absorption spectra of the microsomal FAD-containing monooxygenase in the

oxidized (solid line), reduced (dot line), and peroxyflavin (dash line) forms. [*13*]

(Reprinted with permission)

1.2.2.1 Peroxyflavin as a nucleophile

Peroxyflavin (FlOO⁻) can work as a nucleophilic agent in FMOs. A Baeyer-Villiger

oxidation is typically involved in these types of reactions. The Baeyer-Villiger oxidation

mechanism of oxidative cleavage involves the attack of the peroxy group on the substrate

to form a FlOO-substrate complex; then a rearrangement reaction converts the substrate

from a ketone to an ester (Scheme 1.5).
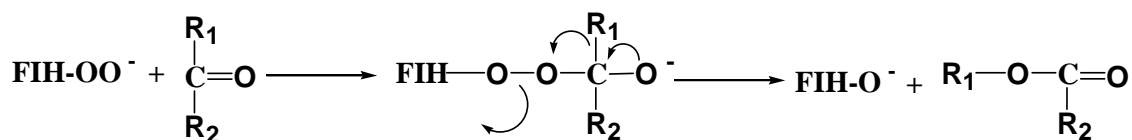
Scheme 1.5 Baeyer-Villiger reaction by C4a-peroxyflavin.

A well-characterized C4a-peroxyflavin is generated in cyclohexanone

monooxygenase, where the peroxyflavin is generated extremely rapidly. Cyclohexanone

monooxygenase catalyzes the insertion of an oxygen atom into the cyclohexanone

substrate to form a 6-hexanolide product. The C4a-peroxyflavin intermediate can be

generated in the absence of cyclohexanone substrate. This oxygenated-flavin intermediate

is relatively unstable; however, the binding of product $NADP^+$ can greatly improve the

stability of $FADOO^-$ [25]. Peroxyflavins have been shown to be unstable in aqueous

environments, so $NADP^+$ may prevent this intermediate from accessing the solvent. The

16

decay of the peroxyflavin intermediate is accelerated in the presence of the cyclohexanone substrate. When cyclohexanone is present, enzyme-bound FADOO$^-$ makes a nucleophilic attack on the ketone group (C=O) followed by a Baeyer-Villiger rearrangement to form the ϵ-ecaprolactone product (Scheme 1.6). The product is released from the enzyme forming an enzyme-bound FADOH, which decays to FAD and water. By this mechanism, one oxygen atom is inserted into the cyclohexanone substrate while the other oxygen is released as water from FADOH.

Another well characterized example where peroxyflavin behaves as a nucleophile is bacterial luciferase. This is an unusual enzyme in that reduced FMN is a substrate instead of a tightly bound cofactor. The reduced FMN is formed by a separate NAD(P)H-flavin reductase. An enzyme-stabilized peroxyflavin has been identified and even purified in the luciferase reaction in the absence of aldehyde substrate. These reduced flavin-dependent monooxygenases like luciferase always follow a strict substrate binding order. Bacterial luciferase binds FMNH$_2$, and enzyme-bound FMNH$_2$ reacts with dioxygen to form a C4a-peroxyflavin intermediate, which has a long half-life at low temperatures. The luciferase-FMNOO$^-$ intermediate works as a nuclophilic agent to attack a wide range of aldehyde substrates along with a Baeyer-Villiger rearrangement to produce the corresponding alcohol, light and FMN [*54*]. The catalytic mechanism of bacterial luciferase will be further discussed in a later section.

17
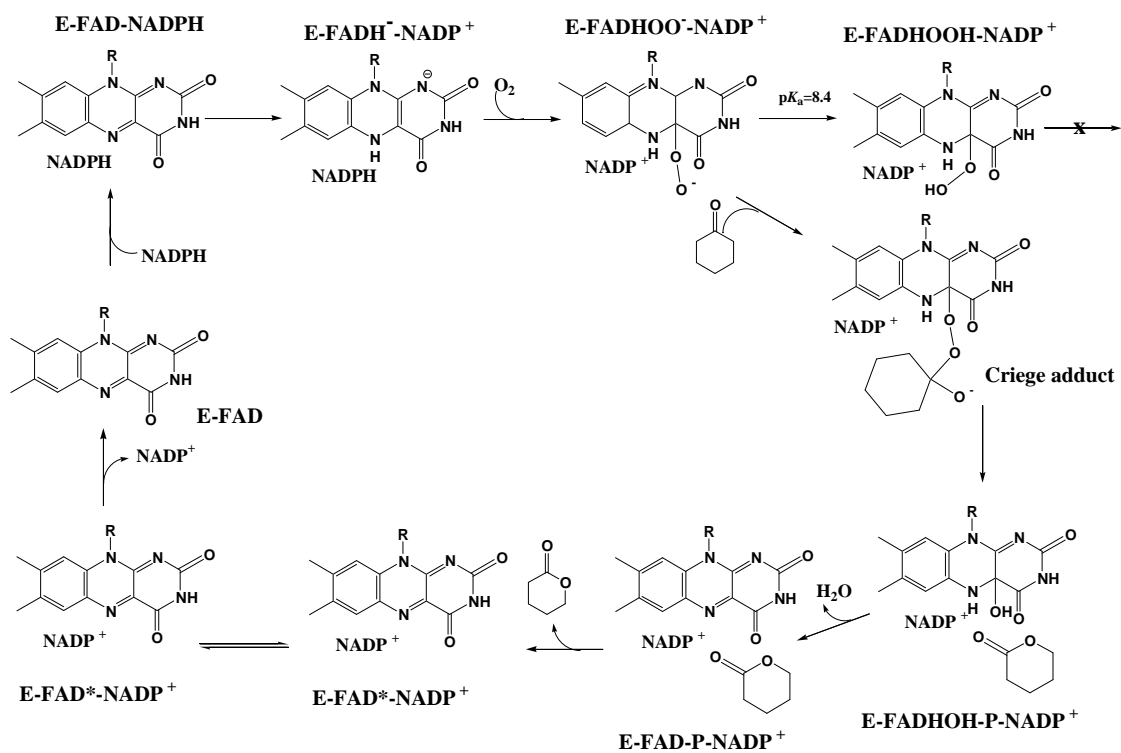
Scheme 1.6 Mechanism of cyclohexanone monooxygenase: C4a-hydroperoxyflavin as a

nucleophile

1.2.2.2 *Hydroperoxyflavin as an electrophile*

The C4a-hydroperoxyflavin (FlOOH) intermediate, acting as an electrophilic agent, can also be an active form in catalysis [*1, 2*]. The most widely and extensively studied FMOs involves the hydroxylation of an activated aromatic substrate. The C4a-hydroperoxyflavin intermediate was first observed experimentally in this class of enzymes [*2*]. Phenol hydroxylase and *p*-hydroxybenzoate hydroxylase are classic examples where hydroperoxyflavin behaves as an electrophilic oxygenating agent. Scheme 1.7 shows the mechanism of phenol hydroxylase. The hydroperoxyflavin intermediate is generated before the substrate is directly involved in the reaction. Only the protonated form of the peroxyflavin (FlOOH, I_s^*) can actively oxidize the phenol substrate by electrophilic addition. The subsequent steps are quite similar to those enzymes in which peroxyflavin intermediates work as nucleophile agents. As the product is released from the enzyme complex, an enzyme bound FADOH intermediate is formed, which decays to FAD and H_2O. *p*-Hydroxybenzoate hydroxylase (PHBH), which is one of the most thoroughly studied aromatic hydroxylase, catalyzes the oxygenation of *p*-hydroxybenzoate to produce protocatechuate [*26*].The catalytic mechanism has been investigated in detail and is consistent with nucleophilic displacement by the substrate of the terminal oxygen of the flavin hydroperoxide [*27*]. In the PHBH mechanism, protein and flavin dynamics involving the protein and flavin are crucial in catalysis [*28*].

As stated, FMO is widely distributed in mammals, plants and bacteria. FMOs from different sources have different structures and biological functions. Examples of FMOs from different sources will be summarized and compared in the following sections.
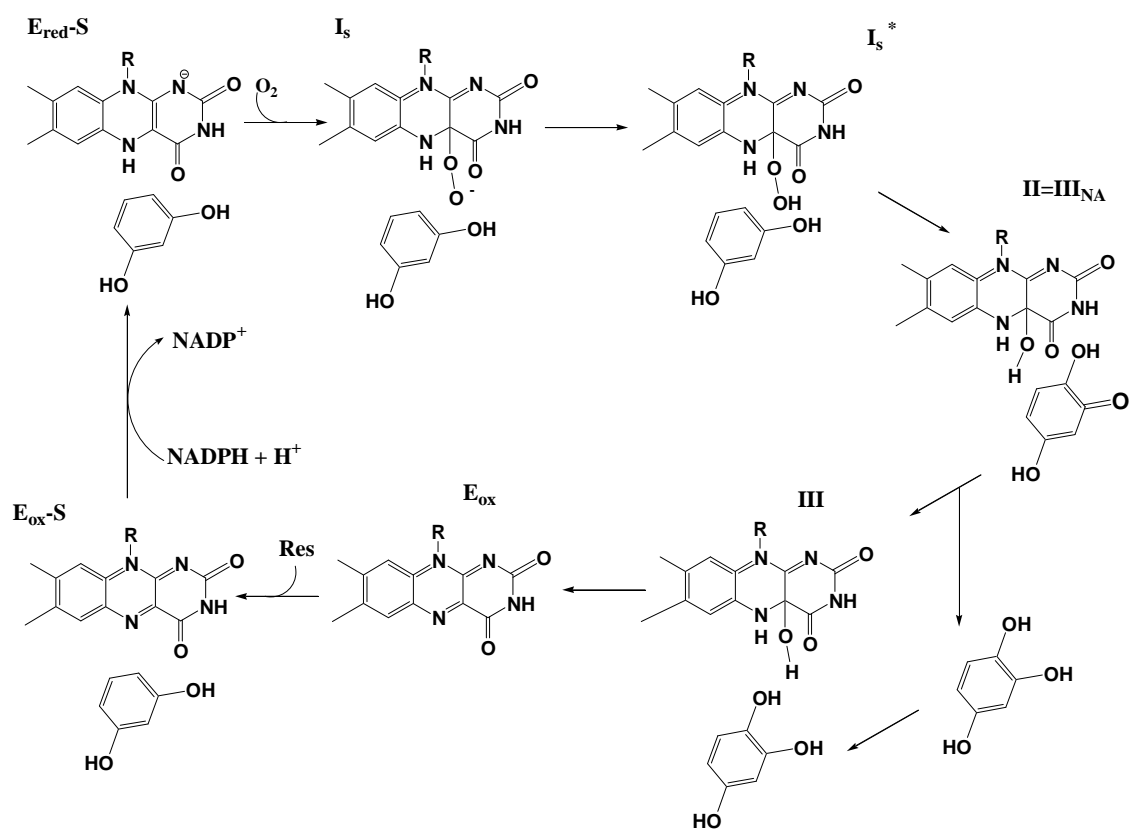
Scheme 1.7 mechanism of phenol hydroxylase: hydroperoxyflavin as an electrophile

1.2.3 FMO from mammals

Mammalian FMOs, are widely distributed in various tissues, such as liver, brain, kidney, lung and small intestine. These FMOs oxygenate nucleophilic heteroatom-containing chemicals and drugs and generally convert them into harmless, polar, readily excreted metabolites. Sometimes, however, FMOs bioactivate chemicals into reactive materials that can cause toxicity. Therefore, mammalian FMOs have extremely important pharmacological and toxicological significance [*13, 14*]. The general function of FMO is considered to be as a xenobiotic detoxication catalyst. Similar to cytohrome P450, FMOs have envolved to protect mammals from the assault of lipophilic nucleophilic chemicals especially in the early environment [*29*]. In some cases, FMOs can be highly selective. This is exemplified by the detoxication and deoderation of trimethylamine (TMA) [*30*]. The inability to *N*-oxygenate TMA because of a defective FMO3 causes a condition called trimethylaminuria, which is also known as fish odor syndrome [*31*]. On the other hand, FMOs can oxygenate a wide range of heteroatom-containing compounds to remove unwanted natural products [*13*]. Like cytochrome P450, FMOs appears to sacrifice considerable enzyme velocity to bind a wide range of substrates in its substrate binding domain [*22*]. Sometimes, FMO oxygenates physiological compounds to their corresponding oxide, leading to the pharmacological activity of the compound. FMOs are also known to convert some nucleophiles to more oxygenated compounds with greater electrophilicity that can result in a product with higher toxicity [*32-34*].

Because of their pharmacological and toxicological significance, FMOs from humans have been extensively studied and well characterized [*14*]. The FMO gene family

in humans arose as a duplication of an ancestral gene or through a series of independent gene duplication events [35]. FMOs with sequence identities >40% have been grouped in the same family, indicated by the first numeral. According to this systematic nomenclature based on the primary sequence identity, there are five well characterized FMO groups: FMO1-FMO5.

FMO1 is a prominent form of FMO in adult human kidney, esophageal, and nasal mucosa. It is unlikely that FMO1 contributes extensively to amine *N-* and other chemical oxygenation reactions unless the amine or chemical is present at relatively elevated substrate concentrations [14]. Evidence indicates that human FMO1 may accept larger N- and S-containing nucleophiles than other FMO enzymes. Furthermore, FMO1-mediated pesticide metabolism may represent an example where FMO1 plays a larger detoxification role than previously thought [14]. Because FMO1 is the major form in fetal human liver, there may be instances of altered metabolism in the fetus owing to FMO1 variants.

Although FMO2 is a prominent FMO expressed at high levels in the lungs of nonhuman primates and other mammals, it is not a prominent functionally active enzyme in human lung [14]. FMO2 wild-type enzyme showed efficient activity for *S*-oxygenation of sulfur-containing chemicals, such as thioureas and thioamides, and because the sulfenic acids of thioureas are chemically reactive, humans with full-length FMO2 may be more susceptible to toxicity of certain thiourea-containing chemicals. On the other hand, thioether-containing pesticides may be detoxifited by *S*-oxygenation by full-length FMO2, and individuals with wild-type FMO2 may show increased protection from the toxic properties of thioether-containing pesticides.

Full-length FMO3 mRNA is strongly detected in adult human liver, but at relatively low levels in adult kidney and lung. In view of the high prevalence of FMO5 in adult and fetal liver, it is not clear which FMO form (FMO3 or FMO5) predominates. It may be that the role of FMO3 versus FMO5 depends on the chemical structure of the substrate. In general, human FMO3 prefers to oxygenate nucleophilic heteroatom–containing substrates that are slightly smaller that those accepted for human FMO1. Based on limited information, FMO5 substrate specificity is poorly defined, although it is apparently distinct from FMO3. Apparent pharmacogenetic effects of FMO3 on drug metabolism have been observed. For example, the extent of benzydamine *N*-oxygenation was correlated to the FMO3 genotype in groups of individuals with trimethylaminuria [*31*]. Prototypical chemicals have been examined as *in vitro* substrates for FMO3 variants [*14*], and the oxygenation of methimazole, TMA, and the probe substrate 10-(*N*,*N*-dimethylaminopentyl)-2-(trifluoromethyl) phenothiazine (5-DPT) were all significantly decreased [*31*].

Human FMO4 is present in adult liver and kidney to approximately the same extent. About ten-fold less FMO4 is present in human fetal liver and the small intestine compared with adult liver. FMO4 is unstable and cDNA expression is problematic, and the activity of the expressed enzyme is poor. For this reason it has been difficult to establish extensive FMO4 substrate specificity.

In light of the prominence of FMO5 in adult human liver and the small intestine examination of FMO5 has taken on new significance. FMO5 does not oxygenate typical FMO3 substrates, and is apparently an atypical FMO. However, an increasing number of compounds are reported to be oxygenated by FMO5 [*14*], including compounds with

functionalities not typically associated with FMO activity (i.e., thioethers with proximal carboxylic acids). Currently, however, FMO3 is the enzyme associated with the vast majority of human FMO-mediated hepatic metabolism. As more information is discovered about FMO4 and FMO5, revision of their role in drug and chemical metabolism is likely.

1.2.4 FMO from plants

The first functional characterization of a plant FMO was reported in 2001, almost 40 years after the enzymes had been discovered in animals [*15*]. The FMOs have been studied mostly in the model plant *Arabidopsis*, in which 29 distinct genes encode proteins that share motifs typically found in FMOs. Comparison of the putative FMO proteins of those plants for which the genome sequence is available revealed that the FMOs from plants fall into three clades: (i) Clade I contains two *Arabidopsis* proteins, FMO1 and a closely related pseudogene, for which no expression has been detected, three FMOs from rice and six from poplar (Populus trichocharpa); (ii) in Clade II, 11 Arabidopsis YUCCA proteins are found together with eight FMOs from rice and 12 from poplar; (iii) Clade III is comprised of 16 Arabidopsis FMOs, of which one can S-oxygenate glucosinolates, seven FMOs from rice, and four poplar FMOs (Figure 1.4). As mentioned, the physiological function of animal FMOs appear to be the detoxification of a vast spectrum of xenobiotics. Interestingly, research has shown that plant FMO can catalyze specific steps in the biosynthesis of auxins or in the metabolism of glucosinolates. Auxins are a class of plant growth substances (often called phytohormones or plant hormones), and play an essential role in coordination of many growth and behavioral processes in the

24
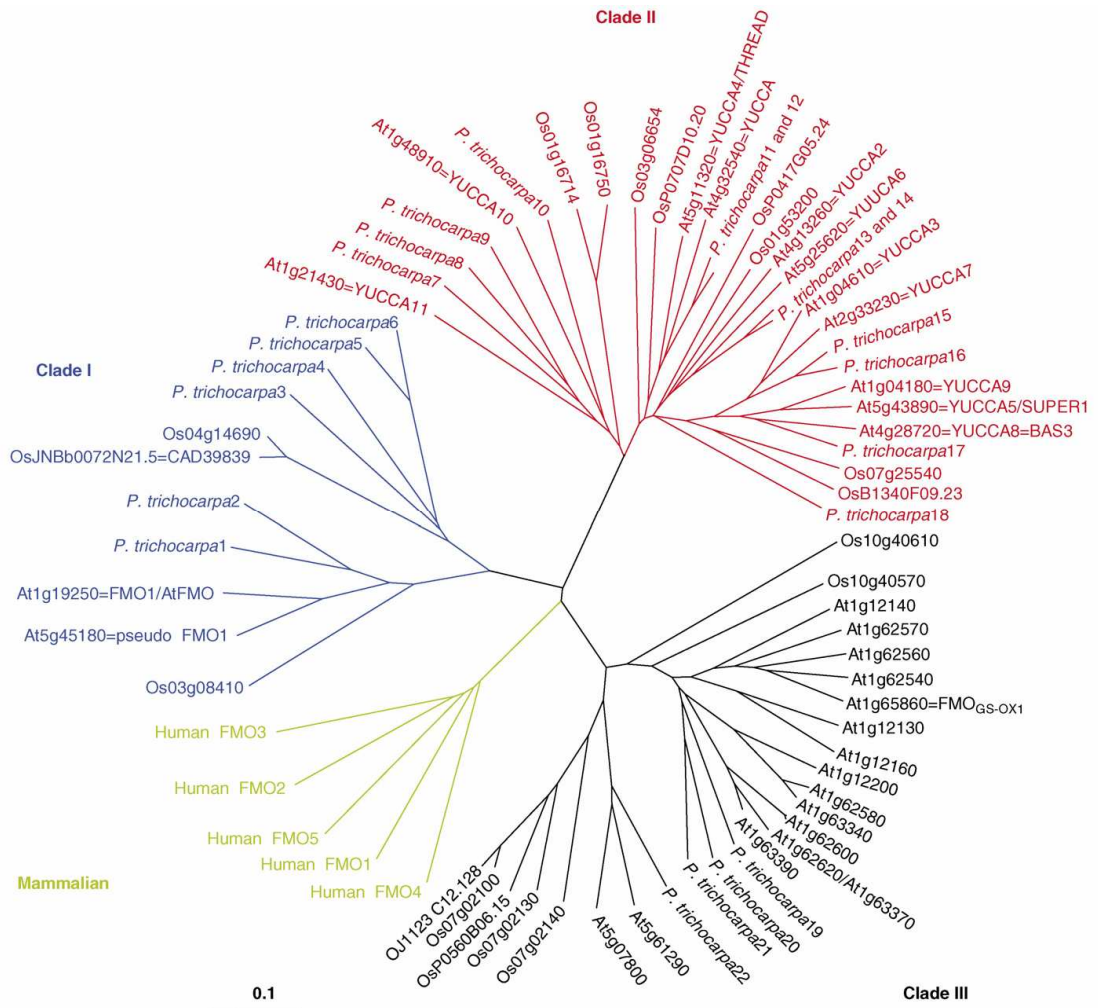
Figure 1.4 Phylogenetic tree of Arabidopsis, rice, poplar and human FMOs. Clade I FMOs (pathogen defense clade) are in blue; Clade II FMOs (YUCCA clade involved in auxin biosynthesis) in red; Clade III FMOs (S-oxygenating clade) are in black and the human FMOs (detoxification clade) in green [15]. (Reprinted with permission)

plant life cycle [36]. The glucosinolates are a class of organic compounds that contain sulfur, nitrogen, and a functional group derived from glucose. Plants use substances derived from glucosinolates as natural pesticides and as a defense against herbivores [15]. Experiments showed that two mutants of YUCCA proteins, a group of plant FMOs, are responsible for the biosynthesis of auxin. YUCCA probably catalyzes the rate-limiting step in auxin biosynthesis from tryptamine to N-hydroxyl tryptamine, because the recombinant YUCCA protein was able to catalyze this conversion in vitro. Moreover, the plant FMO1 (AtFMO) has been reported to be involved in defense against pathogens [37]. In *Arabidopsis*, there are multiple-layered defenses against pathogens. Basal resistance helps to limit the multiplication and spread of virulent pathogens and the severity of disease symptoms, to which pathogen-derived toxins contribute. This kind of defense is not specific to a certain isolate or strain of pathogen. In plants, another defense layer can be involved. When host-adapted pathogens inject into the plant cell, effector proteins that are recognized by resistance (R) genes-encoded proteins are activated. Most R genes encode nucleotide-binding, leucine rich repeat (NB-LRR)-containing proteins. In Arabidopsis, two major classes of NB-LRR proteins have been defined based on the presence at their N-termini of either a coiled-coil domain (CC-NBLRRs) or a domain showing sequence similarity to the Toll or Interleukin receptors of animals (TIR-NB-LRRs). The *Arabidopsis* EDS1 and PAD4 genes, two signaling genes that mediate some but not all *R* responses, have been shown to be involved in basal defense reactions, and also in defense reactions mediated by TIR- but not CC-NBLRR-resistance proteins. The FMO1 gene has been identified as an EDS1- and PAD4-dependent gene in a microarray study [38]. Increasing evidence indicates FMO1 is important for basal

defenses as well as R gene-mediated defenses, similarly to EDS1 and PAD4 [*38*].

Significantly more FMO-like genes have been found in plants than in mammals, which indicate that plant FMOs may have the ability to perform other functions in addition to detoxification. As stated above, some plant FMOs are involved in essential reactions in biosynthesis and the defense against pathogens. Research on plant FMOs has already changed the somewhat simplistic view of FMOs as broad substrate-accepting detoxifying enzymes.

1.2.5 FMO from bacteria

There are hundreds of FMOs found in bacteria. In all FMOs known from mammals and plants, flavin is present as a prosthetic group, however, this is not always the case for bacterial FMOs. There are two different types of FMOs: flavin present as a cofactor or utilized as a substrate. Moreover, flavin is always present as FAD in either mammals or plants FMOs, while both FMN and FAD have been identified in bacterial FMOs.

As mentioned, the overall reaction catalyzed by FMOs is a very complicated reaction, which typically includes the reduction of flavin by NAD(P)H, the activation of dioxygen to form a C4a-(hydro)preoxyflavin intermediate, and substrate oxygenation by C4a-(hydro)preoxyflavin. Each of these processes has unique requirements. Two general strategies are utilized by FMOs to manage this complicated reaction mechanism. First, in the case of single-component flavoprotein monooxygenases, the enzymes undergo significant protein and flavin dynamics during catalysis. The isoalloxazine ring of flavin moves along with the significant conformational change of enzymes [*7*]. This indicates

the flavins switch their position inside the enzyme by conformational changes to modify their varied functions. The other approach uses two enzymes working together to separate flavin reduction and substrate oxidation by using a reductase to generate reduced flavin, and another enzyme, the monooxygenase, to receive the reduced flavin, and active dioxygen for the oxygenation of substrates [7]. Compared to the well characterized single-component FMO, very little information about the mechanism of these two-component enzymes is known. The mechanism of reduced flavin transfer between two-component systems has also generated a great deal of interest.

Unlike mammals and plants, both one enzyme and two-enzyme FMOs have been found in bacteria. Recent studies on these two types of FMOs in bacteria will be summarized in the following sections.

1.2.5.1 Bacterial FMOs: flavin as a prosthetic group

The FMO enzymes in bacteria perform a variety of diverse reactions by oxidizing a wide range of aromatic and aliphatic compounds [5, 13, 22, 39]. Flavin is tightly bound to these flavoprotein monooxygenases. According to the release of the $NADP^+$ or NAD^+ product, sequence and structural similarity, bacterial FMOs can be divided into two classes. In class A, $NADP^+$ or NAD^+ is released immediately upon flavin reduction; while in class B enzymes the $NADPH/NADP^+$ cofactors remain bound during catalysis. In the following sections, the substrate specificity, sequence similarity and specific structural features of each class will be summarized and discussed, respectively.

Class A monooxygenases

Typical substrates of class A monooxygenases are aromatic compounds that contain an activating hydroxyl or amino group. The C4a-hydroperoxyflavin is the oxygenating flavin species, which performs an electrophilic attack on the aromatic ring. All structural known monooxygenases from this subclass contain two sequence motifs for flavin binding: an N-terminal GxGxG sequence that binds to the ADP moiety of FAD and the amino acid sequence, GD, that is in contact with the riboflavin moiety of FAD. On the other hand, there is no NAD(P)H binding region in this subclass of enzymes [*40, 41*]. This is not a surprising result, because NAD(P)H only forms a complex to reduce flavin then the product $NAD(P)^+$ is rapidly released. Members of the class A flavoprotein monooxygenases usually are involved in microbial degradation of aromatic compounds by *ortho-* or *para* hydroxylation of the aromatic ring and display a narrow substrate specificity. A typical enzyme of this subclass is 4-hydroxybenzoate 3-monooxygenase from *Pseudomonas*, which participates in benzoate degradation via hydroxylation and 2,4-dichlorobenzoate degradation [*42, 43*]. Interestingly, a class A monooxygenase has been identified that catalyzes a Baeyer–Villiger oxidation. This bacterial enzyme (MtmOIV) is involved in the biosynthesis of mithramycin, an anticancer drug and calcium lowering agent [*44, 45*]. It will be interesting to elucidate how this class A monooxygenase catalyzes a Baeyer-Villiger rearrangement as these reactions typically utilize a C4a-peroxyflavin intermediate while Class A monooxygenases utilize a C4a-hydroperoxyflavin intermediate.

Class B monooxygenases

This subclass of enzymes is also referred to as multifunctional flavin containing monooxygenases, because these monooxygenases are able to catalyze the oxygenation of substrate with either carbon atoms or heteroatoms. Monooxygenases that belong to this subclass play an essential role in detoxification and biodegradation. These enzymes catalyze an atypical oxygenation reaction: the Baeyer-Villiger oxidation of ketone or aldehyde to an ester or lactone. The flavin-related Baeyer-Villiger oxidation includes the nucleophilic attack of C4a-peroxyflavin on the oxygenating substrate. Cyclohexanone monooxygenase and phenylacetone monooxygenase are examples of monooxygenases in this subclass. The crystal structure of phenylacetone monooxygenase, which inserts an oxygen atom into phenylacetone to form the product benzyl acetate, has been determined [*46*]. The structure is composed of two binding domains for flavin and NADPH, respectively. Coenzyme NAD(P)H/NAD(P)$^+$ remains bound to the monooxygenases of this subclass during the entire catalytic process. The binding of NAD(P)H/NAD(P)$^+$ is catalytically important to the enzymatic reaction. Increased stability of the cyclohexanone bound peroxyflavin intermediate was observed by the binding of NADP$^+$ [*25*].

Significant protein and flavin dynamics

The reactions catalyzed by flavoprotein monooxygenases are complicated processes. To satisfy different requirements, significant protein and flavin dynamics are critical in reactions catalyzed by single-component flavoprotein monooxygenases. The PHBH enzyme, one of the most thoroughly studied flavoprotein monooxygenases, catalyzes the oxidation of *p*-hydroxybenzoate to protocatechuate. Three conformations were detected

during the catalytic reaction of PHBH by X-ray crystallography and kinetic analyses of wild-type and variant enzymes [43, 47-49]. An *out* conformation allows NADPH to access the exposed flavin and initiate the PHBH reaction by reducing the isoalloxazine ring. An *in* conformation shields the flavin from solvent, thus protecting the reactive FADOOH intermediate formed when $FADH_2$ reacts with O_2. Finally, an *open* conformation permits trafficking of substrate and product in and out of the active site. These dynamic properties afford multiple sites for carrying out separate phases of catalysis, thereby optimizing each step in the reaction pathway.

In summary, these complicated conformational changes are essential to FMOs to stabilize the C4a-(hydro)peroxyflavin intermediate while also adjusting the orderly sequence of chemical events. With PHBH it can be seen that once initiated, the series of mechanistic steps proceeds like a "domino effect" to bring about efficient catalysis.

1.2.5.2 Bacterial FMOs: flavin is utilized as a substrate

Flavins are a tightly bound prosthetic group in numerous flavoproteins, however, in some enzymes the flavin can also be utilized as a substrate. As mentioned, the reactions catalyzed by flavoprotein monooxygenases are complicated and involve multiple processes. In addition to the single polypeptide flavoprotein monooxygenases discussed above, two-component flavin-dependent monooxygenases have been discovered, where reductive and oxidative reactions are catalyzed by two separate enzymes, a flavin-reductase and a monooxygenase. In the two-component flavin-dependent monooxygenases, the flavin is reduced by a separate NAD(P)H-dependent reductase, and then transferred to the monooxygenase enzyme. The overall catalytic mechanism of these

two-component monooxygenase systems is quite similar to the flavin containing monooxygenases. Since there are actually two enzymes involved in flavin reduction and substrate oxygenation, a major area of focus has been the mechanism of reduced flavin transfer from the reductase to the monooxygenase. For the monooxygenase component, the activation of dioxygen by reduced flavin, the structural and functional relationship of the enzymes, and the substrate binding order are usually the focus of the mechanistic studies. A stabilized hydroperoxyflavin intermediate has also been identified even isolated in some well characterized two-component monooxygenase systems. A combination of structural and biochemical approaches were performed to explore the ability of these monooxygenases to stabilize the hydroperoxyflavin intermediate. In the following section, three different aspects of the overall mechanism of these two-component flavin-dependent monooxygenase enzymes will be discussed: 1) the mechanistic and structural studies of the flavin reductase component; 2) the mechanistic and structural studies of the monooxygenase component and 3) the mechanism of the reduced flavin transfer between these two components.

1.2.5.2.1 Flavin reductases

Reduced flavin, as a product, is generated by the catalytic reactions of NAD(P)H-flavin reductases in the following reaction:

$$Fl + NAD(P)H + H^+ \rightarrow FlH_2 + NAD(P)^+ \tag{1.1}$$

where Fl stands for oxidized flavin substrate and FlH_2 refers to the reduced flavin product. In addition to reducing flavins for oxidation reactions by flavin-dependent monooxygenase, these reductases are also involved in reducing iron complexes [*50, 51*].

32

The size of flavin reductase monomers are generally small, ranging from 13 to 34.5 kDa [6].

Flavin reductases are usually classified into three groups based on substrate specificity: FRP, NADPH-preferring flavin reductases; FRD, NADH-preferring reductases, and FRG, the general flavin reductases that utilizes NADH and NADPH with similar efficiencies. Flavin reductases are also divided into two classes based on the role of the flavin: flavoprotein class I and non-flavoprotein class II. In class I flavin reductases, the flavin is present as a cofactor, while the flavin is a substrate in class II reductases [6]. The preference for FMN or FAD has no direct relationship on whether flavin is required as a cofactor.

The FRP from *Vibrio harveyi*, and Fre from *Escherichia coli* are two extensively characterized flavin reductases. The *V. harveyi* FRP, which favors NADPH as a substrate, belongs to Class I [52]. This enzyme is a homodimeric enzyme with each subunit comprising two domains and containing one bound FMN per monomer. The first and major domain contains four-stranded antiparallel β-sheet flanked by helices on either side. The second domain reaches out from one subunit to interact with the first domain of the second subunit [6]. A disordered nine-residue loop (A_{201}-S-R-T-S-N-G-K_{209}) is present in the crystal structure. Moreover, the Arg203 residue within this loop is critical for NADPH recognition and binding [53]. A NADPH/NADP$^+$ shuttle mechanism between an open and closed conformation during catalysis has been proposed based on structural studies of *V. harveyi* FRP [54]. The *V. harveyi* luciferase and FRP enzyme was used as a model for the elucidation of the reduced flavin transfer mechanism between the reductase and monooxygenase [55]. After the formation of specific complex(es) between FRP and

luciferase, the reduced flavin cofactor is transferred directly to luciferase for bioluminescence.

The *E.coli* Fre/FRII represents a non-flavoprotein Class II reductases that does not contain any flavin cofactor. Fre is able to utilize both FMN and FAD as cosubstrate; however this enzyme shows a moderate preference for FMN [56] and a strong preference for FAD [57]. Fre exhibits a sequential kinetic mechanism with ordered substrate binding of NAD(P)H followed by flavin, with the reduced flavin product released first before NAD^+. Although Fre does not contain a bound flavin, Fre may be closely related to a flavoprotein family of which the spinach ferredoxin-$NADP^+$ reductase (FNR) is a structural prototype. The Fre enzyme contains a four-residue motif similar to a sequence in FNR known to interact with flavin. Ser49 residue within this motif is indeed critical to flavin binding and catalytic activity [58]. The Fre and FNR flavin reductases also have certain mechanistic similarities in that charge transfer complex intermediates detected in the Fre reaction are similar to those observed for FNR.

1.2.5.2.2 Flavin-dependent monooxygenases

Two-component flavoprotein monooxygenases are widely distributed in bacteria to catalyze the oxygenation of a variety of substrates, which usually are aromatic compounds or compounds containing heteroatoms. These compounds typically are very stable in nature and difficult to oxidize. In two-component flavoprotein monooxygenases, the reduced flavin is acquired from the flavin reductase.

$$S + FH_2 + O_2 \rightarrow S\text{-}O + F + H_2O \tag{1.2}$$

The reduced flavin is first converted to the C(4a)-hydroperoxyflavin intermediate for

substrate oxygenation and released as an oxidized flavin product. This group of monooxygenases catalyze oxidative half-reaction only.

The mechanism of flavin-dependent monooxygenases in the two-component systems has been studied for decades, however, most of the mechanistic and structural information regarding these two-component monooxygenases have only recently been reported. Some catalytic reactions have been well-characterized, such as bacterial luciferase [56], *p*-hydroxyphenylacetate hydroxylase (HPAH) from *P. aeruginosa*, and *A. baumannii* [48, 49], and RebH [57], an oxygenase responsible for halogenating tryptophan in the biosynthesis of rebeccamycin. The mechanism of these enzymes will be discussed in the following section.

These two-component monooxygenases have been grouped into two subclasses in terms of flavin substrates. To be consistent with the classification of single-component monooxygenases, class D ($FMNH_2$-dependent monooxygenases) and class E ($FADH_2$-dependent monooxygenases) will be used.

Class D monooxygenases: $FMNH_2$-dependent monooxygenases

A number of monooxygenases belong to the Class D group of flavin-dependent monooxygenases based on substrate specificity and sequence homology. These enzymes use reduced FMN as substrate, which is generated by the reductase. Structurally, the subunit(s) display a TIM-barrel fold. The most extensively studied representatives are bacterial luciferases. The luciferases exist as a heterodimeric structure (α & β subunits); however, the two subunits of the heterodimer are very similar in sequence and structure [58]. The elucidated crystal structure of the luciferase from *Vibrio harveyi* has revealed

35

that both subunits exhibit a TIM-barrel fold with the only major difference being a flexible loop located only in the α-subunit (LuxA). Individual subunits are inactive, but when recombined under appropriate conditions they recover nearly full activity. Although they are similar in sequence and structure, the two subunits are functionally distinct. Substrate binding and catalytic properties appear to reside on the α-subunit. The function of the β-subunit (LuxB) is required for the high quantum yield and protein stability [*58*].

LadA, a long-chain alkane monooxygenase, utilizes a terminal oxidation pathway for the conversion of long-chain alkanes to their corresponding primary alcohols. The structure of LadA and its complex with FMN were reported recently. LadA, a homodimeric enzyme, shows a TIM-barrel architecture similar to bacterial luciferase, and alkanesulfonate monooxygenase (SsuD) from *E.coli*. The LadA:FMN binary complex structure and a Lad:FMN:alkane model revealed that the flavin ring lies in a hydrophobic cavity [*59*]. The LadA monomer differs from the prototypical TIM barrel structure by five extended insertion regions and an extension at the C-terminus of the polypeptide chain. In LadA, dimerization is promoted by a parallel four-helix bundle formed by α2 and α3 of each subunit. The dimerization interface is flat and is predominantly built up by hydrophobic residues. The same dimer arrangement was also found in other monooxygenases in this two-component family, suggesting the functional importance of dimeric forms of these enzymes.

Except for bacterial luciferases, the catalytic mechanism of flavoprotein monooxygenases in this subclass is still not clear. Bacterial luciferase catalyzes the production of visible light from the reaction of reduced FMN, long-chain aldehyde and

dioxygen. This reaction has an unusual slow turn-over rate, which may be caused by a long lifetime enzymatically-stabilized C4a-(hydro)peroxyflavin intermediate [*56*]. The reaction pathways and intermediates involved in the luciferase reaction are shown in Scheme 1.8. After the initial binding of luciferase and $FMNH_2$, this complex reacts with dioxygen extremely fast to form a hydroperoxyflavin (Intermediate II). In the absence of aldehyde substrate, this hydroperoxyflavin has a relatively long lifetime, which can be isolated and characterized using low-temperature techniques [*61*]. As mentioned, this oxygen-containing intermediate differs from both reduced and oxidized flavin; it has absorption peaks in the visible range at 372 nm, and fluorescence emission centered at 490 nm. In the presence of aldehyde, peroxyflavin inserts an oxygen atom into the aldehyde substrate to form the corresponding acid and emitting intermediate [FMNOH]*, which further decays to FMNOH to emit light.

Class D monooxygenases: FADH₂-dependent monooxygenases

In this monooxygenases subclass, reduced FAD is utilized as substrate. Structurally, these enzymes show more diverse structures than class C monooxygenases. Sequence homology suggests that a number of class D monooxygenases have structural similarities with the acyl-CoA dehydrogenase fold. Typical substrates of these monooxygenases are aromatic compounds. The prototypical example is *p*-hydroxyphenylacetate hydroxylase (HPAH), which catalyzes the hydroxylation of *p*-hydroxyphenylacetate (HPA) to form 3,4-dihydroxyphenylacetate (DHPA) in a number of bacteria. More recently, the three-dimensional structure of HPAH has been solved along with the structure of the
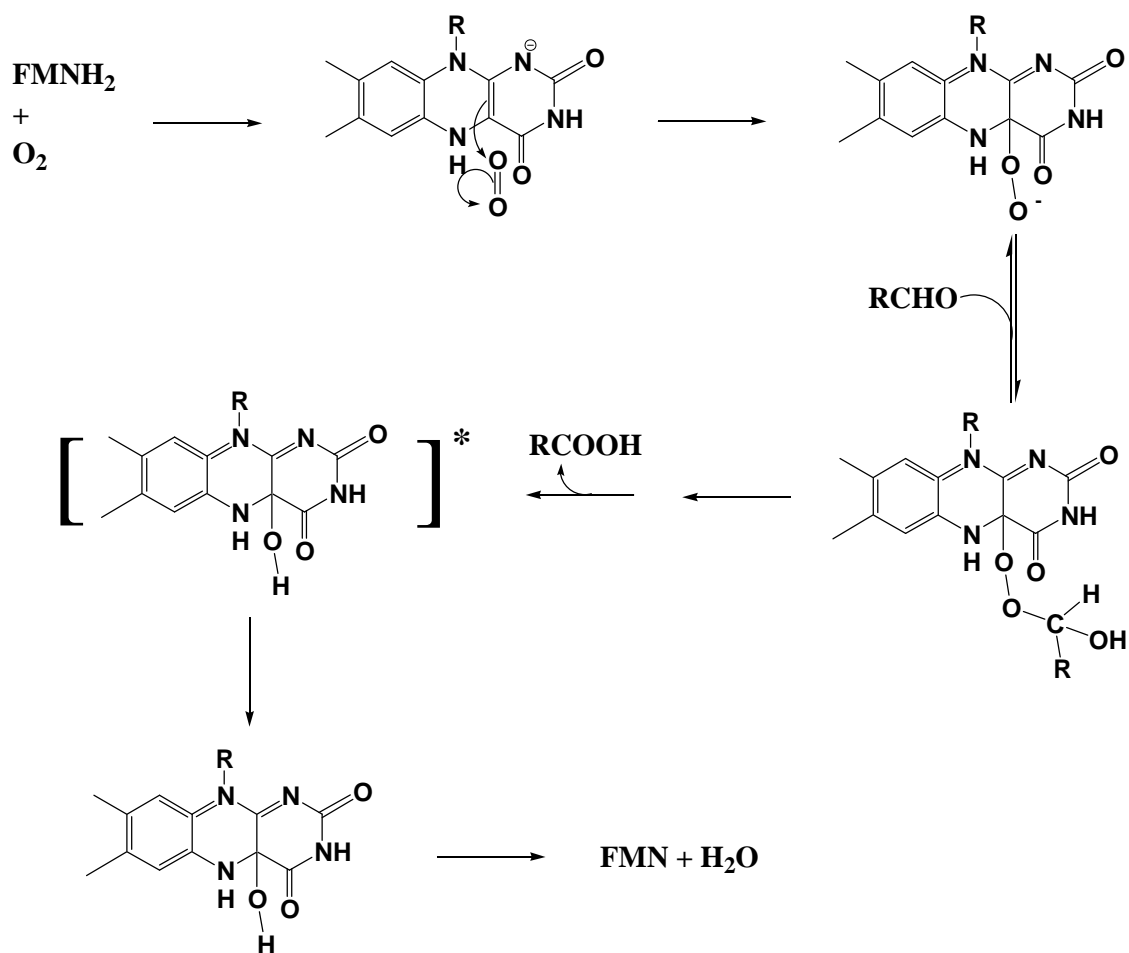
Scheme 1.8 Reaction sequence and intermediates involved the reaction of bacterial

luciferase with FMNH$_2$

HPAH-FADH$_2$ complex [*62*]. The HPAH is a homotetrameric structure with four identical subunits. Each monomer is made of three domains; the N-terminal domain, the β-sheet domain, and the C-terminal domain. Interactions between the subunits of the tetramer are mediated by helical bundles in the C-terminal domains. The reduced flavin bound HPAH structure shows a hydrophobic cavity essential in stabilizing the hydroperoxyflavin intermediate. This hydrophobic cavity is able to protect the hydroperoxyflavin intermediate from accessing solvent.

Styrene monooxygenase from *Pseudomonas sp* catalyzes the degradation of styrene to 2, 5-dihydroxyphenylacetate and includes only one dinucleotide binding domain (FAD). This structural information indicates an evolutionary link with the Class A flavoprotein monooxygenases. Some halogenation reactions occurring in nature are catalyzed by two-component flavoprotein monooxygenases. One of the best studied flavin-dependent halogenases is tryptophan 7-halogenase (RebH) [*57*]. The tryptophan 7-halogenase structure is a dimer with each subunit forming a single domain. The halogenase subunit contains a helical substrate binding module. A hydroperoxyflavin intermediate is generated during catalysis, and it is proposed that a chloride ion will perform a nucleophilic attack on the hydroperoxyflavin resulting in the formation of HOCl. This highly reactive molecule will travel through a tunnel to reach and halogenate the bound tryptophan molecule.

Active sites of the two-component monooxygenases

As single-component flavin-containing monooxygenases, the two-component flavin-dependent monooxygenases are capable of stabilizing the C4a-(hydro)peroxyflavin

intermediate. Attempts have been made to determine what structural properties lead to the stabilization of the oxygen-flavin intermediates [*62, 63*]. Another general property for this family of monooxygenases is that the monooxygenase component always has a higher affinity for the reduced flavin over the oxidized flavin, although the structure and size of both states are quite similar to each other. This preference for reduced rather than oxidized flavin plays important roles in flavin transfer between the reductase and the monooxygenase components.

As mentioned, bacterial luciferase is the most extensively studied enzyme in this two-component monooxygenase family. The crystal structure of bacterial luciferase from *Vibrio harveyi* has been elucidated [*58*], however the binding sites for the FMN and aldehyde substrates have not been identified. The α subunit (LuxA) is primarily responsible for catalysis; however, the presence of the β subunit is essential for high catalytic efficiency [*56*]. The active site thus is believed to be located in the α subunit with the phosphate moiety of FMN anchored at an electron dense inorganic phosphate site located on LuxA [*56*]. Amino acid substitutions have been carried out to probe the binding sites of both substrates, and the catalytic roles of conserved residues in the luciferase reaction [*64-67*]. A model of the luciferase-flavin complex structure based on the structural activity data, energetic criteria, and the geometric requirement for catalysis has been proposed [*68*]. In this model, the location of the phosphate moiety was used as the anchor in a flexible docking procedure performed by a conformational search. As shown in Figure 1.5, the resulting model of the bacterial luciferase-FMN complex is consistent with the reported experimental data. Based on the model, bound FMN is surrounded by several hydrophobic residues, which help to form a relatively hydrophobic

environment. Considering the C4a-(hydro)peroxyflavin is extremely unstable under aqueous conditions [1, 2], this hydrophobic environment may be critical in stabilizing this oxygen-flavin intermediate. This agrees with results from mutagenesis studies on contribute to the hydrophobic cavity. A conserved hydrophobic residue, Phe46, was replaced by Asp resulting in an enzyme C4a-(hydro)peroxyflavin intermediate with a shorter half-life due to the change of the hydrophobic enviroments [69]. In addition, the reduced flavin preference of luciferase may be explained by this structural information. The N5 hydrogen atom of reduced flavin may be hydrogen-bounded to the *cis*-peptide between Ala75 and Ala74, while the oxidized flavin cannot form this type of bond [68]. Cys106, a conserved active site residue in bacterial luciferase, plays an important role in the stabilization of the C4a-(hydro)peroxyflavin intermediate. Mutation of Cys106 to alanine, valine, and serine was shown to reduce bioluminescence and destabilize the C4a-(hydro)peroxyflavin intermediate. [70]

The crystal structure of HPAH also shows a hydrophobic cavity in front of the reduced FMN in the HPAH-FMNH$_2$ complex [62]. The shape and position of this cavity are perfect fit for housing the oxygen atoms of the flavin C4a-hydroperoxide intermediate and prevent it from accessing the solvent. Figure 1.6 shows the hydrophobic residues surrounding reduced flavin in the active site of HPAH. The reduced flavin is embedded in a protein scaffold formed by several stretches of amino acid residues. The flavin is kept in position by a network of hydrogen bonds and hydrophobic interactions. The shape and position of this cavity are specifically arranged for housing the oxygen atoms of the C4a-(hydro)peroxyflavin intermediate.
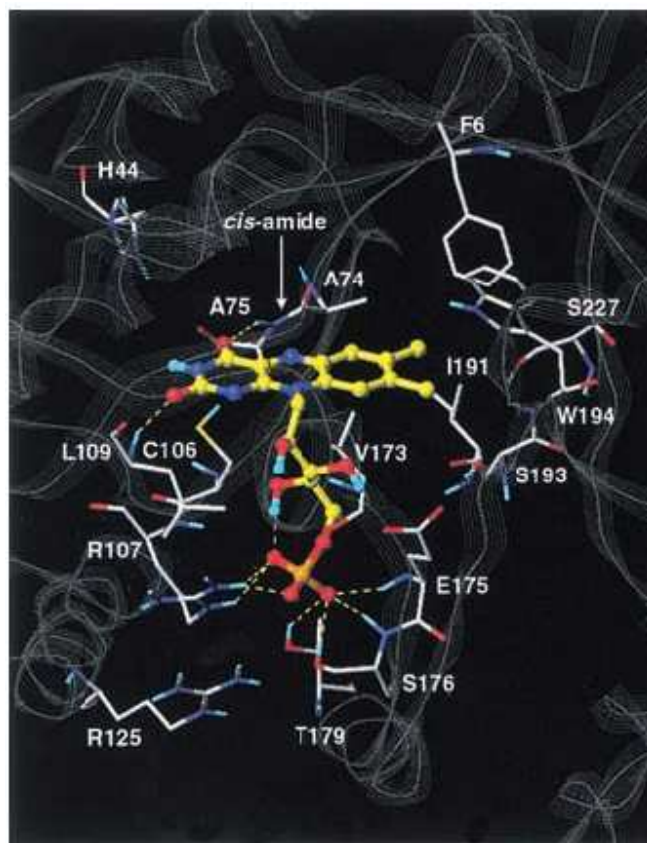
Figure 1.5 The modeled luciferase-FMN complex structure. The FMN ligand is shown in ball-and-stick. Selected protein residues lining the binding site are shown as capped-sticks and labeled. Inter- and intra-molecular hydrogen bonds formed by the FMN are shown as dashed lines [68]. (Reprinted with permission)
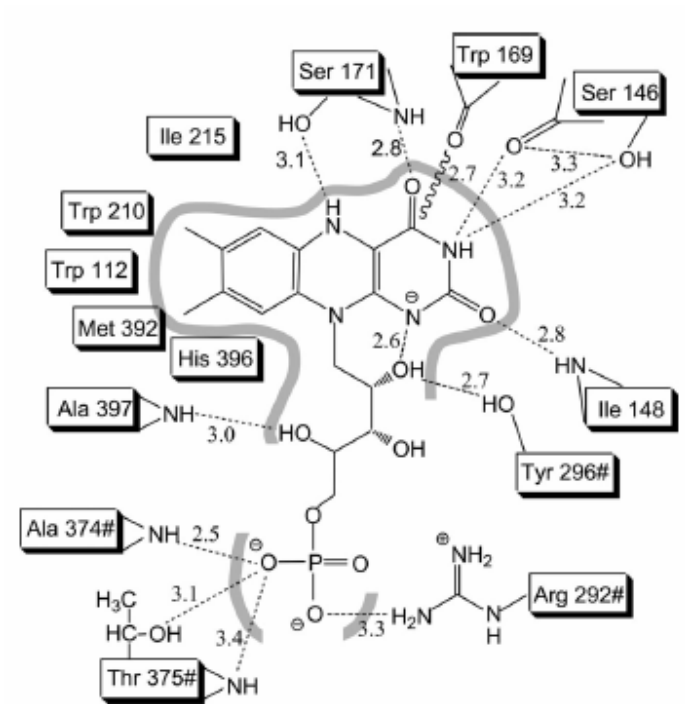
Figure 1.6 Interactions between reduced FMN and HPAH [*62*]

(Reprinted with permission)

1.2.5.2.3 Mechanism of reduced flavin transfer

As mentioned, reduced flavin is quite unstable in an aqueous environment because of a series of self-catalytic reactions which generate reactive oxygen radicals. Therefore, direct reduced flavin transfer between the reductase and the monooxygenase should overcome this unstable property of reduced flavin. Reduced flavin transfer in several two-component monooxygenases has been explored in flavin reductase-bacterial luciferase, styrene monooxygenase, *p*-hydroxyphenylacetate hydroxylase, and alkanesulfonate monooxygenase. Generally, there are two possible flavin transfer mechanisms: 1) free diffusion of reduced flavin to the monooxygenase; 2) direct channeling of reduced flavin from donor to acceptor. Each transfer mechanism has been demonstrated depending on the system under study. More interestingly, recent studies reveal that both diffusion and direct channeling mechanisms occur in reduced flavin transfer from the reductase to bacterial luciferase.

Direct channeling of reduced flavin transfer from reductase to monooxygenase

Reduced flavin transfer between the reductase and luciferase was the first extensively studied system. Although bacterial luciferase relies on reduced flavin transferred from an external reductase, luciferase can obtain reduced flavin from multiple reductases. Other well characterized flavin-dependent monooxygenases are usually co-expressed with a reductase to provide reduced flavin. Evidence suggests that $FMNH_2$ can be directly transferred from the reductase to luciferase. When luciferase receives $FMNH_2$ by free diffusion, it can be reasoned that the K_m of the reductase for the flavin and pyridine nucleotide substrates should be the same in both the reductase single-enzyme assay and

the reductase-luciferase coupled assay. On the other hand, knowing that the turnover rate of luciferase is markedly slower than the reductase, the overall efficiency of a reductase-luciferase functional complex will be limited by luciferase. In various reductase-luciferase systems, substantially lower K_m values were observed in coupled assays than in single-enzyme assays monitoring flavin reduction by the reductase [55]. Therefore, direct transfer of $FMNH_2$ was proposed in the reductase-luciferase reaction.

The *Vibrio harveyi* NADPH-FMN oxidoreductase (FRP) and luciferase pair were chosen as a model for further studies of the reduced flavin transfer mechanism. The steady-state kinetic mechanism of the reductase (FRP) was altered in the presence of luciferase, as shown in scheme 1.9. The reductase shows a typical ping-pong mechanism in single enzyme assays. Interestingly, a sequential mechanism was observed in the luciferase-coupled assay. This implies a direct transfer of reduced flavin to luciferase [55]. However, the reduced flavin transfer mechanism proposed for the *V. harveyi* FRP-luciferase couple does not preclude other mechanisms for reduced flavin transfer to luciferase. In fact, the results from the the *Photobacterium fischeri* NAD(P)H-FMN oxidoreductase (FRG) and luciferase coupled assay showed the ping-pong mechanism of the FRG remained unchanged in reductase-luciferase coupled assays. However, K_m values of both substrates for reductase were significant lower in coupled assays than those measured in single-enzyme assay. This also supported a direct transfer of reduced flavin from FRG to luciferase [55].

A.

```
         NH H              F FH₂
         ↓  ↑              ↓  ↑
  EF ─┴──┴─ EFH₂ ─┴──┴─ EF
```

B.

```
      F              NH N            LFH₂
      ↓              ↓  ↑              ↑
  E ─┴── EF ─┴──┴─ EFH₂ ──┴─ E
                                 L
```
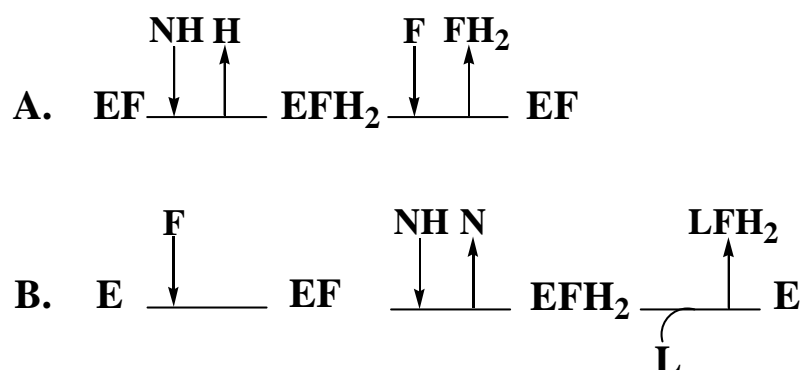
Scheme 1.9 (A) Ping-pong mechanism of flavin reductase from *V. fischeri* and *V. harveyi* in the respective single-enzyme reactions. (B) Sequential mechanism of flavin reductase in the reductase-luciferase coupled reactions. (E: reductase; NH: NADPH; F: oxidized flavin; FH_2: reduced flavin; N: $NADP^+$; L: luciferase)

Free diffusion of reduced flavin from reductase to monooxygenase

A free diffusion transfer mechanism has been proposed in the two-component *p*-hydroxyphenylacetate hydroxylase (HPAH) [*71*]. Because of the fast reoxidation of reduced flavin, the monooxygenase should bind to reduced flavin extremely fast to avoid reoxidation if the reduced flavin is transferred by free diffusion. Their findings imply the important role of HPA in regulating the rapid transfer of reduced flavin between components in the HPAH system. Without HPA, the reduction of flavin by the reductase is about 15 s^{-1}, while in the present of HPA, the reduction rate of flavin is 20 fold faster. Thus it would appear that HPA, a substrate for the monooxygenase component, allosterically influences the reactivity of the reductase and controls the overall rate of production of reduced flavin. However, the kinetic effect of the monooxygenase

46

substrate on reductase activity actually shows the interaction between these two enzyme components.

More recently Tu and colleagues investigated the *Vibrio harveyi* luciferase and flavin reductase (FRP) kinetic reaction by using O_2 concentrations as a probe. The reductase activity was evaluated in both single and coupled enzyme assays at various oxygen concentrations [72]. If reduced flavin is transferred by a directly channeling mechanism, the oxidation of reduced flavin during coupled-enzyme assays should be independent of increased oxygen concentrations. If a rate dependence on oxygen concentration is observed in coupled-enzyme assays, free diffusion may also be involved in flavin transfer. Results show that increases in oxygen concentration led to gradual decreases in the peak bioluminescence intensity, $K_{m, FMN}$, and $K_{m, NADPH}$ of FRP in the coupled reaction. This implied that some reduced flavin may transfer to the monooxygenase by free diffusion. Therefore, a mixed transfer mechanism including both free diffusion and direct transfer in the FRP/luciferase system was proposed based on these experiments. This conclusion was based on an assumption that the FPR-bound and luciferase-bound $FMNH_2$ were stable at various oxygen concentrations. However, there is a possibility that the oxidation of enzyme-bound reduced $FMNH_2$, especially FRP-bound $FMNH_2$, occurs at higher oxygen concentrations. Regardless of how the reduced flavin is transferred, the transfer efficiency would be decreased as oxygen concentration increases which will result in a gradual decrease in bioluminescence intensity.

1.3 Two-component flavin-dependent alkanesulfonate monooxygenase from E. coli

The alkanesulfonate monooxygenase system from *E .coli* includes two enzymes: an NAD(P)H:FMN reductase (SsuE); and an $FMNH_2$-dependent alkanesulfonate monooxygenase (SsuD). This system belongs to the two-component flavin-dependent monooxygenase family. FMN is reduced by SsuE with NADPH and is then transferred to SsuD, which directly catalyzes the oxidation of alkanesulfonate to aldehyde and sulfite in the presence of dioxygen. The overall reaction mechanism of this two-component system is shown in Scheme 1.10 [73]. The biological function of this enzymatic system is to find an alternative sulfur source by catalyzing the desulfonation of alkanesulfonate compounds under sulfur starvation conditions. In the following sections, sulfonate-sulfur metabolism in *E.coli*, some related sulfur starvation induced (Ssi) proteins, and previous mechanistic and structural studies on the alkanesulfonate system will be summarized and reviewed.
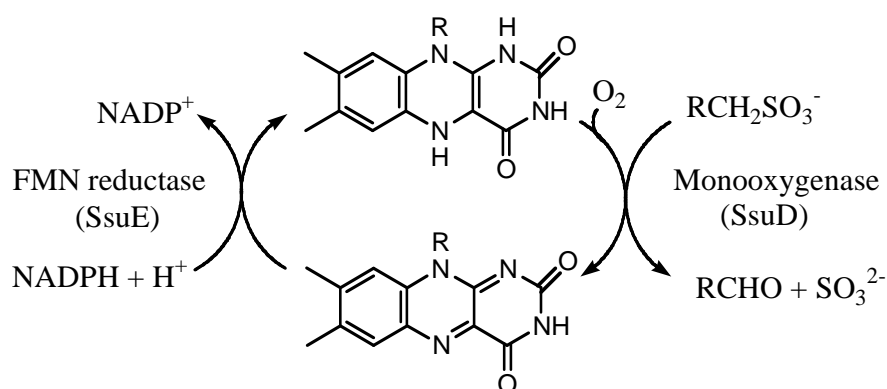
Scheme 1.10 Reaction mechanism of the alkanesulfonate monooxygenase system

1.3.1 Sulfonate-sulfur metabolism in and sulfur-starvation-induced (Ssi) proteins

Sulfur is an essential element for bacterial growth, which can be assimilated from different sources. As shown in Figure 1.7, cysteine is the preferred source of sulfur for *E. coli* and other bacteria. Sulfonate can be assimilated through a series of reductions and incorporated into cysteine. However, under sulfur starvation conditions, bacteria must find alternative sources for obtaining sulfur. Some organic sulfur compounds are utilized by bacteria during sulfur limiting conditions [74]. In *E.coli*, alkanesulfonate and taurine are the two most common alternative sources for acquiring sulfur.

E. coli is primarily found in the gut, an environment with suitable sulfate and cysteine levels. Surprisingly, *E. coli* are able to grow in soil environments where inorganic sulfate may be limiting. Under sulfur starvation conditions, Ssi proteins are induced and expressed. They play different roles in releasing sulfite from organic sulfur sources. Based on the assumption that the expression of Ssi proteins would be repressed by sulfate and cysteine, these proteins have been identified by comparing the protein expression of cell growth with and without cysteine and sulfate. Some of the eight Ssi proteins were identified as proteins involved in uptake of cystine (cystine binding protein, FliY) or in the biosynthesis of cysteine from sulfate (O-acetylserine-(thiol)-lyase, CysK), and a sulfate binding protein (Sbp). Two important gene clusters, *tauABCD* and *ssuEADCB,* were later identified and shown to be directly involved in sulfur acquistion [74]. Both gene clusters encode an ABC transport system (TauABC and SsuABC) and an oxygenase system (*tauD* and *ssuDE*). The *tauABCD* gene cluster is involved in the desulfonation of taurine [75]; while the *ssu* gene cluster participates in the release of sulfite from

Sulfate (external)   **Taurine (external)**   **Alkanesulfonates (external)**

CysP CysT CysW CysA sbp   **TauABC**   **SsuABC**

Sulfate (internal)   **Taurine (internal)**   **Alkanesulfonates (internal)**

ATP sulfurylase CysD CysN

APS

Taurine Dioxygenase TauD   *Alkasulfonates monooxygenase SsuD*

APS Kinase CysC

PAPS

FMN redutase SsuE

PAPS sulfotransferase CysH

Sulfite

Acetyl-CoA

Sulfite redutase CysI CysJ CysG

Serine acetrytransferase CysE

O-Acetyl-serine ——— **Sulfide**

Serine

Cysteine

Figure 1.7 Cysteine biosynthesis from sulfate and alkanesulfonates in *E. coli.*

alkanesulfonates [*76*].

For the ABC-type transporters, A proteins are periplasmic binding proteins, B proteins are ATP-hydrolyzing enzymes, and C proteins are the integral membrane components of the corresponding transporter. Taurine can only be transported into a cell by the TauABC transport system and desulfonated by TauD, while most long-chain aliphatic sulfonates were exclusively transported by the SsuABC system and desulfonated by the SsuE/D system (Figure 1.7). Interestingly, a few alkanesulfonate substrates can be transported by both systems. In some cases, these substrates can be catalyzed by both oxygenase systems.

1.3.2 Taurine Dioxygenase

Taurine dioxygenase is an α-ketoglutarate-dependent dioxygenase. The TauD enzyme converts taurine to sulfite and aminoacetaldehyde, and is dependent on the presence of Fe(II) and α-ketoglutarate [*77*]. Besides taurine, other sulfonate substrates, for example butanesulfonate, pentanesulfonate, and MOPS (3-(N-morpholino) propanesulfonic acid) can serve as substrates for TauD with lower affinity than taurine [*74*].

The kinetic mechanism of TauD was proposed based on stopped-flow kinetic analyses (Scheme 1.11) [*78*]. The α-ketoglutarate coenzyme binds first in a six-coordinate Fe(II) complex. Taurine binding releases the water ligand to form a five-coordinate Fe(II) complex, so O_2 can access the iron center. Succinate and carbon dioxygen are then cleaved to form a Fe(IV)=O intermediate, from which oxygen is inserted into taurine. In the final step, sulfite and aminoacetaldehyde are released from

Alkanesulfonates   **Taurine**

External

Periplasm

SsuA   TauA

SsuC | SsuC   TauC | TauC

SsuB | SsuB   TauB | TauB

Cytoplasm

$R\text{-}CH_2SO_3^-$ $R\text{-}CH_2SO_3^-$ ^-OOC $\quad$ COO^-

$NAD(P)H + H^+$ $\quad$ $FMNH_2$ $\qquad$ O_2

$\qquad\qquad$ SsuE $\qquad$ SsuD $\qquad\qquad$ TauD $|$ Fe^{2+} $\qquad$ O_2

$NAD(P)^+$ $\qquad$ FMN $\qquad\qquad\qquad\qquad\qquad\qquad$ CO_2

$RCHO + H^+ + SO_3^{2-}$ $\qquad$ $RCHO + H^+ + SO_3^{2-}$ $\qquad$ ^-OOC $\quad$ COO^-
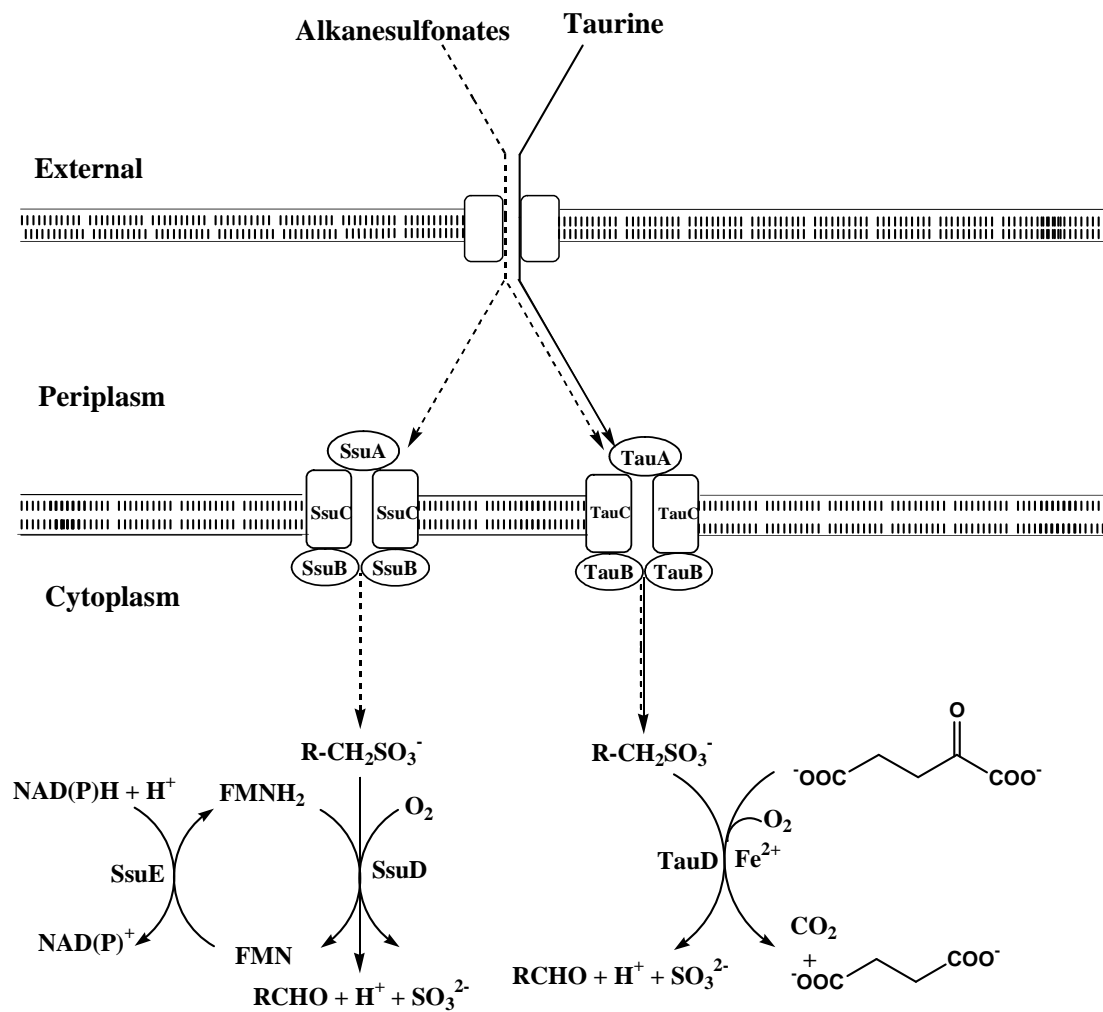
Figure 1.7 Uptake and desulfonation of taurine and alkanesulfonates in *E. coli*.

52
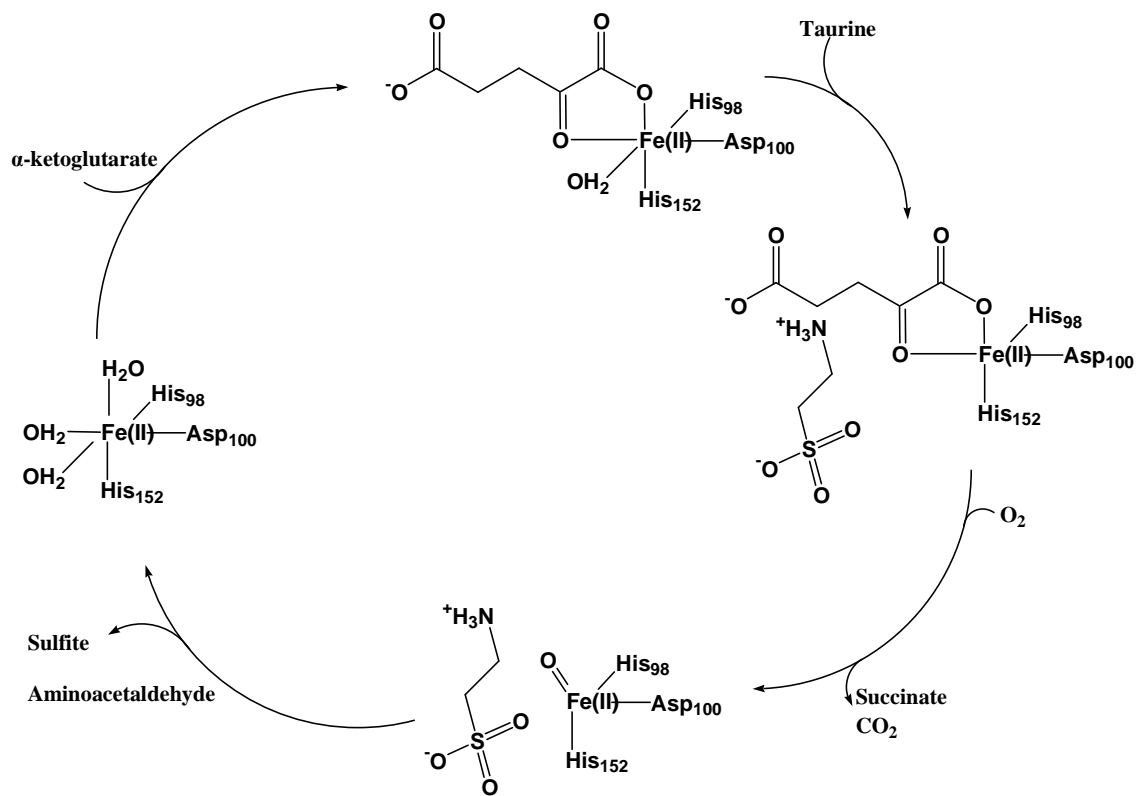
Scheme 1.11 Catalytic mechanism of TauD

the active site.

1.3.3 Substrate ranges of SsuD and TauD: two complementary systems

As mentioned, both the Ssu and Tau system help in the acquisition of inorganic sulfur during limited sulfur conditions. These two systems are complementary to help *E.coli* survive under sulfur starvation conditions with alternative sulfur sources. Table 1.1 summarizes the substrate ranges of both SsuD and TauD. SsuD utilize a wider range of substrates range than TauD. One of the common properties of flavin-containing/dependent monooxygenase is their ability to catalyze a wide range of

Sulfonated Substrate	Relative Activity	
	SsuD	TauD
	%	
Taurine	0.0	100.0
N-Phenyltaurine	65.5	0.0
4-Phenyl-1-butanesulfonic acid	42.4	2.5
HEPES	10.6	5.0
MOPS	36.4	34.2
PIPES	29.2	3.1
2-(4-Pyridyl)ethanesulfonic acid	87.4	0.5
1,3-Dioxo-2-isoindolineethanesulfonic acid	100.0	30.1
Sulfoacetic acid	19.8	--[a]
L-Cysteic acid	0.0	0.0
Isethionic acid	14.3	1.2
Methanesulfonic acid	0.7	0.0
Ethanesulfonic acid	5.2	0.8
Propanesulfonic acid	14.0	2.3
Butanesulfonic acid	17.8	8.4
Pentanesulfonic acid	40.4	22.5
Hexanesulfonic acid	43.8	11.3
Octanesulfonic acid	46.3	--
Decanesulfonic acid	43.2	--
Dodecanesulfonic acid	20.1	3.3
Tetradecanesulfonic acid	2.9	--

--[a], not determined

Table 1.1 Substrate ranges of SsuD and TauD: two complementary systems

substrates [*73*]. SsuD was able to desulfonate C-2 to C-10 unsubstituted alkanesulfonates, substituted ethanesulfonic acids, as well as N-phenyltaurine, 4-phenyl-1-butanesulfonic acid, and sulfonated buffers. The TauD enzyme is more substrate specific in the catalysis of taurine along with MOPs buffer and several alkanesulfonates. Taurine actually is not an abundant amino acid in nature, therefore it is uncertain whether taurine is the natural substrate for TauD.

1.3.4   Flavin-dependent two-component alkanesulfonate monooxygenase system

Many characterized bacterial enzymes catalyze a single distinct reaction; however, enzymes working as complex systems with multifunctions have increasingly been identified [*39*]. Enzyme systems coexpressed on the same operon under the control of a single promoter are usually involved in a similar function. The alkanesulfonate monooxygenase system is an example of a complex system involved in the desulfonation reaction of alkanesulfonates [*73*]. The SsuD enzyme directly catalyzes the desulfonation reaction of alkanesulfonate substrates in the presence of dioxygen and reduced flavin, provided by SsuE (Scheme 1.10). The alkanesulfonate monooxygenases system has also been identified in other bacterial soil organisms including *Bacillus subtilis, Pseudomonas aeruginosa* and *Pseudomonas putida*. This enzyme system has also been detected in several bacterial pathogens, such as *E.coli 0157:H7, Bacillus anthracis* and *Yersinia pestis*, but the alkanesulfonate monooxygenase system has not been identified in higher organisms [*74*].

1.3.4.1 SsuE and FMNH₂ transfer mechanism in the alkanesulfonate monooxygenase system

SsuE, a homodimeric protein of 58.4 kDa, catalyzes the reduction of FMN by NAD(P)H. Similar to other characterized flavin reductases, the steady-state kinetic mechanism of SsuE proceeds by an ordered sequential mechanism with NADPH binding to SsuE first followed by FMN to form a ternary complex. After the reduction of the flavin, the $FMNH_2$ product is released first followed by $NADP^+$ (As shown in scheme 1.12) [79]. In the presence of SsuD and the alkanesulfonate substrate, the kinetic mechanism of SsuE is changed to a rapid equilibrium ordered mechanism where the NADPH substrate and $NADP^+$ product are in equilibrium with free enzyme. This suggests that SsuD and the alkanesulfonate substrate ensure the reaction is driven in the forward direction even in the presence of low concentrations of NADPH. The altered mechanism of SsuE in the presence of SsuD and the octanesulfonate substrate support a model that involves protein-protein interactions between SsuE and SsuD. Moreover, direct protein-protein interactions between SsuD and SsuE have been detected through several biochemical approaches. Therefore, a direct channeling mechanism for reduced flavin transfer has been proposed in the alkanesulfonate monooxygenase system.
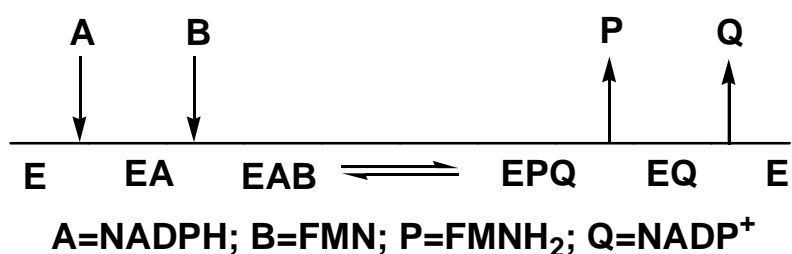
Scheme 1.12 Ordered sequential mechanism of SsuE

Rapid reaction kinetic analyses were performed to define the flavin reduction mechanism by SsuE [80]. The typical mechanism of flavin by reductases, where flavin is a tightly bound prosthetic group, proceeds through charge-transfer intermediates. These charge-transfer intermediates have a broad UV-vis absorbance peak in the range of 500-800 nm. The kinetic trances recorded at 550 nm showed that reduction of FMN occurs in three distinct phases (Scheme 1.13). Following a possible rapid equilibrium binding of FMN and NADPH to SsuE (MC-1) that occurs before the first detectable step, an initial fast phase (241 s^{-1}) corresponds to the interaction of NADPH with FMN (CT-1). The second phase is a slow conversion to form a charge-transfer complex of reduced FMNH$_2$ with NADP$^+$ (CT-2), and represents electron transfer from the pyridine nucleotide to the flavin. The third step is the decay of the charge-transfer complex to SsuE with bound products (MC-2).
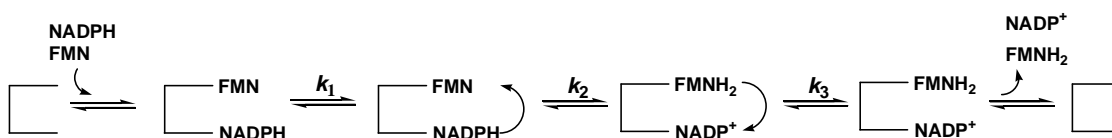
Scheme 1.13 Proposed mechanism of flavin reduction by SsuE

1.3.4.2 FMNH$_2$-dependent Alkanesulfonate monooxygenase (SsuD)

SsuD is the two-component monooxygenase, where reduced flavin is present as a substrate. The FMNH$_2$ needed for the desulfonation reaction of SsuD is provided by SsuE, which is co-expressed with SsuD from the same *ssuEADCB* gene cluster [73].

The three dimensional structure shows SsuD has an unusual homotetrameric structure in the two-component $FMNH_2$-dependent monooxygenase class, where most known structures exist as a dimer [60]. The SsuD monomer consists of a single domain in an eight-stranded β/α-barrel motif, which classifies SsuD as a member of the TIM-barrel family. The SsuD structure differs from the prototypical TIM-barrel structure by four extended insertion regions located in segments connecting β-strands and α-helices (Figure 1.9).

SsuD shares little sequence identity with other TIM barrel flavoproteins. Bacterial luciferase LuxAB (15% sequence identity), and the F_{420}-dependent N^5,N^{10}-methylenetetrahydromethanopterin reductase Mer (19% sequence identity) are
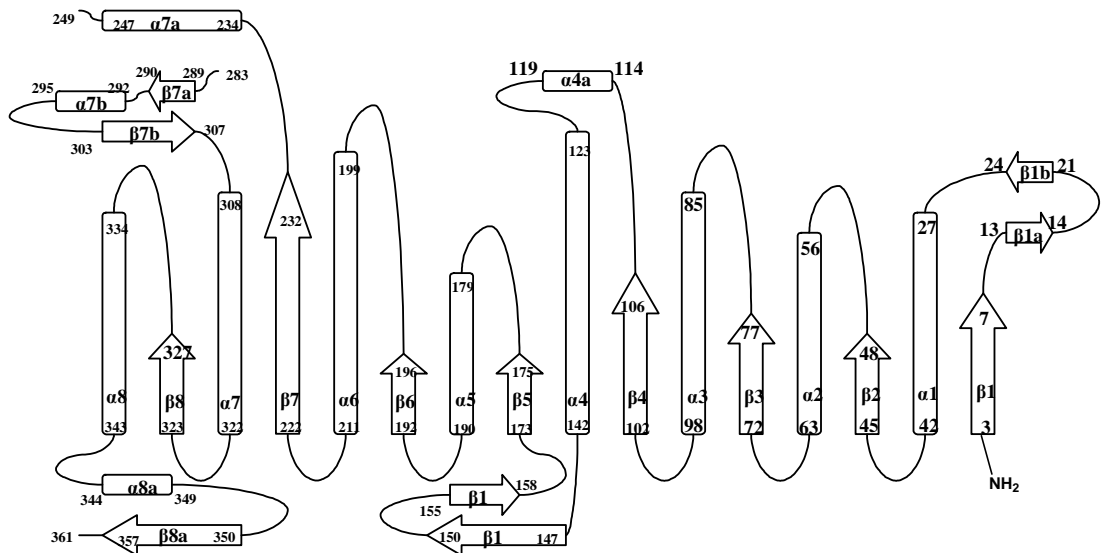
Figure 1.9 Topology diagram showing the secondary structural elements of SsuD

identified as the closest structure homologues to SsuD. Attempts to grow SsuD crystals in the presence of FMN have failed and various alkanesulfonate substrates could not bind to SsuD crystals. Therefore, the active site of SsuD has not been definitively identified. The amino acid residues Cys54, His11, His333, Tyr331, His228 and Arg226 flank the wall of a cavity, located at the C-terminal end of of the β-barrel, where active sites are commonly observed in TIM-barrel enzymes. Even through, there is low amino acid sequence identity with luciferase, amino acid residues Cys54, His228 and Tyr331 of SsuD have a similar spatial arrangement as Cys106, His44 and Tyr110 of LuxA, which have been identified as important to catalysis. The role of Cys106 has been extensively investigated by both site-directed mutagenesis and chemical modification studies in bacterial luciferase. Substitution of Cys106 to valine showed both a decrease in aldehyde utilization and destabilization of the C4a-(hydro)peroxyflavin intermediate. The stability of the C4a-(hydro)peroxyflavin in the C106V variant was significantly decreased dramatically in stopped-flow analyses [70]. His44 has been implicated as a catalytic base in the mechanism of bacterial luciferase. The luciferase bioluminesence activity of the His44 variants was reduced around 10^3-fold. The addition of imidazole rescued 30% of the activity at increasing pH (pH >6.5) [66]. Bacterial luciferase shows an alpha-beta heterodimeric structure with two structurally similar and functionally distinct subunits. The major structural difference between α and β subunits of bacterial luciferase is a flexible loop which only located between β7-α7 loop of α subunit. This flexible loop is essential to substrate binding and conformational changes in the bacterial luciferase reaction. Interestingly, a flexible loop was observed between β7-α7 loop of SsuD monomer structure. Initial cloning of SsuD led to an abherrent mutantion of Arg297 on

the flexible loop of SsuD that abolished catalytic activity [73]. The roles of the conserved amino acids at the putative active site of SsuD are currently being investigated.

1.4 Summary

Flavoprotein monooxygenases, which are widely distributed in mammals, plants, and bacteria, are able to catalyze a variety of mechanistic reactions. Substrates of flavoprotein monooxygenase are typically aromatic compounds or chemicals containing heteroatoms, which are very stable in nature and are difficult to oxygenate. In mammals, there are five groups of FMOs (1-5) distributed in different tissues. They play essential roles in xenobiotic metabolism, especially in detoxication. There are more FMO-like genes identified in plants than mammals; more interestingly, FMOs from plants are also involved in the biosynthesis of plant hormones and other metabolins, and some plant FMOs may also play roles in gene defense. FMOs are also widely distributed in bacteria and are essential in bacterial detoxification, biodegradation, and biosynthesis. A number of two-component flavin-dependent monooxygenases have also been identified in bacteria along with the single-component flavoprotein monooxygenases. All two-component monooxygenases are composed of a flavin reductase and a flavin-dependent monooxygenase. Flavin reduction and substrate oxygenation are performed by two separate enzymes. The flavins are reduced by the reductase then transferred to the monooxygenase. These two-component flavin-dependent monooxygenases are divided into two subclasses: $FMNH_2$-dependent monooxygenases

(Class C) and FADH$_2$-dependent monooxygenases (Class D). All structures of known Class C monooxygenases show a TIM barrel structure; however, the structures of Class D monooxygenases are diverse. The alkanesulfonate monooxygenase (SsuD) belongs to Class C, the FMNH$_2$-dependent monooxygenases. Considering the instability of reduced flavin in the presence of dioxygen, two flavin transfer mechanisms have been proposed: channeling and dissociative. Each transfer mechanism has been demonstrated depending on the system under study.

Even though flavoprotein monooxygenases are diverse in their substrate specificity, structural assembly, and biological functions, the overall catalytic mechanisms are similar. All reactions catalyzed by flavoprotein monooxygenases include a reductive and an oxidative reaction. Flavin is reduced by coenzyme NAD(P)H, and the reduced flavin activates dioxygen to form a enzyme-bound C4a-(hydro)peroxyflavin, which serves as a oxygenating agent to directly insert an oxygen atom into the substrate. Both protonated (FlOOH) and deprotonated (FlOO$^-$) are able to oxidize substrates. FlOOH is usually involved in the oxygenation of aromatic substrates as an electrophilic agent; while FlOO$^-$ acts as a nucleophilic agent to attack chemicals containing heteroatoms. Compared to other flavoproteins and free reduced flavin, the C4a-(hydro)peroxyflavin of flavoprotein monooxygenases is relatively stable. Structurally, a hydrophobic cavity is required to prevent this hydroperoxyflavin intermediate from solvent decomposition.

The two-component alkanesulfonate monooxygenase system is able to desulfonate a wide range of alkanesulfonate compounds. Working along with other Ssi proteins, the

alkanesulfonate monooxygenase system helps *E.coli* utilize aliphatic sulfonates as a alternative source of sulfur. Previous studies show that the reduction of flavin by SsuE proceeds through the formation of two charge transfer intermediates, which is similar to reductases with a tightly bound flavin prosthetic group. The flavin is transferred from SsuE to SsuD by a direct channeling mechanism based on kinetic analyses and the detection of protein-protein interactions between SsuE-SsuD. However, the catalytic mechanism of SsuD is still not clear. In the following chapters, the catalytic mechanism of SsuD will be probed and discussed.

CHAPTER TWO

CATALYTIC IMPORTANCE OF THE SUBSTRATE BINDING ORDER FOR THE FMN-DEPENRENT ALKANESULFONATE MONOXYGENASE ENZYME

2.1 INTRODUCTION

In *Escherichia coli,* sulfur is typically acquired from inorganic sulfate and assimilated through the cysteine biosynthetic pathway [*81, 74-75*]. Alternative sulfur sources including organic sulfonate and sulfate esters are utilized when inorganic sulfate is limiting in the environment. Sulfate limitation induces specific proteins that enable the organism to acquire and metabolize these alternative sulfur sources. Proteins produced from the *ssu* operon are involved in the uptake and desulfonation of alkanesulfonates in the environment. In addition to an ABC-type transporter, a two-component protein system is required for sulfur acquisition [*73*]. The NAD(P)H[1]-dependent FMN reductase (SsuE) catalyzes the reduction of FMN by NAD(P)H followed by the transfer of reduced flavin to the monooxygenase (SsuD), which catalyzes the oxygenolytic cleavage of alkanesulfonate to aldehyde and sulfite (Scheme 2.1) [*73*]. The released sulfite is reduced and assimilated into sulfur-containing compounds.
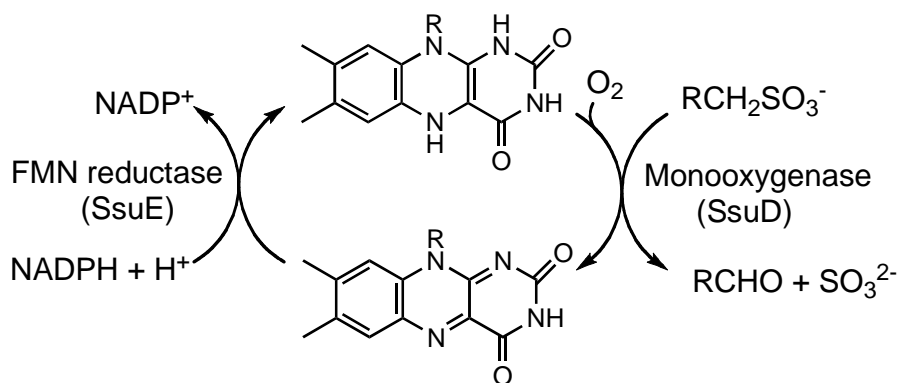
Scheme 2.1 Reaction mechanism of the alkanesulfonate monooxygenase system

Several bacterial flavin reductases associated with two-component systems have been kinetically evaluated [*79-85*]. Although SsuE shares little sequence identity with other flavin reductases, the mechanism of flavin reduction is similar. In steady-state kinetic assays, the results have shown that SsuE follows an ordered sequential mechanism, with NADPH as the first substrate to bind and $NADP^+$ as the last product to dissociate. Reduction of the flavin by NADPH leads to immediate transfer from SsuE to SsuD. While the steady-state kinetic parameters of the system were not significantly altered in the presence of SsuD and octanesulfonate, the kinetic mechanism of SsuE is altered to a rapid equilibrium ordered mechanism. These results suggested that protein-protein interactions are relevant to flavin transfer [*79*]. Results from rapid reaction kinetic studies of flavin reduction by SsuE identified the formation of charge-transfer intermediates between the pyridine nucleotide and flavin substrate [*86*]. Therefore, the mechanism of flavin reduction involving formation of charge-transfer complexes is similar to standard flavoproteins. Additional studies have been performed to better understand the mechanism of reduced flavin transfer between SsuE and SsuD [*86*].

Stable protein-protein interactions were identified between the alkanesulfonate monooxygenase proteins through affinity chromatography and spectroscopic analyses. These studies further support a model involving direct flavin transfer from the reductase to the monooxygenase enzyme.

While the flavin reductase belonging to the alkanesulfonate monooxygenase system has been well characterized, much less is known about the catalytic mechanism of the monooxygenase component. The reaction mechanism of SsuD involves the oxygenolytic cleavage of the carbon-sulfur bond of alkanesulfonates. The α-ketoglutarate-dependent taurine dioxygenase from *Escherichia coli* is another enzyme that utilizes primary aliphatic sulfonates as sulfur sources [*77*]. The mechanism involved for sulfur acquisition by taurine dioxygenase is notably different from the alkanesulfonate monooxygenase system. Taurine dioxygenase utilizes α–ketoglutarate and an iron center to activate O_2 for cleavage of the carbon-sulfur bond, while the alkanesulfonate monooxygenase relies on a reduced flavin for dioxygen activation [*73*]. The SsuD enzyme was previously shown to catalyze the desulfonation of a wide range of alkanesulfonate substrates, and this catalysis was dependent on reduced flavin and dioxygen [*73*]. Comparison of the amino acid sequence identity of SsuD with other two-component monooxygenase enzymes is low; however SsuD is structurally related to bacterial luciferase [*60, 68, 87*]. Specifically, there are several conserved and spatially similar active site residues common to each protein. The catalytic role for several of these residues has been determined in bacterial luciferase, however their corresponding role in the desulfonation reaction by SsuD remains to be elucidated [*64-66, 70, 88-89*].

While the initial characterization of SsuD has been performed, the detailed

mechanism of sulfur acquisition by this enzyme has not been fully explored [*73*]. A C4a-(hydro)peroxyflavin intermediate is proposed to be the reactive O_2 species for SsuD and other monooxygenase components belonging to these systems [*2, 61, 90-92*]. Several groups have identified the formation of a flavin adduct when the monooxygenase enzyme is mixed with reduced flavin in the presence of oxygen. Detailed presteady state kinetic analysis of aromatic hydroxylation by *p*-hydroxyphenylacetate 3-hydroxylase has provided valuable insight into the mechanism of hydroxylation [*71,91*]. The desulfonation of alkanesulfonates by SsuD likely involves the formation of a C(4a)-(hydro)peroxyflavin intermediate similar to *p*-hydroxyphenylacetate 3-hydroxylase, however the kinetic mechanism may be more closely related to bacterial luciferase given their structural and catalytic similarities. Presteady state evaluation of the SsuD reaction has been performed, and a mechanism for sulfur acquisition and substrate binding is described in these studies.

2.2 MATERIAL & METHODS

2.2.1 Materials.

FMN, NADPH, EDTA, potassium phosphate (monobasic anhydrous and dibasic anhydrous), sodium chloride, sodium hydrosulfite (dithionite), and 5,5-dithiobis(2-nitrobenzoic acid) (DTNB), glucose, glucose oxidase, and urea were from Sigma (St. Louis, MO). Glycerol was purchased from Fisher (Pittsburgh, PA). Standard buffer contains 25 mM potassium phosphate, pH 7.5, and 10% glycerol unless otherwise noted. SsuD and SsuE enzymes were expressed and purified as previously described [79]. The concentrations of SsuD and SsuE proteins were determined from A_{280} measurements using a molar extinction coefficient of 47.9 $mM^{-1}cm^{-1}$ and 20.3 $mM^{-1}cm^{-1}$, respectively.

2.2.2 Binding ratio of reduced flavin to SsuD

The binding ratio of $FMNH_2$ by SsuD was measured by the method of Hummel and Dreyer [100-101]. A FPLC system (Biorad) was used for the analysis. A Sephadex G-25 column (1.6×2.5 cm) was equilibrated with 25 mM potassium phosphate buffer, pH 7.5, containing $FMNH_2$ (10 μM, reduced with dithionite). Samples containing SsuD (9 μM) and various concentrations of $FMNH_2$ (0-18 μM) were injected into the column at a rate of 0.5 ml/min, and the protein eluted from the column with equilibration buffer. The flavin concentration was determined by measuring the absorbance at 450 nm after the flavin in all samples had been completely reoxidized. The absorbance at 450 nm was plotted against the fraction number. The area of the second peak (free flavin) varies linearly with increasing flavin concentrations in the sample over the quantity contained in the elute buffer. The X-intercept corresponds to the quantity of flavin bound by the

protein.

2.2.3 Reduced flavin binding.

Reduced flavin binding to SsuD and SsuE was measured by spectrofluorimetric titration using a similar method described for oxidized flavin [*74*]. Spectra were recorded on a Perkin Elmer LS 55 luminescence spectrometer (Palo Alto, CA) with an excitation wavelength at 280 nm and an emission wavelength of 344 nm. Anaerobic SsuD or SsuE enzyme solutions were prepared in a glass titration cuvette by at least 15 cycles of evacuation followed by equilibration with ultra high purity argon gas. Glucose (20 mM) and glucose oxidase (10 units) were added to remove trace amounts of dioxygen. Flavin prepared in standard buffer was added to an air-tight titrating syringe with an oxygen-scrubbing system of glucose (20 mM) and glucose oxidase (10 units). The syringe was incubated in an anaerobic glove-box for 20 min to remove O_2. The anaerobic FMN solution was photoreduced by irradiation for 30 min in the presence of EDTA (10 mM), and the titration apparatus was assembled in the anaerobic glove-box.

For the titration of SsuD with reduced flavin, a 1 mL solution of SsuD (0.5 μM) in standard buffer was titrated with reduced flavin (0.16-7.8 μM) and the fluorescence spectra recorded following a two min incubation after each addition. The titration of SsuE (0.5 μM) with reduced flavin was performed as described for SsuD, however the reduced flavin concentration used for the titration ranged from 0.5-97.0 μM. Bound $FMNH_2$ was determined using the following equation [*93*]:

$$[S]_{bound} = [E]\frac{(I_0 - I_c)}{(I_0 - I_f)}$$
(2.1)

Where $[S]_{bound}$ represents the concentration of enzyme bound substrate. [E] represents the

initial concentration of enzyme, I_0 is the initial fluorescence intensity of enzyme prior to the addition of substrate, I_c is the fluorescence intensity of enzyme following each addition, and I_f is the final fluorescence intensity. The concentration of FMNH$_2$ bound was plotted against the free substrate to obtain the dissociation constant (K_d) according to Eq. 2.2.

$$Y = \frac{B_{\max} X}{K_d + X} \tag{2.2}$$

Y and X represent the concentration of bound and free substrate, respectively, following each addition. $B_{\max}$ is the maximum binding at equilibrium with the maximum concentration of substrate. K_d is the dissociation constant for the substrate.

2.2.4 Octanesulfonate binding.

Octanesulfonate binding to SsuD or the SsuD-FMNH$_2$ complex were performed by similar spectrofluorimetric methods used in the flavin binding experiments. A 1 mL solution of SsuD (1 μM), either alone or with reduced flavin (2 μM), was made anaerobic in a glass titration cuvette as described. Aliquots of octanesulfonate (2.7-54 μM or 2.7-108 μM) in an air-tight titrating syringe were added to SsuD or the SsuD-FMNH$_2$ complex. The fluorescence spectra were recorded with an excitation wavelength at 280 nm and emission intensity measurements at 344 nm following a two min incubation. The concentration of bound octanesulfonate was determined by Eq. 1, and plotted against the concentration of free octanesulfonate to determine the dissociation constant (K_d) according to Eq. 2.2.

2.2.5 Rapid reaction kinetic analyses.

Stopped-flow kinetic analyses were carried out on a thermostatted Applied

Photophysics SX. 18 MV stopped-flow spectrophotometer. The stopped-flow instrument was made anaerobic by filling with an O_2 scavenging system containing 25 mM phosphate buffer, pH 7.5, 10% glycerol, 100 mM NaCl with 20 mM glucose and 10 units of glucose oxidase in the inner system and drive syringe. The oxygen-scrubbing solutions were allowed to stand in the system overnight and were thoroughly rinsed with anaerobic standard buffer prior to performing the experiments. All reactions were carried out in standard buffer at 4°C. Alternate mixing of the enzyme and substrates were performed in these studies, however all experiments contained 45 µM SsuD and 15 µM $FMNH_2$. The $FMNH_2$ solutions were made anaerobic in a glass tonometer and then photoreduced by irradiation for 30 min in the presence of EDTA (10 mM). The O_2 concentration remained constant at 210 µM (air-saturated buffer), or when evaluating the O_2 dependence was varied from 0.1-1.0 mM. The O_2 concentrations were determined on a Hansatech oxygen electrode (Norfolk, UK). The O_2-saturated buffer in experiments monitoring dioxygen dependence was prepared by bubbling 100% O_2 in standard buffer for 30 min in an air-tight syringe. Solutions containing different concentrations of O_2 were prepared by mixing different volumes of O_2-saturated buffer with anaerobic buffer solutions. When included in the reaction, the octanesulfonate concentration was constant (100 or 200 µM), or when monitoring the octanesulfonate dependence varied from 0.5-1.0 mM. All experiments were carried out in single-mixing mode by mixing equal volumes of the various solutions, and monitored by single wavelength analyses at 370 and 450 nm.

2.2.6 Activity assay.

SsuD activity was assayed based on a previously described method with some modifications [73]. Reactions were initiated by the addition of NADPH (500 µM) into a

reaction mixture containing SsuD (0.2 μM), SsuE (0.6 μM), FMN (1 μM), and a range of octanesulfonate concentrations (5-2000 μM) in standard buffer with 100 mM NaCl at 25 ˚C. After a three min incubation, the reaction was stopped by the addition of urea (2.0 M), and DTNB (1 mM) was added to a 200 μl aliquot of the reaction solution. The colorimetric reaction was allowed to develop at room temperature for two min, and the absorbance measured at 412 nm using a molar extinction coefficient for the TNB anion of 14.1 $mM^{-1}cm^{-1}$.

An assay was also developed to compare the formation of aldehyde product using alternate mixing of reaction components, analogous to reactions carried out in the stopped-flow instrument. The contents of syringe A and B are shown in Table 2.2, and all reactions were performed in 25 mM potassium phosphate buffer, pH 7.5, 25 ˚C. Solutions in syringe A always contained the flavin substrate either in the presence or absence of SsuD and the octanesulfonate substrate. Reduced flavin was prepared in an air-tight syringe with an O_2-scrubbing system containing glucose (20 mM) and glucose oxidase (10 units). Syringe A was incubated in an anaerobic glove-box for 20 min to remove O_2, and the flavin was photoreduced in the presence of EDTA (10 mM). The solution in syringe A was then mixed with the solution in syringe B to give a total volume of 1 mL. The reaction mixture was incubated at 25 ˚C for five min, and 1 mL methylene chloride was added to extract the octanal product from the reaction solution. A standard curve was generated with a range of octanal concentrations (1-20 μM) in 1 mL methylene chloride, and 50 μM pentadecane added as the internal standard (retention time: 15.9 min). The methylene chloride extract solution was analyzed on a Shimadzu gas chromatograph G-15A equipped with a flame ionization detector. A 1 μL sample was chromatographed

71

on a 300× 0.25 cm HP-1 (crosslinked methyl silicone gum) column with nitrogen at 180 ˚C, and the detector temperature at 250 ˚C.

2.2.7 Data analysis.

Initial analyses of the single wavelength stopped-flow traces at 380 and 450 nm were performed with the PROKIN software (Applied Photophysics, Ltd.) installed on the stopped-flow spectrophotometer. Global analysis was applied to discern the steps involved in flavin oxidation. A two- or three-step sequential reversible model was adopted during the fitting, and the kinetic traces were resolved into two or three distinct phases depending on the wavelength evaluated. All single wavelength traces at 370 and 450 nm were imported and fitted with Kaleidagraph software (Abelbeck Software, Reading, PA). The single-wavelength traces were fitted to a double or triple exponential using the following equations:

$$A = A_1 \exp(-k_1 t) + A_2 \exp(-k_2 t) + C \tag{2.3}$$

$$A = A_1 \exp(-k_1 t) + A_2 \exp(k_2 t) + A_3 \exp(-k_3 t) + C \tag{2.4}$$

where k_1 k_2, and k_3 are the apparent rate constants, A is the absorbance at time t, A_1, A_2, A_3 are amplitudes of each phase, and C is the absorbance at the end of the reaction.

The data for the concentration dependence of octanesulfonate on k_1 were fitted with a simplified hyperbolic equation:

$$k_{obs} = k_{lim}[S]/k_d + [S] \tag{2.5}$$

where k_{obs} is the observed rate constant, k_{lim} is the limiting rate constant for flavin reduction, K_d is the dissociation constant for the enzyme-substrate complex, and S is the substrate concentration.

2.3 RESULTS

2.3.1 Binding ratio of SsuD and reduced flavin

The binding of $FMNH_2$ to SsuD was initially measured by the Hummel-Dreyer method [*100-101*]. A Hitrap^{TM} Sephadex G-25 column (1.6 × 2.5 cm) was pre-equilibrated with 25 mM potassium phosphate buffer, pH 7.5, containing $FMNH_2$. Samples of SsuD at varying $FMNH_2$ concentrations were injected into the pre-equilibriated column, and eluted with a buffer containing the same $FMNH_2$ concentration as equilibrium buffer. As shown in Figure 2.1A, two flavin peaks were generated. The first peak represents the protein-bound flavin, and the second peak was a negative peak due to the deficit of free reduced favin bound by SsuD. When the $FMNH_2$ concentration of the injected sample was higher than the elute buffer (10 µM), positive peaks were observed at the retention time of free flavin. Negative peaks were also observed at the same retention time if the $FMNH_2$ concentration of the injected sample was lower than elute buffer (10 µM). The area of the second peak of $FMNH_2$ varies linearly with the excess of $FMNH_2$ in the injected sample over the quantity contained in the elute buffer (Figure 2.1B). The X-intercept with the x-axis corresponds to the quantity of $FMNH_2$ bound by the protein. Our results showed 9 µM SsuD monomer could bind about 9.5 µM $FMNH_2$ with an approximate 1:1 binding ratio.

73
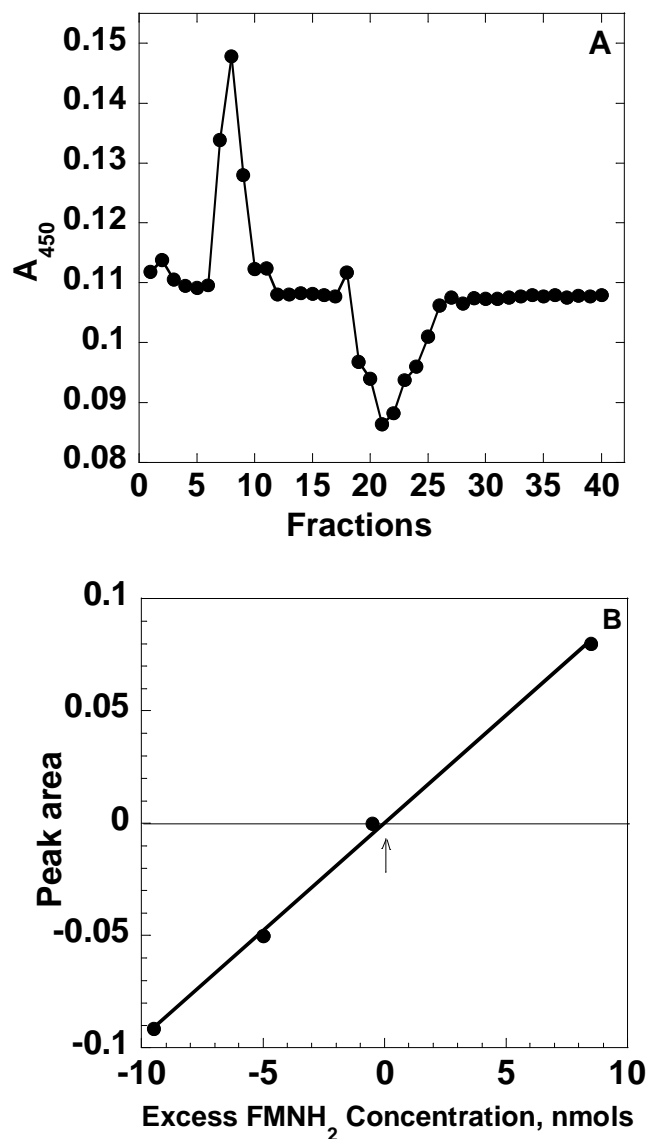
Figure 2.1. FMNH₂ binding measurements by gel filtration chromatography. A. Chromatographic profile. Column: Hitrap^{TM} Sephadex G-25 column (1.6×2.5 cm). Eluent: 25 mM patossium phosphate Buffer, pH 7.5, 10% glycerol, 10 µM FMNH₂, 1mg/mL dithionite. Sample: 9 µM SsuD, 0.5 mL. B. peak area of FMNH₂ plotted against excess FMNH₂. The arrow indicates the quantity of FMNH₂ bound by SsuD. 9 µM SsuD can bind 9.5 µM FMNH₂. FMNH₂ binds to SsuD with a 1:1 stoichiometry.

2.3.2 Reduced flavin binding

Previous studies have shown that each protein in the two-component monooxygenase family has a specific affinity for the oxidized or reduced form of the flavin [*79*]. The dissociation constants for the binding of reduced flavin to SsuE and SsuD were determined by fluorimetric titrations. The decrease in the intrinsic protein fluorescence emission intensity due to the binding of $FMNH_2$ was monitored at 344 nm for each protein. The concentration of bound and free $FMNH_2$ was calculated according to Eq. 2.1, and the concentration of flavin bound to each enzyme was plotted against the concentration of free $FMNH_2$ added with each aliquot (Figure 2.2). The dissociation constants for FMN and $FMNH_2$ binding to each alkanesulfonate monooxygenase enzyme are summarized in Table 2.1. The average K_d value for $FMNH_2$ binding to SsuD was 0.32 $\pm$ 0.15 µM with a binding stoichiometry of one reduced flavin bound per SsuD monomer. A similar binding ratio was also obtained by equilibrium gel filtration. The average K_d value for $FMNH_2$ binding to SsuE was 15.5 $\pm$ 1.3 µM. As a substrate of SsuE and product of SsuD, the K_d for oxidized flavin binding to each alkanesulfonate monooxygenase enzyme was previously determined by similar fluorimetric titration methods described for reduced flavin. The dissociation constants for FMN binding to SsuE and SsuD were 0.015 $\pm$ 0.004 µM and 10.2 $\pm$ 0.4 µM, respectively (*5*). These results show that SsuE has a higher affinity for oxidized FMN, while SsuD has a higher affinity for reduced flavin. These contrasting affinities ensure that once SsuE reduces the flavin, it is immediately released and transferred to SsuD.
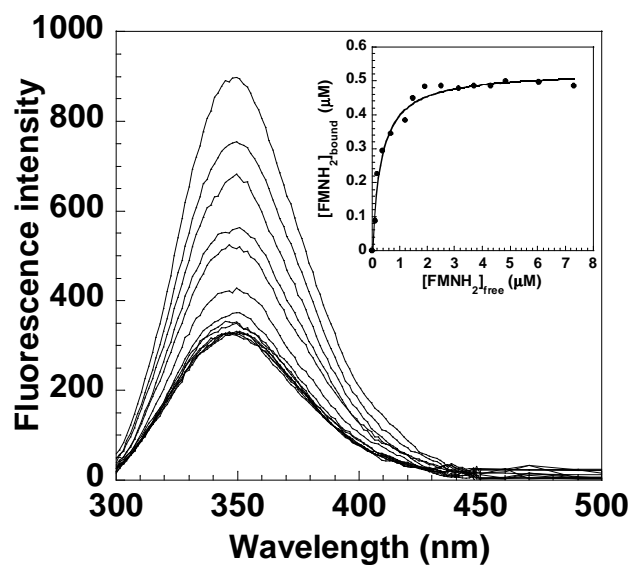
Figure 2.2. Fluorimetric titration of the alkanesulfonate monooxygenase with $FMNH_2$. The SsuD enzyme (0.5 µM) was titrated with $FMNH_2$ (0.16-7.8 µM). Emission intensity measurements at 344 nm were measured using an excitation wavelength at 280 nm. The change in fluorescence of the SsuD enzyme following the addition of $FMNH_2$ was converted to the estimated concentration of bound $FMNH_2$ (Eq. 2.1) and plotted against the concentration of free $FMNH_2$. Inset: Change in the emission intensity at 344 nm. The solid line represents the fit of the titration curve to Eq. 2.2. Each titration was performed in triplicate.

Table 2.1 Dissociation constants for FMN and $FMNH_2$ binding

	SsuE	SsuD
	μM	μM
FMN[a]	0.015 ± 0.004	10.2 ± 0.4
$FMNH_2$[b]	15.5 ± 1.3	0.32 ± 0.15

[a] Previously reported [5].

[b] Determined under anaerobic conditions as described in *Materials & Methods*.

2.3.3 Kinetic studies of flavin oxidation by SsuD

The short half-life of reduced flavin in the presence of dioxygen often makes it difficult to assay the activity of the monooxygenase in the absence of the flavin reductase for the two-component monooxygenase enzymes. However, stopped-flow kinetic analyses have been used successfully to probe the kinetic mechanism of these monooxygenases from the flavin-dependent two-enzyme systems [*57, 91-92, 94-96*]. Stopped-flow kinetic studies in the absence of alkanesulfonate were performed to monitor the oxidation of $FMNH_2$-bound SsuD at 370 and 450 nm. The formation of the C4a-(hydro)peroxyflavin by SsuD should be observed in a step prior to conversion of the flavin to the oxidized form in the kinetic traces obtained at 370 nm. Single-wavelength kinetic traces were also obtained for the reaction of free $FMNH_2$ with air-saturated buffer in the absence of SsuD (data not shown). The oxidation of free $FMNH_2$ was best fit to a double-exponential equation with rates of 2.20 s^{-1} (k_1), 1.19 s^{-1} (k_2) at 370 nm and 2.04 s^{-1} (k_1), 1.43 s^{-1} (k_2) at 450 nm, respectively. For the oxidation of $FMNH_2$-bound SsuD, a higher concentration of SsuD (45 µM) was used relative to $FMNH_2$ (15 µM) to ensure that the enzyme-catalyzed oxidation of reduced flavin was monitored. Under these conditions, the kinetic traces at both wavelengths increased at almost identical rates in two distinct phases at 370 and 450 nm. These kinetic traces were best fit to a double-exponential equation with rates of 0.43 s^{-1} (k_1), and 0.15 s^{-1} (k_2) at 370 nm and 0.50 s^{-1} (k_1), and 0.16 s^{-1} (k_2) at 450 nm (Figure 2.3A). The rate of oxidation for $FMNH_2$-bound SsuD at both wavelengths was significantly slower than the oxidation of free $FMNH_2$. There was no direct evidence for the formation of a stabilized C4a-(hydro)peroxyflavin intermediate generated during flavin oxidation by SsuD under

78
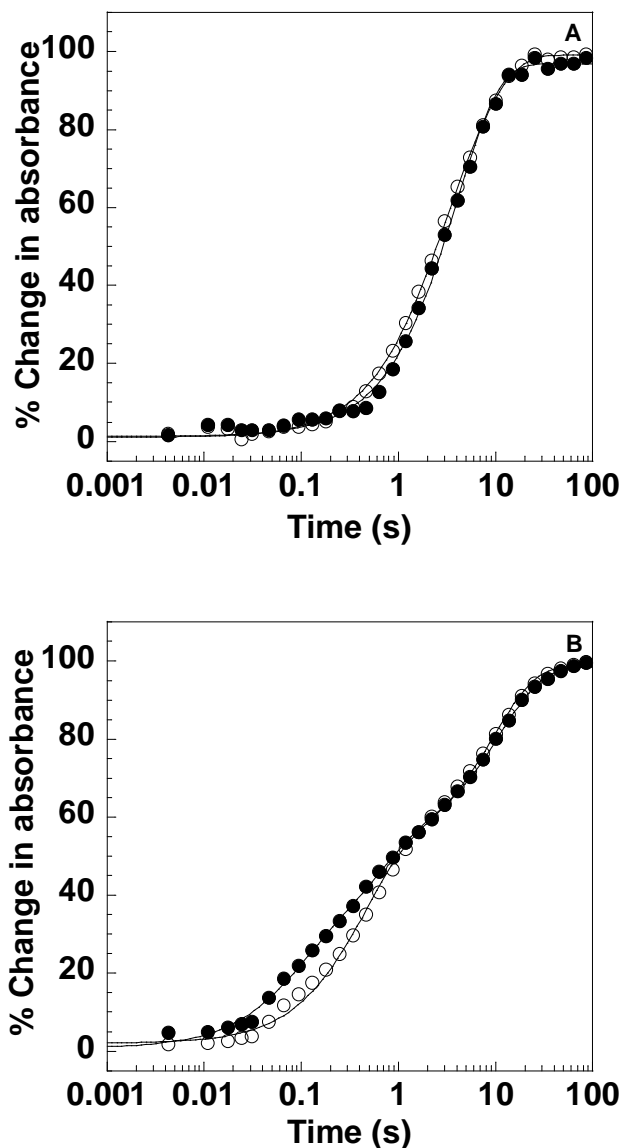
Figure 2.3. The kinetics of flavin oxidation by SsuD with alternate mixing of $FMNH_2$ and O_2 in the absence of octanesulfonate. A: Premixed SsuD-$FMNH_2$ (SsuD: 45 μM, $FMNH_2$ 15 μM) was mixed with air-saturated buffer. Kinetic traces of flavin oxidation were monitored at 370 (●) and 450 nm (○). B: Free $FMNH_2$ solution was mixed with SsuD (45 μM) in air-saturated buffer. Kinetic traces of flavin oxidation were monitored at 370 (●) and 450 nm (○).

these conditions. The two phases observed in the kinetic traces can be attributed to flavin oxidation.

Additional stopped-flow kinetic experiments were conducted to obtain information on the binding and oxidation of $FMNH_2$ by SsuD. When $FMNH_2$ was mixed with SsuD in air-saturated buffer, the kinetic traces were significantly altered from the oxidation of pre-mixed SsuD and $FMNH_2$ (Figure 2.3B). An initial fast phase was now observed in the reaction at 370 nm that was best fit to a triple-exponential equation with rates of 12.9 s^{-1} (k_1), 0.95 s^{-1} (k_2), and 0.08 s^{-1} (k_3), while the kinetic trace at 450 nm was best fit to a double-exponential equation with rates of 1.3 s^{-1} (k_1), and 0.09 s^{-1} (k_2). The increase at 370 nm should be correlated with the C4a-(hydro)peroxyflavin, and implies that the flavin adduct is only observed when reduced flavin and SsuD are not premixed. To determine if the fast phase is dependent on dioxygen, free $FMNH_2$ was mixed with SsuD at varying O_2 concentrations at 370 nm. Interestingly, the rate constant for the first phase was not dependent on increasing O_2 concentrations. The lack of an effect on the fast phase with varied O_2 concentrations may indicate that a slow binding or conformational step masks this dependence, or that the phase represents a step unrelated to formation of the C4a-(hydro)peroxyflavin.

2.3.4 Kinetic parameters for octanesulfonate

The steady-state kinetic parameters for SsuD were determined by measuring the amount of TNB anion formed at 412 nm from the reaction of the sulfite product with DTNB. The SsuE enzyme was included in the reaction to provide reduced flavin to the monooxygenase enzyme, and was in excess relative to SsuD so reduced flavin would not be limiting in the reaction. there was no measurable amount of TNB anion produced
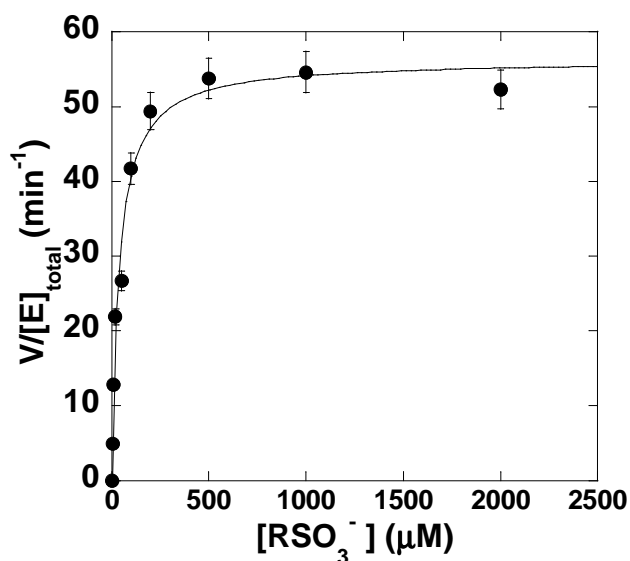
Figure 2.4 Initial velocities of SsuD with octanesulfonate. SsuD activity was measured by a modified SsuE-SsuD couple enzyme assay as reported [73]. Reactions was initiated by the addition of NADPH (500 µM) into a reaction mixture containing SsuD (0.2 µM), SsuE (0.6 µM) and a range of octanesulfonate concentrations (0.05-2 mM) in standard buffer at 25 ˚C. The reactions were stopped by the addition of Urea (2 M) and DTNB was added to reaction solution. After 2 mins colorimetric reaction, the absorbance was measured at 412 nm using a molar extinction coefficient for the TNB anion of 14.1 mM^{-1} cm^{-1}.

Table 2.2 Kinetic parameters for octanesulfonate of SsuD

Kinetic parameters	k$_{cat}$ (min^{-1})	K$_m$ (µM·min^{-1})
SsuD	56.2 $\pm$ 3.3	34.2 $\pm$ 5.8

due to side reactions with protein thiols. The K_m and k_{cat} values for octanesulfonate were 34.2 ± 5.8 µM and 56.2 ± 3.3 min^{-1}, respectively (Figure 2.4, & Table 2.2). The value for the catalytic efficiency (k_{cat}/K_m) of the enzyme with octanesulfonate was 1.65 ± 0.22 µM^{-1} min^{-1}.

Octanesulfonate was also used to determine the binding affinity of the alkanesulfonate substrate to SsuD. Aliquots of an octanesulfonate solution were added to SsuD under anaerobic conditions, however there was no observable change in the intrinsic protein fluorescence at an emission wavelength of 344 nm (Figure 2.5A). These results suggest that octanesulfonate is not able to bind directly to SsuD. Ordered binding of the alkanesulfonate substrate to SsuD site may be contingent upon the binding of other substrates required for catalysis. The binding of octanesulfonate to the SsuD-FMNH$_2$ complex was evaluated under anaerobic conditions to determine if flavin-bound SsuD promotes the binding of octanesulfonate. To ensure that all SsuD was bound to FMNH$_2$, a 2:1 ratio of FMNH$_2$ to SsuD was used in these studies. The addition of octanesulfonate showed a decrease in the intrinsic fluorescence of the SsuD-FMNH$_2$ complex at an emission wavelength of 344 nm (Fig. 2.5B). The concentration of bound octanesulfonate and free octanesulfonate was calculated according to Eq. 2.1. The concentration of octanesulfonate bound to the SsuD-FMNH$_2$ complex plotted against the concentration of free octanesulfonate after each addition is shown in the inset of Figure 2.5B. The K_d value for octanesulfonate binding to the SsuD-FMNH$_2$ complex was 17.5 ± 0.9 µM with a 1:1 stoichiometric ratio of octanesulfonate to SsuD. These results indicate that the octanesulfonate substrate can bind to SsuD only if FMNH$_2$ is initially bound, and suggests that octanesulfonate binding may be dependent on a conformational
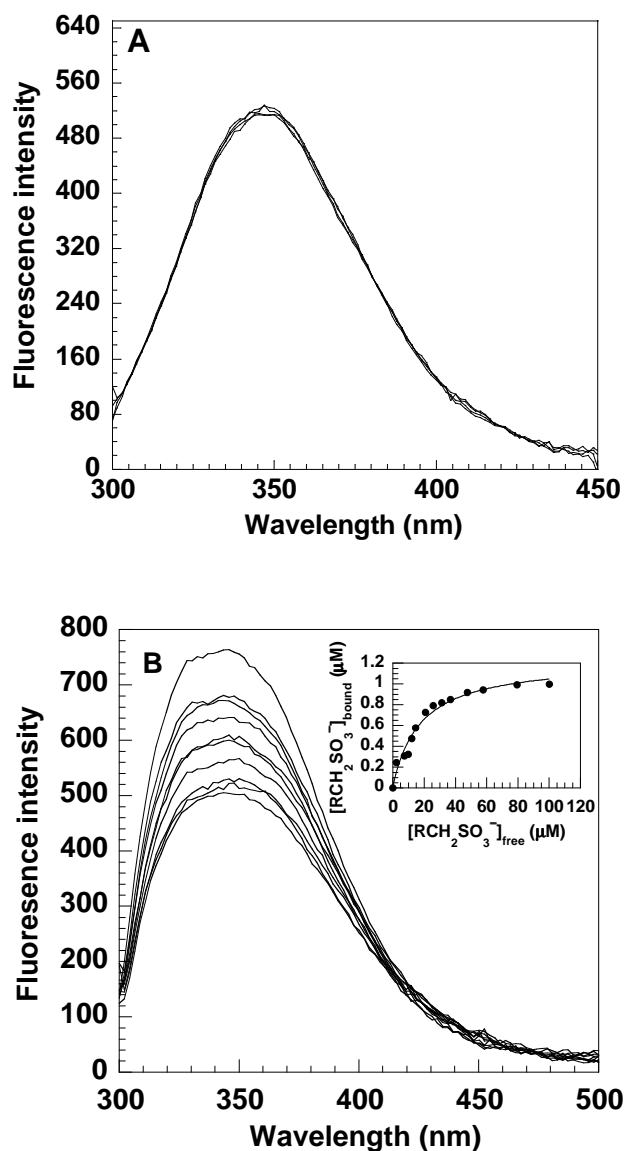
Figure 2.5. Fluorimetric titration of the SsuD enzyme and SsuD-FMNH$_2$ complex with octanesulfonate. A: Titration of SsuD with octanesulfonate in the absence of FMNH$_2$. SsuD enzyme (1 µM) was titrated with octanesulfonate (2.7-54 µM). B: Titration of the SsuD-FMNH$_2$ complex with octanesulfonate. SsuD (1 µM) was premixed with FMNH$_2$ (2 µM), and the complex was titrated with octanesulfonate solution (2.7-108 µM). Inset: Change in the emission intensity at 344 nm.

change induced by FMNH$_2$.

2.3.5 Kinetic studies of flavin oxidation by SsuD in the presence of octanesulfonate

Flavin oxidation by SsuD in the presence of octanesulfonate was investigated through stopped-flow kinetic analyses at 370 and 450 nm mixing free FMNH$_2$ with SsuD and octanesulfonate in air-saturated buffer. At low octanesulfonate concentrations ($\leq$ 100 µM), the kinetic traces at 370 nm were best fit to a triple exponential equation (Figure 2.6). However, as the concentration of octanesulfonate increased the kinetic traces were best fit to a double exponential (data not shown). For the reactions monitored at 370 nm, the k_{obs} for the first (when observed at low octanesulfonate concentrations) and third phase did not vary with the octanesulfonate concentration , while the second phase showed a hyperbolic dependence on the octanesulfonate concentration that was best fit to Eq. 2.4 to give a K_d of 93 µM and a limiting rate constant of 2.4 s^{-1} (Figure 2.6, Inset A). These results are consistent with octanesulfonate binding in two steps. A rapid equilibrium step is involved in the initial binding of octanesulfonate to the enzyme followed by either an irreversible isomerization or chemical step. The chemical step could involve the formation of the C4a-(hydro)peroxyflavin intermediate or carbon-sulfur bond cleavage if O$_2$ reacts with reduced flavin prior to octanesulfonate binding. Kinetic traces recorded at 450 nm under similar experimental conditions were best fit to a double-exponential equation. The k_{obs} for the first phase again displayed a hyperbolic dependence on the octanesulfonate concentration with a K_d of 85 µM and a limiting rate constant of 2.8 s^{-1} (Figure 2.6, Inset B), similar to the kinetic parameters obtained at 370 nm.

A fast initial phase was observed when reduced flavin was mixed with the SsuD at low octanesulfonate concentrations. The observed formation and accumulation of the putative C4a-(hydro)peroxyflavin intermediate may be directly related to increased product formation. To determine if the initial fast phase could be correlated with C4a-(hydro)peroxyflavin formation, a single turnover reaction assay for SsuD, analogous to reactions carried out in the stopped-flow instrument, was developed to directly measure the aldehyde product. Product octanal was measured by GC-FID and figure 2.7 shows the GC-FID chromatography of octanal and the internal standard. The ratios of the octanal peak area at various concentrations (1-20 µM) to 50 µM internal standard are linear relative to the octanal concentration (Figure 2.8). Single-turnover reaction conditions were established to ensure that the oxidation of reduced flavin was directly coupled to product formation. The SsuD enzyme and substrate were mixed in different orders according to Table 2.3. The results from these assays showed that 5.8 µM octanal was produced when $FMNH_2$ was reacted with premixed SsuD and octanesulfonate in air-saturated buffer, a 4-fold increase compared to the reaction of SsuD-$FMNH_2$ mixed with octanesulfonate and air-saturated buffer (1.5 µM octanal). The amount of the octanal produced in each reaction should be directly correlated with the amount of C4a-(hydro)peroxyflavin intermediate observed in each reaction. Therefore, increased formation of the C4a-(hydro)peroxyflavin intermediate occurs when reduced flavin is reacted with premixed SsuD and octanesulfonate in air-saturated buffer.

Figure 2.6. Kinetics of flavin oxidation by SsuD in the presence of octanesulfonate. Experiments were performed by stopped-flow kinetic analysis at 4 °C. Flavin oxidation of free $FMNH_2$ (15 µM) mixed with SsuD (45 µM) and octanesulfonate (50 µM) in air-saturated buffer monitored at 370 (●) and 450 nm (○). Inset A: Octanesulfonate concentration dependence on the k_{obs} for the second phase at 370 nm. Inset B: Octanesulfonate concentration dependence on the k_{obs} for the first phase at 450 nm. The kinetic traces shown are the average of three separate experiments. The solid lines are the fits of the kinetic traces to Eq. 2.3 or 2.4.
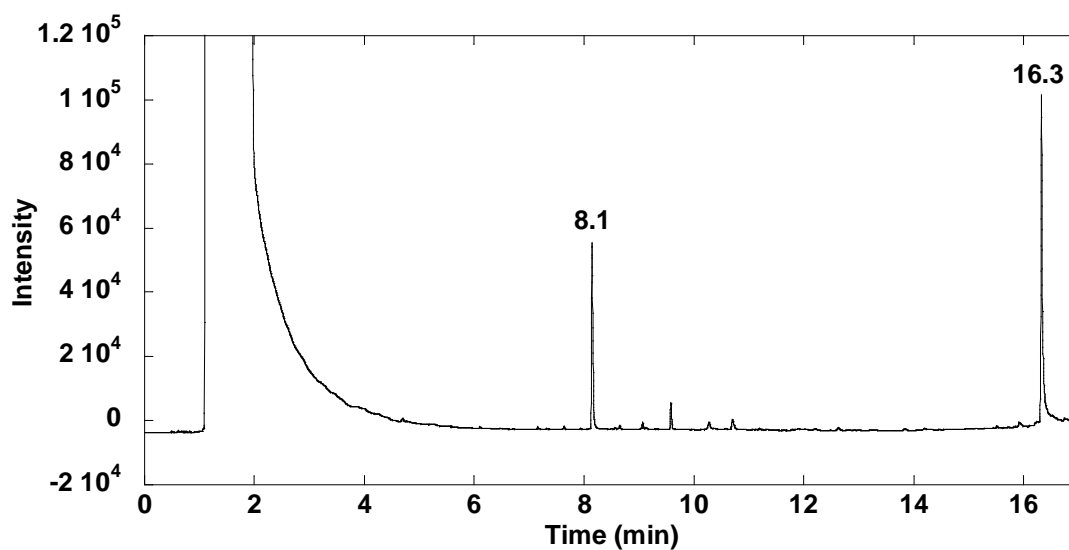
Figure 2.7 Detection of octanal by gas chromatography. The methylene chloride solution containing 20 µM octanal (retention time: 8.1 min) and 50 µM pentadecane (retention time: 16.3 min) was analyzed on a Schimadzu gas chromatograph G-15A equipped with a flame ionization dector. 1 µL sample was chromatographed on a 300 X 0.25 cm HP-1 column (crosslink methyl silicone gum).
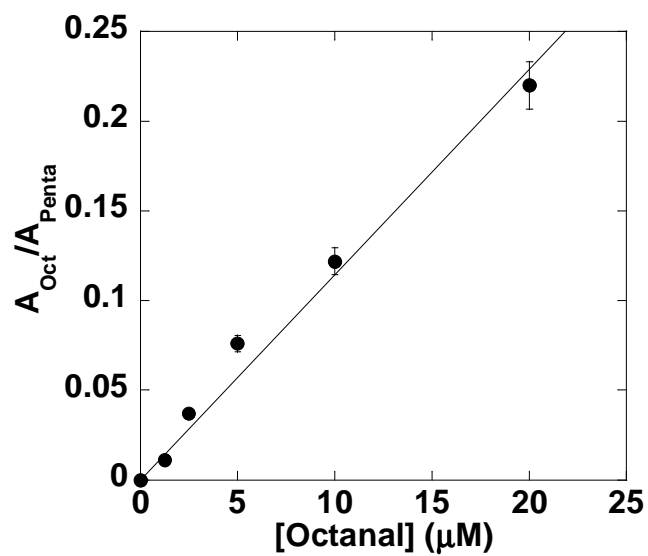
Figure 2.8 Standard line of octanal measurement by GC-FID. A series sample containing various octanal (1-20 µM) and 50 µM pentadecane were analyzed by gas chromatograph. The peak area ratios of octanal and pentadecane were plotted against octanal concentrations giving a lineal dependence on octanal concentrations.

Table 2.3 Determination of octanal product from single turnover reactions of SsuD[a]

Type of reaction	Octanal
Syringe A/Syringe B	*µM*
[FMNH$_2$]/[SsuD, octanesulfonate, O$_2$]	5.8
[SsuD,FMNH$_2$]/[octanesulfonate, O$_2$]	1.5

[a]All reactions were carried out in 25 mM potassium phosphate buffer, pH 7.5, 25 ˚C. The solutions of SsuD (80 µM), FMNH$_2$ (80 µM), octanesulfonate (200 µM) and oxygenated buffer (0.21 mM) were mixed in two air-tight syringes according to the table. The octanal product was extracted as described in *Materials & Mthods* and analyzed by gas chromatography. Under the experimental conditions, the retention time of octanal and pentadecane (internal standard) was 8.1 min and 16.3 min, respectively.

2.3.6 Kinetic studies of flavin oxidation by SsuD with alternate octanesulfonate mixing

The results suggest that the binding of $FMNH_2$ to SsuD induces an isomerization promoting octanesulfonate binding. However, it was not clear if octanesulfonate binding induced a second isomerization step. If there is an isomerization step following binding of the octanesulfonate substrate, then the oxidation of premixed SsuD-$FMNH_2$-octanesulfonate should be faster than that of the SsuD-$FMNH_2$ complex with octanesulfonate and O_2. Figure 5A shows the kinetic traces at 450 nm for two alternate mixing conditions. Two phases were also observed in the reaction of the SsuD-$FMNH_2$-octanesulfonate complex mixed with air-saturated buffer, a fast phase (k_1) followed by a slower phase (k_2). At 200 µM octanesulfonate concentration, the data was best fit to a double-exponential equation with rates of 2.31 s^{-1} (k_1), 0.18 s^{-1} (k_2). The rate of the fast phase (k_1) for the SsuD-$FMNH_2$-octanesulfonate complex reaction with O_2 was approximately 2-fold faster than that of SsuD-$FMNH_2$ complex reaction with octanesulfonate in air-saturateed buffer (1.30 s^{-1}). The rate dependence on octanesulfonate concentration was performed to determine if any of the individual steps were dependent on the alkanesulfonate concentration. Kinetic analyses at 450 nm for the oxidation of the SsuD-$FMNH_2$-octanesulfonate complex at varying octanesulfonate concentrations mixed with air-saturated buffer showed a clear hyperbolic dependence on k_1 (Figure 2.9). A fit of the data gave a K_d value of 37.4 µM and a limiting rate constant of 2.8 s^{-1}. The octanesulfonate-dependent experiments were repeated by mixing the SsuD-$FMNH_2$ complex with increasing amounts of octanesulfonate in air-saturated buffer. The k_{obs} for the first phase also showed a hyperbolic dependence on the octanesulfonate concentration with a K_d value of 100.8 µM and a limiting rate constant of 1.9 s^{-1} (Figure

2.9B). The lower K_d value and higher rate observed with the reaction of the FMNH$_2$-bound SsuD and octansulfonate complex with air-saturated buffer supports the existence of an isomerization step following octanesulfonate binding.
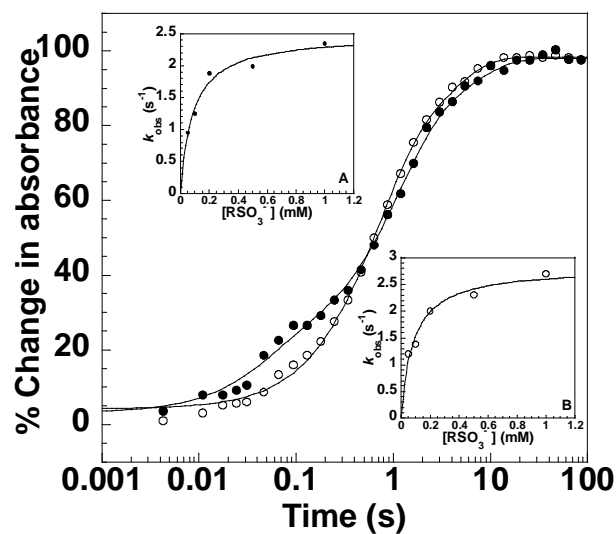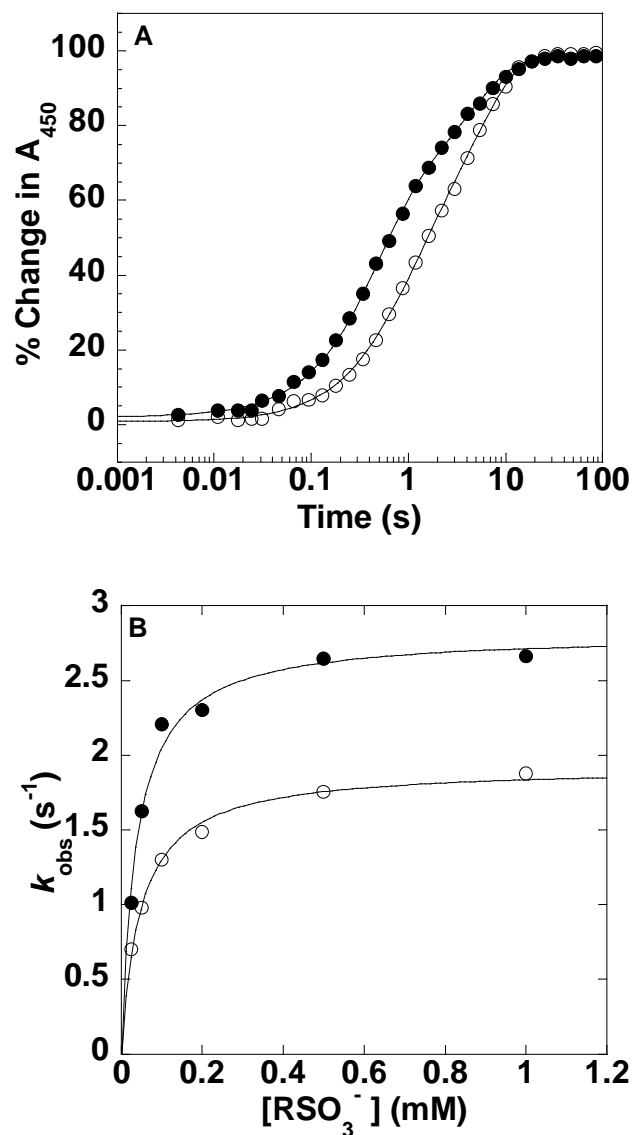
Figure 2.9. Kinetics of flavin oxidation by SsuD with alternate mixing in the presence of octanesulfonate. Experiments were performed by stopped-flow kinetic analyses at 4 ºC. A: Kinetic traces of flavin oxidation at 450 nm. (○) Kinetic trace of SsuD-FMNH$_2$ (SsuD: 45 μM, FMNH$_2$: 15 μM) mixed with octanesulfonate (200 μM) in air-saturated buffer; (●) Kinetic trace of SsuD-FMNH$_2$-octanesulfonate (SsuD: 45 μM, FMNH$_2$: 15 μM,

octanesulfonate: 200 µM) mixed with air-saturated buffer. The kinetic traces shown are the average of three separate experiments. The solid lines are the fits of the kinetic traces to Eq. 2.3. B: Octanesulfonate concentration dependence on the k_{obs} for the first phase at 450 nm. (○) Plot of k_{obs} for the first phase when SsuD-FMNH$_2$ is mixed with varied octanesulfonate solutions. (●) Plot of k_{obs} for the first phase when SsuD-FMNH$_2$-octanesulfonate is mixed with air-saturated buffer. The solid line represents the fit of the curve to Eq. 2.5.

2.4 DISCUSSION

While the kinetic mechanism of the flavin reductase has been extensively studied in the two-component alkanesulfonate monooxygenase system [*79, 80*], the mechanism of the monooxygenase enzyme in this system is still not well understood. The detailed mechanism of SsuD should prove interesting given the unique role of this enzyme in carbon-sulfur bond cleavage. Several groups have shown that rapid reaction kinetic analyses are a valuable tool for probing the reaction mechanism of the two-component monooxygenase enzymes [*57,91-92, 94-96*]. The results from these substrate binding studies and rapid reaction kinetics analyses provide insight into the substrate binding specificity of SsuD, and apparent protein isomerizations relevant to catalysis. Understanding the catalytic mechanism of SsuD is important to further probe the role of this enzyme system in bacterial sulfur acquisition.

Studies focused on determining the affinity of both SsuE and SsuD for $FMNH_2$ were central in establishing the preferred redox form of the flavin for each enzyme. Results from equilibrium gel filtration chromatography and fluorescent titration experiments show that both SsuD and SsuE bind $FMNH_2$ with a 1:1 ratio, which is consistent with the binding stoichiometry of one oxidized FMN to SsuE and SsuD [*79*]. SsuD had a 40-fold lower K_d value than SsuE for $FMNH_2$, while SsuE showed a 600-fold lower K_d value compared to SsuD for FMN (Table 2.1). Based on these results the monooxygenase has a much stronger affinity for $FMNH_2$ than the flavin reductase, while the flavin reductase can bind FMN more tightly than the monooxygenase. The preference of the flavin reductase for FMN and the monooxygenase for $FMNH_2$ is a commonly observed feature

in the two-component monooxygenase family [*71, 90, 93, 97*]. The preference of the flavin reductase and monooxygenase for different redox forms of the flavin appears to play an essential role in flavin transfer between these two enzymes. Previously studies showed that there is a direct interaction between SsuE and SsuD [*86*]. Once the flavin is reduced by SsuE it is directly transferred to SsuD, thereby preventing uncoupling of the desulfonation reaction due to autoxidation of the reduced flavin.

A C4a-(hydro)peroxyflavin is widely accepted as a common intermediate for flavin-dependent monooxygenase reactions [*61, 71, 90-92*]. The flavin-dioxygen adduct can either act as an electrophile or nucleophile depending on the reaction catalyzed. A C4a-(hydro)peroxyflavin is also thought to be the reactive flavin intermediate in the desulfonation of alkanesulfonates by SsuD [*73*]. More specifically, the C4a-peroxyflavin ($Fl–OO^-$) would seem the plausible intermediate in the reaction making a nucleophilic attack on the sulfonate functional group to form an initial alkanesulfonate peroxyflavin intermediate (Scheme 2.2). A Baeyer-Villiger rearrangement of the flavin adduct would lead to the generation of the aldehyde and sufite products. Given the structural similarity of SsuD to bacterial luciferase it was expected that the peroxyflavin would be a highly stable intermediate observable at a range between 300 and 400 nm (*34-37*). However, results from stopped-flow analyses in the absence of the alkanesulfonate substrate show that the order of addition of $FMNH_2$ and O_2 determines whether the formation of the putative C4a-(hydro)peroxyflavin intermediate is easily observed at 370 nm (Figure 2.3). The overall oxidation of pre-mixed $FMNH_2$-bound SsuD is significantly slower than that of free $FMNH_2$. This is likely due to the protected nature of the $FMNH_2$ within the active site of SsuD. The kinetic traces obtained at 370 and 450 nm for the premixed SsuD
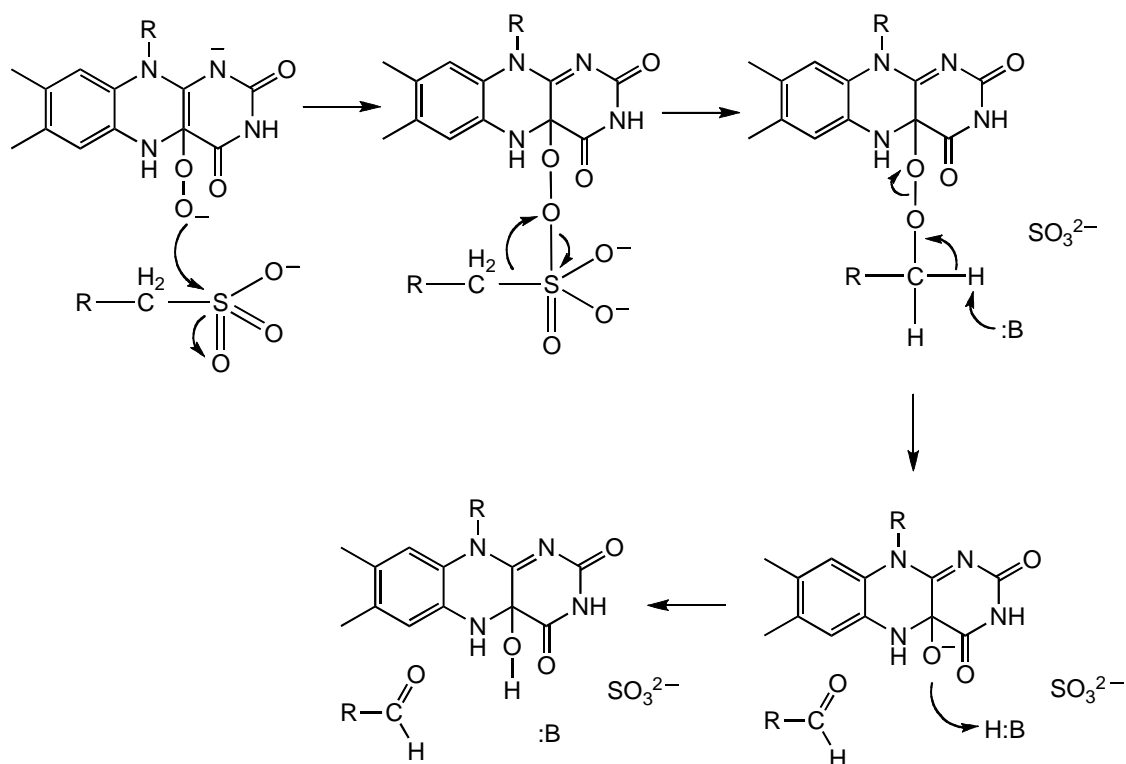
Scheme 2.2. Proposed mechanism of the SsuD desulfonation reaction

solution increased at almost identical rates in two distinct phases with a faster initial

phase (k_1) and a slower second phase (k_2) (Figure 2.3). There was no direct evidence for

the formation of a stabilized C4a-(hydro)peroxyflavin intermediate, and the kinetic traces

observed represent the generation of the FMN. However, when free FMNH$_2$ was mixed

with SsuD in oxygenated buffer, the kinetic traces show a different pattern compared to

the oxidation of premixed SsuD-FMNH$_2$ and free FMNH$_2$ (Figure 2.3). The kinetic trace

now showed three phases, and a new fast phase (k_{obs} at 12 s^{-1}) was observed in the kinetic

traces obtained at 370 nm that was absent from the kinetic traces obtained with premixed SsuD and $FMNH_2$. This fast phase was also absent in the kinetic traces obtained at 450 nm. The rates obtained for the last two phases were similar to the rates obtained with premixed SsuD and $FMNH_2$ (k_1 and k_2), and are assigned to the decay of the flavin intermediate back to the oxidized form. This initial fast phase following mixing of $FMNH_2$ with SsuD in oxygenated buffer may represent a flavin adduct that forms prior to regeneration of FMN. In the absence of octanesulfonate, the probable intermediate is the C4a-(hydro)peroxyflavin. These results suggest that a C4a-(hydro)peroxyflavin intermediate is likely generated in the desulfonation reaction catalyzed by SsuD and the identification of this intermediate is dependent on the order of addition of $FMNH_2$ and O_2 to SsuD. It was expected that the initial fast phase identified in the kinetic trace at 370 nm would be dependent on O_2 concentration, but there was no clear dependence observed. This could be due to a slow binding or conformational step that masks this dependence.

The dependence on the enzyme and substrate mixing order for the observed formation of the C4a-(hydro)peroxyflavin was also reported for the flavin-dependent halogenase RebH [*57*]. A three-form model for binding and complex formation of RebH and $FADH_2$ has been proposed in this enzymatic reaction. An active ternary complex was initially formed that readily reacted with O_2 to form the C4a-(hydro)peroxyflavin intermediate. Under anaerobic conditions, the ternary complex appears to convert to an inactive form that is not immediately reactive with O_2, but can undergo a moderately slow conversion back to the active ternary complex once O_2 is available. This slow conversion back to the active form would not allow the C4a-(hydro)peroxyflavin to accumulate to detectable levels. Double-mixing experiments also provided evidence for

the conversion of the inactive complex to a dead-end complex. For the dead-end complex, $FADH_2$-bound RebH reacts with O_2 to form oxidized flavin with no significant accumulation of C4a-(hydro)peroxyflavin. Similar protein dynamics could be involved in the SsuD reaction, which would explain the lack of accumulated C4a-(hydro)peroxyflavin when SsuD and $FMNH_2$ are premixed. While evidence was obtained for the readily reversible inactive form, double-mixing experiments will need to be performed to fully determine if the ternary dead-end complex is also formed in SsuD. Alternatively, the formation of the C4a-(hydro)peroxyflavin intermediate may form rapidly in SsuD within the dead time of the instrument. When SsuD is mixed with $FMNH_2$ the observed intermediate may be caused by a slower isomerization step that precedes the formation of the C4a-(hydro)peroxyflavin. This would alter the time scale in which the flavin intermediate is formed allowing the C4a-(hydro)peroxyflavin to accumulate.

The stability of C4a-(hydro)peroxyflavin intermediates formed in two-component monooxygenase reactions are quite variable depending on the enzyme under investigation. Strong kinetic evidence supports the formation of a C4a-(hydro)peroxyflavin intermediate in numerous two-component monooxygenase systems [*61, 71, 90-92*]. In luciferase, this intermediate is so stable in the absence of the aldehyde substrate that it was isolated at 4 °C (*23*). Recent structural studies of *p*-hydroxyphenylacetate hydroxylase from *Acinetobacter baumannii* suggest that a hydrophobic cavity lies in front of C4a on the isoalloxazine ring [*62*]. A packed hydrophobic cavity may be required to create a solvent-free environment that prevents rapid breakdown of the unstable flavin intermediate. The C4a-(hydro)peroxyflavin intermediate signal in the SsuD reaction is

weak compared to other two-component monooxygenase enzymes, which implies this intermediate may show decreased stability due to lower hydrophobicity within the SsuD active site. While SsuD shares low amino acid sequence identity with bacterial luciferase, the arrangement of conserved residues within the putative active site are highly similar [*60, 87*]. Therefore, one would expect to observe increased stability of the C4a-(hydro)peroxyflavin in SsuD as seen with bacterial luciferase. Obtaining the structure of SsuD with flavin bound will help to determine the nature of the flavin environment within the active site.

Results from fluorimetric titrations imply that octanesulfonate is not able to bind to SsuD unless $FMNH_2$ is first bound, as there is no observable intrinsic fluorescence intensity change with the addition of octanesulfonate to SsuD. The fluorescence intensity was significantly quenched with the addition of octanesulfonate to the SsuD-$FMNH_2$ complex giving a K_d value of 17.5 µM (Figure 2.5). These results suggest that the alkanesulfonate substrate is not the first substrate that binds to SsuD, and an $FMNH_2$-induced conformational change is necessary to allow octanesulfonate to bind. The addition of substrates to SsuD likely occurs through a partial ordered process initiated by the binding of reduced flavin. An ordered binding mechanism has been demonstrated through kinetic analyses for several two-component monooxygenase enzymes [*57, 71, 95*]. The reduced flavin is always the first substrate to bind, and the subsequent addition of substrates varies depending on the enzyme being evaluated. In bacterial luciferase, the aldehyde substrate can bind before or after reaction of the O_2 with reduced flavin [*95*]. For *p*-hydroxyphenylacetate 3-hydroxylase, the reduced flavin also binds first and the addition of either O_2 or hydroxyphenylacetate is random. However,

double-mixing stopped-flow experiments support the reaction of O_2 with the $FMNH_2$ to form the C4a-(hydro)peroxyflavin prior to binding of *p*-hydroxyphenylacetate [57].

The C4a-(hydro)peroxyflavin intermediate was also detected at 370 nm at low octanesulfonate concentrations when $FMNH_2$ was mixed with SsuD and octanesulfonate in air-saturated buffer, and three distinct phases were observed (Figure 2.7). However, this oxygenated flavin intermediate did not accumulate to detectable levels at higher octanesulfonate concentrations. This indicates at high octanesulfonate concentrations the reaction of octanesulfonate with the C4a-(hydro)peroxyflavin would be rapid and does not accumulate to significant levels. The decay of the C4a-(hydro)peroxyflavin showed a hyperbolic dependence on the octanesulfonate concentration, which suggests the binding of octanesulfonate occurs in two steps. The octanesulfonate binds in rapid equilibrium to SsuD followed by an isomerization step or direct carbon-sulfur bond cleavage. However, there was still no observed O_2 dependence on the initial fast phase at 370 nm seen at lower octanesulfonate concentrations. When premixed SsuD and $FMNH_2$ were mixed with octanesulfonate in oxygenated buffer there was no initial increase at 370 nm corresponding to the formation of the C4a-(hydro)peroxyflavin. An assay analogous to reactions carried out in the stopped-flow instrument was developed to measure the aldehyde product. Higher product formation should be observed if the initial fast phase at 370 nm attributed to C4a-(hydro)peroxyflavin correlates with product formation. As a single turnover reaction, the amount of product is dependent on the intermediates generated in each reaction. There was a 4-fold increase in the amount of octanal

produced when $FMNH_2$ alone was reacted with premixed SsuD-octanesulfonate-O_2 compared to the reaction of SsuD-$FMNH_2$ with octanesulfonate and O_2 (Table 2.3). The octanesulfonate is unable to bind to SsuD unless $FMNH_2$ is first bound, therefore even though octanesulfonate is present with SsuD it is not yet bound to the enzyme. These results further supported the presence of an inactive complex between SsuD and $FMNH_2$. The lower octanal product produced with premixed SsuD and $FMNH_2$ may be due to the slow conversion of the SsuD- $FMNH_2$ binary complex back to the active form in the presence of octanesulfonate and O_2. When SsuD is not premixed with the reduced flavin, the inactive complex is unable to form. The previous results suggest that an isomerization step precedes octanesulfonate binding. Evidence to support this observation was obtained by alternate mixing experiments monitored at 450 nm: SsuD-$FMNH_2$ mixed with octanesulfonate in oxygenated buffer, and premixed SsuD-$FMNH_2$-octanesulfonate mixed with oxygenated buffer. The k_1 for the decay of the reaction when octanesulfonate was premixed with SsuD and $FMNH_2$ is 2-fold faster than the reaction that had not been premixed with octanesulfonate (Figure 2.9A). As a result, the decay of the flavin intermediate occurs at a faster rate if octanesulfonate is premixed with SsuD and $FMNH_2$. The faster rate for the decay of the flavin intermediate is directly correlated with an increase in product formation (data not shown). In addition, the K_d value is 3-fold lower when SsuD, $FMNH_2$, and octanesulfonate are premixed (Figure 2.9B). An isomerization step would be masked in this reaction because octanesulfonate would already be bound to
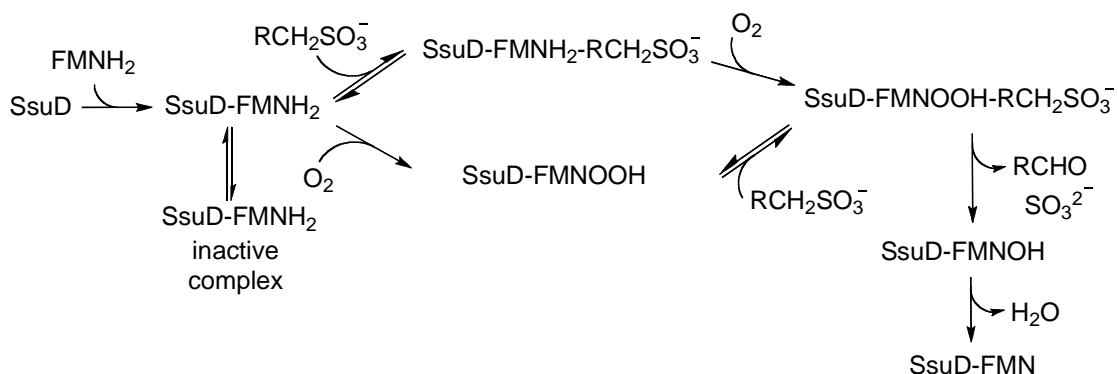
Scheme 2.3. Order of substrate binding for SsuD

form the ternary complex, and the net effect would be a rate increase and decrease in the octanesulfonate binding affinity.

A minimal model for substrate binding can be defined by the described experiments. After binding of reduced flavin to SsuD to from the SsuD-FMNH$_2$ complex, the enzymecan carry out the reaction through one of two paths: 1) SsuD-FMNH$_2$-octanesulfonate is formed prior to reacting with O$_2$, and 2) the SsuD-FMNH$_2$-O$_2$ intermediate is formed prior to reacting with octanesulfonate. A faster rate and lower K_d value for octanesulfonate binding was observed with premixed SsuD, octanesulfonate, and FMNH$_2$ suggesting that octanesulfonate binds prior to O$_2$. Based on these experiments it would appear that O$_2$ is the last substrate to bind thereby ensuring that formation of the C4a-(hydro)peroxyflavin is fully coupled to desulfonation, however both paths are represented in the model.

In summary, this study has elucidated the reaction mechanism of the alkanesulfonate monooxygenase component (Scheme 2.3). The results suggest an ordered substrate

binding mechanism where SsuD binds $FMNH_2$ first leading to a conformational change that promotes the binding of octanesulfonate. Reaction of $FMNH_2$ with O_2 to form aC4a-(hydro)peroxyflavin intermediate is directly involved in desulfonating the alkanesulfonate substrate to produce the corresponding aldehye and sulfite. This substrate binding order plays an essential role in catalysis, and significant protein dynamics during the course of the reaction was shown to be involved in both $FMNH_2$ and alkanesulfonate binding.

CHAPTER THREE

ON THE CATALYTIC ROLE OF THE CONSERVED RESIDUE His228 LOCATED IN THE PUTATIVE ACTIVE SITE OF THE ALKANESULFONATE MONOOXYGENASE

3.1 INTRODUCTION

In *Escherichia coli*, cysteine, sulfate or inorganic sulfur starvation induces the synthesis of a set of proteins involved in acquiring sulfur from alternate sulfur sources. The two-component alkanesulfonate monooxygenase system, comprised of a NAD(P)H:flavin reductase (SsuE) and an alkanesulfonate monooxygenase (SsuD), is expressed along with other proteins to utilize a broad range of alkanesulfonates as an alternative sulfur source. In the overall reaction, FMN is reduced by SsuE in the presence of NAD(P)H, then the reduced flavin is further transferred to SsuD [*73*]. The SsuD bound $FMNH_2$ activates dioxygen to form a C4a-(hydro)peroxyflavin intermediate that directly cleaves the carbon-sulfur bound releasing sulfite and the corresponding aldehyde [*102*].

In our previous studies, the mechanism of SsuD was probed by a combination of biochemical and kinetic approaches. The octanesulfonate substrate was unable to bind to SsuD until $FMNH_2$ was first bound, which implied an ordered substrate binding mechanism in the SsuD reaction. This conclusion was further confirmed by stopped-flow
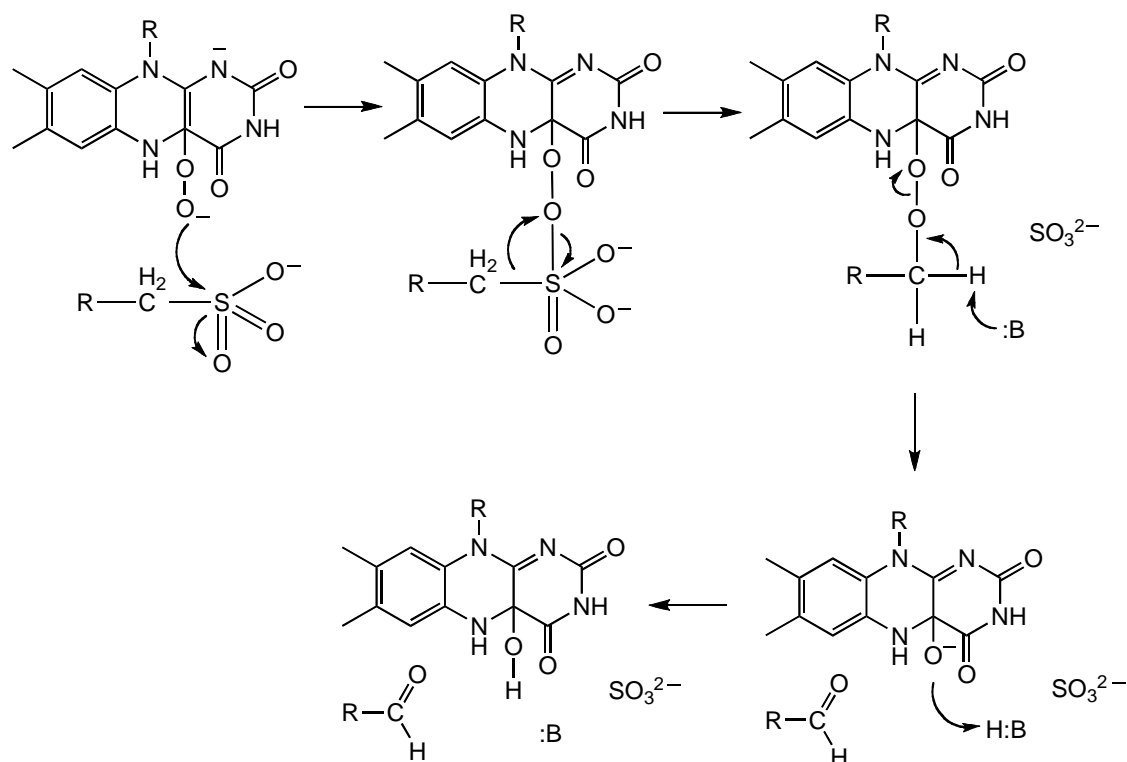
Scheme 3.1 Proposed mechanism of the SsuD desulfonation reaction

kinetic analyses, in which the orders of substrate addition showed different kinetic behaviors. Therefore, the SsuD reaction undergoes an ordered substrate mechanism and this substrate binding mechanism has catalytic significance. A C4a-(hydro)peroxyflavin intermediate has been identified in the SsuD reaction by stopped-flow analyses in the absence or at low concentrations of octanesulfonate. Interestingly, the order of addition of $FMNH_2$ and O_2 determines whether the formation of the C4a-(hydro)peroxyflavin intermediate is observed in stopped-flow kinetic traces. The flavin intermediate signal

was only observed when FMNH$_2$ and SsuD were not premixed under anaerobic conditions, which implied that the initially formed SsuD-FMNH$_2$ complex converted to an inactive complex. The C4a-peroxyflavin is proposed as the oxygenating flavin intermediate during SsuD catalysis. The C4a-peroxyflavin makes a nucleophilic attack on the sulfur group of the alkanesulfonate substrate, then a Baeyer-Villiger rearrangement mechanism is involved in the cleavage of the carbon-sulfur bond (As shown in Scheme 3.1) [102]. A catalytic base has also been proposed to abstract a proton from the alkane peroxyflavin intermediate so the aldehyde product can be released from the enzyme following rearrangement. Identification of this catalytic base would provide valuable information on the desulfonation mechanism by SsuD.

SsuD has an unusual homotetrameric structure in this flavin-dependent two-component monooxygenase family, which is comprised of two homodimers (A/B and C/D) with a monomeric molecular weight of 41,605 Da [60]. Although the amino acid sequence homology is low, SsuD is similar in overall structure to other flavin-dependent monooxygenases; bacterial luciferase and long-chain alkane monooxygenase (LadA). These FMN-dependent monooxygenases display similar TIM barrel architectures. Since there is neither an SsuD-flavin or SsuD-alkanesulfonate complex structure available, the location of the active site is still not clear. The conserved amino acid residues Cys54, His11, His333, Tyr331, His228 and Arg226 form the wall of a cavity. The location of this cavity is in agreement with the observation that the active site of all TIM-barrel enzymes are located at the C-terminal end of the β-barrel. Several amino acids located in the putative active site of SsuD (His228, Tyr331, and Cys54)
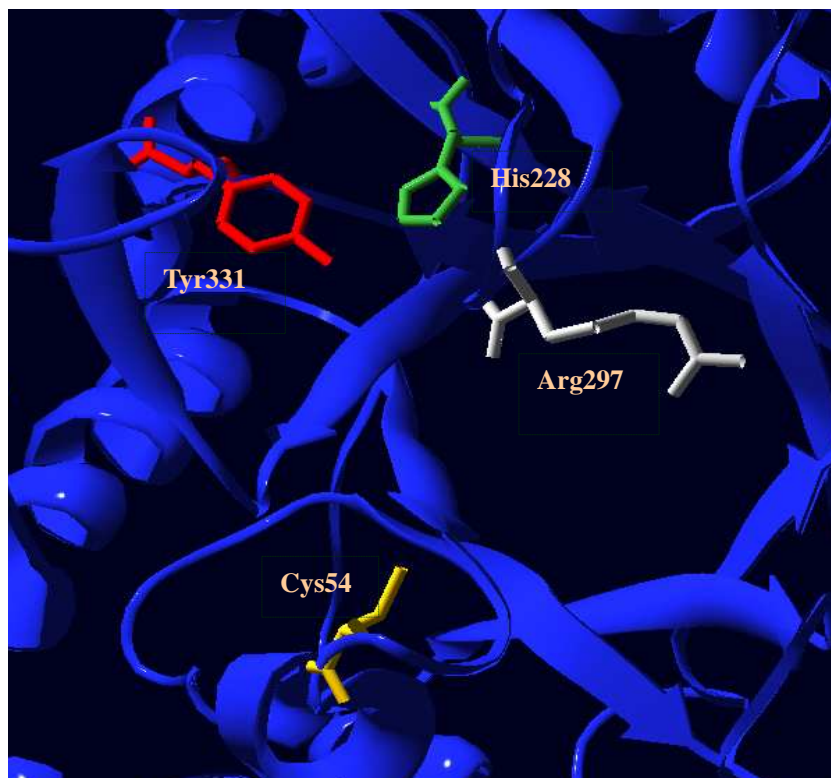
Figure 3.1 Conserved residues in putative active site of SsuD

are in a similar arrangement as catalytically relevant amino acids from bacterial luciferase (His44. Tyr110 and Cys106) and LadA (His138 and Tyr63) (Figure 3.1) [*58, 60, 61*]. The Cys54 was showed to play an important role in stabilizing the C4a-(hydro)peroxyflavin intermediate (unpublished data), which is similar with the catalytic role of Cys106 of bacterial luciferase [*70, 88*]. These results indicate that the conserved residues among the flavin-dependent monooxygenases not only are structural related but also have similar catalytic functions. His44 in the α-subunit of bacterial luciferase has been shown to be a catalytic base in the bioluminescence reaction. Mutation of this histidine residue to alanine showed significant decreases in the intensity of light emitted. It was found that

the enzymatic activity could be rescued with the addition of imidazole to the reaction at increasing pH (pH > 6.5) [66]. Based on the similar spatial arrangement of this residue with bacterial luciferase, His228 of SsuD is proposed to be the putative active site base involved in proton abstraction from the alkane peroxyflavin intermediate.

The present study was performed to determine the role of H228 in the mechanism of desulfonation. Several His variants were constructed and analyzed through steady-state and rapid reaction kinetics. The pH dependence on catalytic steps involving octanesulfonate was performed to further probe the mechanistic role of this His residue. The information obtained from these pH profiles were supplemented with chemical rescue experiments. From these studies a role for the His residue in the mechanism of SsuD is proposed.

3.2 MATERIALS & METHODS

3.2.1 Materials.

E. coli strains including XL-1, BL21(DE3) and QuickChange site-directed mutagenesis kit were purchased from Stratagene (La Jolla, CA). Plasmid vectors and pET21a were obtained from Novagen (Madison, WI). DNA primers were synthesized by Davis Sequencing (Davis, CA). FMN, NADPH, EDTA, potassium phosphate (monobasic anhydrous and dibasic anhydrous), sodium chloride, sodium hydrosulfite (dithionite), Imidazole, streptomycin sulfate, trifluoroacetic acid, trypsin, Tris base, 5,5-dithiobis(2-nitrobenzoic acid) (DTNB), glucose, glucose oxidase, and urea were from Sigma (St. Louis, MO). Ammonium sulfate, ethidium bromide, formaldehyde, glacial acetic acid, isopropyl-Dthiogalactoside (IPTG), 2-propanol, glycerol, sodium carbonate, sodium phosphate and glycerol were purchased from Fisher (Pittsburgh, PA). LB-agar and LB-medium were from BIO 101 Systems (Carlsbad, CA). Streptavidin agarose column matrix was obtained from Invitrogen (Carlsbad, CA). Phenyl Sepharose column matrix was from Amersham Biosciences (Piscataway, NJ). Acrylamide/Bis solution, sodium dodecyl sulfate (SDS), and Macro-prep High Q Support were from Bio-Rad (Hercules, CA). Standard buffer contains 25 mM potassium phosphate, pH 7.5, and 10% glycerol unless otherwise noted. SsuD and SsuE enzymes were expressed and purified as previously described. The concentration of SsuD and SsuE proteins was determined from A_{280} measurements using a molar extinction coefficient of 47.9 $mM^{-1} cm^{-1}$ and 20.3 $mM^{-1} cm^{-1}$, respectively.

3.2.2 Site-directed mutagenesis.

A recombinant pET21a plasmid containing the *ssuD* gene was used for site-directed mutagenesis. Histidine 228 was substituted to alanine (H228A), aspartate (H228D) and lysine (H228K) using the QuickChange site-directed mutagenesis kit from Stratagene (Santa Clara, CA). Primers for each variant were designed as 29 base oligonucleotides containing the desired mutation (3.1). The PCR amplified products were purified with the QIAquick PCR Purification Kit (). The mutant constructs were transformed into *E. coli* XL-1 Blue supercompetent cells for amplification of plasmid DNA and storage. Plasmids were extracted following the QIAprep Miniprep protocol (Gaithersburg, MD) from a 5 mL growth of *E. coli* XL-1 Blue cells incubated overnight in LB-Amp media at 37 °C. The generated mutations were verified by DNA sequence analysis at Davis Sequencing (University of California, Davis). The plasmids containing the desired mutations were transformed into *E. coli* BL21(DE3). The SsuD His228 variant proteins were expressed in *E. coli* BL21(DE3) and purified as previous reported [79]. The purified proteins were frozen and stored at -80 °C.

Table 3.1 Primers used in His228 mutagenesis

	Primers
H228A F[a]	C GGT ATT CGT CTG <u>GCG</u> GTG ATT GTT CGT G
H228A R	C ACG AAC AAT CAC <u>CGC</u> CAG ACG AAT ACC G
H228D F	C GGT ATT CGT CTG <u>GAT</u> GTG ATT GTT CGT G
H228D R	C ACG AAC AAT CAC <u>ATC</u> CAG ACG AAT ACC G
H228K F	C GGT ATT CGT CTG <u>AAA</u> GTG ATT GTT CGT G
H228K R	C ACG AAC AAT CAC <u>TTT</u> CAG ACG AAT ACC G

[a] F: forward; R: reverse

3.2.3 Circular dichroism

Circular dichroism (CD) spectra of the wild-type SsuD and His228 variants (H228A, H228D, and H228K) were obtained with 1.2 μM enzymes in 25 mM potassium phosphate buffer (pH 7.5), 100 mM NaCl at room temperature. Spectra were recorded on a Jasco J-810 Spectropolarimeter (Easton, MD). Measurements were taken in 0.1 nm increments from 300 to 185 nm in a 0.1 cm path length cuvette with a bandwidth of 1 nm and a scanning speed of 50 nm/min. Each spectrum is the average of eight scans; smoothing of the data was performed using the default parameters within the Jasco J-720 software.

3.3.4 Flavin titration

Flavin binding affinities of His228A, H228D, and H228K SsuD were determined by spectrofluorometric titration recorded on a Perkin Elmer LS 55 luminescence spectrometer (Palo Alto, CA) with an excitation wavelength at 280 nm and emission measurements at 344 nm. For the titration of the SsuD variants with FMN, a 1.0 ml solution of SsuD (0.5 μM) in standard buffer was titrated with FMN (2.6-98.6 μM), and the fluorescence spectra recorded following a 2 min incubation after the addition of each aliquot of FMN. Titration of each SsuD variant with reduced FMN was performed under anaerobic conditions. Anaerobic SsuD enzymes (0.5 μM) were prepared in a glass titration cuvette by at least 15 cycles of evacuation followed by equilibration with ultrahigh purity argon gas. Glucose (20 mM) and glucose oxidase (10 units) were added to remove trace amounts of oxygen. Flavin   prepared in standard buffer was added to

an airtight titrating syringe with an oxygen scrubbing system of glucose (20 mM) and glucose oxidase (10 units). The syringe was incubated in an anaerobic glovebox for 20 min to remove oxygen. The anaerobic FMN solution was photoreduced by irradiation for 30 min in the presence of 10 mM EDTA, and the titration apparatus was assembled in the anaerobic glovebox. The fluorescence spectra were recorded after 2 mins following the titration of each SsuD variant with $FMNH_2$ (0.16-7.8 μM). Bound and free flavin were calculated using equation 2.1. The concentration of bound flavin was plotted against free flavin to obtain the dissociation constant (K_d) according to equation 2.2.

3.2.5 Octanesulfonate binding

The binding of octanesulfonate to the SsuD variants complexed with $FMNH_2$ were performed under anaerobic conditions. Anaerobic H228A, H228D, or H228K SsuD and $FMNH_2$ solutions were prepared as previous described. Octanesulfonate solutions were kept in an anaerobic glovebox overnight and an oxygen-scrubbing system of glucose (20 mM) and glucose oxidase (10 units) was added to remove trace oxygen. The titration apparatus was assembled in the anaerobic glovebox. Aliquots of octanesulfonate (2.5-110 μM) were added to the the SsuD variants complexed with $FMNH_2$. The fluorescence spectra were recorded with an excitation wavelength at 280 nm and emission intensity measurements at 344 nm following a 2 min incubation. The concentration of bound octanesulfonate was determined by Eq. 2.1 and plotted against the concentration of free octanesulfonate to determine the dissociation constant (K_d) according to Eq 2.2.

3.2.6 Activity assay

The activities of the H228A, H228D, and H228K SsuD were assayed based on a previously described methods with some modifications [*73*]. Reactions were initiated by the addition of NADPH (500 μM) into a reaction mixture containing each SsuD variant (0.8 μM), SsuE (2.4 μM), FMN (2 μM), and a range of octanesulfonate concentrations (0.01-5 mM) in standard buffer with 100 mM NaCl at 25 °C. After a 3 min incubation, the reaction was stopped by the addition of urea (2.0 M), and DTNB (1 mM) was added to a 200 μL aliquot of the reaction solution. The colorimetric reaction was allowed to develop at room temperature for 2 min, and the absorbance measured at 412 nm using a molar extinction coefficient for the TNB anion of $14.1 \text{ mM}^{-1}\text{cm}^{-1}$.

3.2.7 Rapid reaction kinetic analyses

Stopped-flow kinetic analyses were carried out on a thermostatted Applied Photophysics SX. 18 MV stopped-flow spectrophotometer. The stopped-flow instrument was made anaerobic by filling with an O_2 scavenging system containing 25 mM phosphate buffer, pH 7.5, 10% glycerol, 100 mM NaCl with 20 mM glucose, and 10 units of glucose oxidase in the inner system and drive syringe. The oxygen-scrubbing solutions were allowed to stand in the system overnight and were thoroughly rinsed with anaerobic standard buffer prior to performing the experiments. All reactions were carried out in standard buffer at 4 °C. The $FMNH_2$ (15 μM) solutions were made anaerobic in a glass tonometer and then photoreduced by irradiation for 30 min in the presence of EDTA (10 mM). The solution containing each SsuD variant enzyme (45 μM), oxygen (210 μM) and octanesulfonate (0-1000 μM) was kept in an air-tight syringe. All experiments were carried out in single-mixing mode by mixing equal volumes of the solutions and

113

monitored by single wavelength analyses at 370 and 450 nm. The kinetic traces were fitted to Eq. 2.3 or Eq. 2.4.

3.2.8 Imidazole rescue of H228A SsuD variant

Imidazole solutions were prepared in 50 mM potassium phosphate buffer, 100 mM sodium chloride, 10% glycerol at the desired imidazole concentration (5-200 mM) and pH value (5.5-9.0). The H228A SsuD enzyme activity was assayed under the following conditions: H228A SsuD (1.6 μM), SsuE (4.8 μM), FMN (5.0 μM), NADPH (500 μM) and octanesulfonate (0.02-4 mM) in a total volume of 0.5 mL. The effect of imidazole on the activity of H228A SsuD was determined by measuring the enzymatic activity with octanesulfonate (1 mM) as substrate for the enzyme in the presence of varying concentrations of imidazole (5-200 mM) in 50 mM potassium phosphate (pH: 6.0, 7.0, and 7.5). The effect of imidazole on the turnover number of H228A SsuD was determined by measuring the enzymatic activity with varying concentrations of octanesulfonate substrate (0.02-4 mM) in the presence of 50 mM imidazole at varying pH values (5.5 to 9.0).

3.2.9 The pH dependence of wild-type and H228A SsuD

The effect of pH on the kinetic parameters of octanesulfonate were determined in 50 mM potassium phosphate (pH 5.8–7.8), and Tris-HCl (pH 7.5-9.5), supplemented with 100 mM sodium chloride to maintain the ionic strength. H228A or wild-type SsuD activity was assayed as previous described and the kinetic parameters (k_{cat} and K_m) were determinted by fitting the data to the Michaelis-Menten equation. The pH dependence of

114

k_{cat} and k_{cat}/K_m were fitted to a double ionization model equation 3.1 [*103,104*].

$$k_{obs} = \frac{k_{lim1} \times 10^{(pK_1 - pH)} + k_{lim2}}{1 + 10^{(pK_1 - pH)} + 10^{(pH - pK_2)}}$$

(3.1)

3.3 RESULTS

3.3.1 Circular dichroism of the wild-type and SsuD variants

The far-UV CD spectrum of proteins can reveal important properties regarding their secondary structures. The far-UV CD spectroscopy experiments were performed to compare the secondary structures of H228A, H228D, and H228K and wild-type SsuD. All recorded spectra obtained appeared to overlap with each other (Figure 3.2), suggesting that the single mutation at His228 did not cause any major perturbations in secondary structure.

3.3.2 Oxidized and reduced FMN binding affinity

To determine whether His228 is directly involved in flavin binding, the dissociation constants of oxidized and reduced FMN to His228A, H228D, and H228K SsuD were determined by fluorimetric titration. The decrease in the intrinsic protein intensity was monitored upon the binding of flavin to each SsuD variant. The concentration of bound and free $FMNH_2$ or FMN was calculated according to Eq. 2.1, and the concentration of flavin bound to each enzyme was plotted against the concentration of free $FMNH_2$ or FMN added with each aliquot. Figure 3.3 shows representative spectra of the titration of H228A SsuD titration with $FMNH_2$. The inset shows the plot of bound $FMNH_2$ against free $FMNH_2$ with each addition of $FMNH_2$. The dissociation constants of oxidized and reduced FMN to each SsuD variant are listed and summarized in Table 3.2. The average K_d values for $FMNH_2$ binding to H228A, H228D, and H228K SsuD were 0.39 ± 0.09, 0.56 ± 0.24 and 0.41 ± 0.11, respectively. The average K_d values for FMN are 40- to 50-fold higher than $FMNH_2$, with values of 18.3 ± 2.7 (H228A SsuD), 16.5 ± 3.5

116
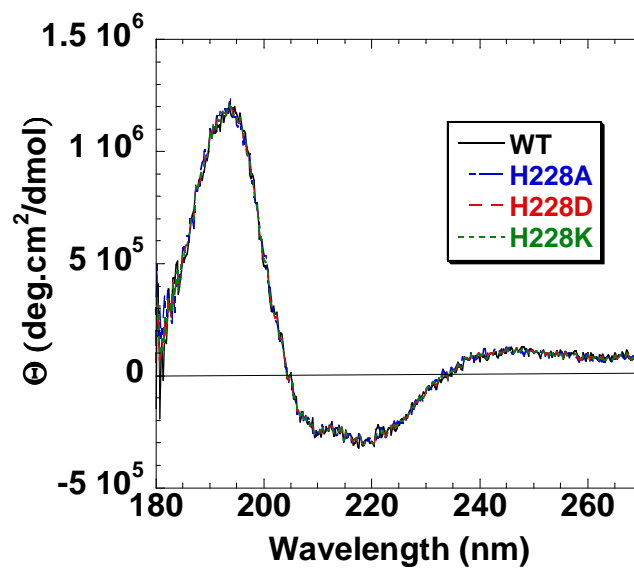
Figure 3.2 Circular dichroism spectra of H228A, H228D, H228K and wild-type SsuD. All experiments were performed with each SsuD enzyme (1.2 μM) in 25 mM potassium phosphate buffer (pH 7.5), 100 mM NaCl at room temperature. Each spectrum is the average of eight scans.
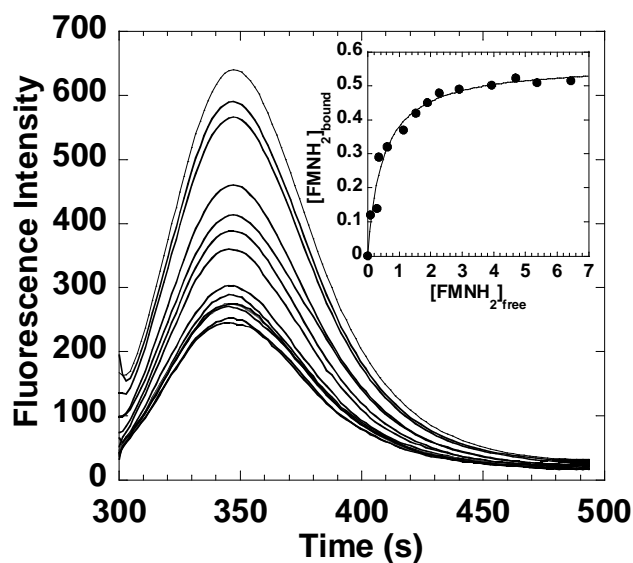
Figure 3.3 Fluorimetric titration of H228A SsuD with $FMNH_2$. H228A SsuD (0.5 μM) was titrated with $FMNH_2$ (0.16-7.8 μM) under anaerobic conditions. Emission intensity measurements at 344 nm were measured using an excitation wavelength at 280 nm. The change in fluorescence of H228A SsuD following the addition of $FMNH_2$ was converted to the estimated concentration of bound $FMNH_2$ (Eq. 2.1) and plotted against the concentration of free $FMNH_2$. Inset: Change in the emission intensity at 344 nm. The solid line represents the fit of the titration curve to Eq. 2.2.

(H228D SsuD), and 22.1 ± 4.4 (H228K SsuD). There was no significant change in the binding affinity of oxidized and reduced flavin between wild-type and the His228 variants, which implies that the His228 residue is not directly involved in the binding of flavin to SsuD.

3.3.3 Octanesulfonate binding to the SsuD variants

The binding affinity of octanesulfonate to each SsuD variant complexed with $FMNH_2$ was determined by fluorimetric titrations under anaerobic conditions. To ensure that all SsuD enzyme was bound to $FMNH_2$, a saturating $FMNH_2$ concentration (2:1 ratio of $FMNH_2$ to SsuD) was used in these studies. Figure 3.4 shows a representative fluorescence spectra recorded during the titration of octanesulfonate to H228A SsuD complexed with $FMNH_2$. The addition of octanesulfonate showed a decrease in the intrinsic fluorescence of the H228A SsuD-$FMNH_2$ complex at an emission wavelength of 344 nm. The concentration of bound octanesulfonate and free octanesulfonate was calculated according to Eq. 2.1. The concentration of octanesulfonate bound to the H228A SsuD-$FMNH_2$ complex plotted against the concentration of free octanesulfonate after each addition is shown in the inset. The K_d value for octanesulfonate binding to the H228A SsuD-$FMNH_2$ complex was 22.8 ± 0.37 μM. The dissociation constants of octanesulfonate to H228D (19.9 ± 0.29 μM) and H228K (28.2 ± 0.46 μM) SsuD complex with $FMNH_2$ are summarized in table 3.2. There was no significant change between wild-type SsuD and the H228 SsuD variants in terms of octanesulfonate binding. These results indicate that His228 is not directly involved in the binding of octanesulfonate to SsuD.
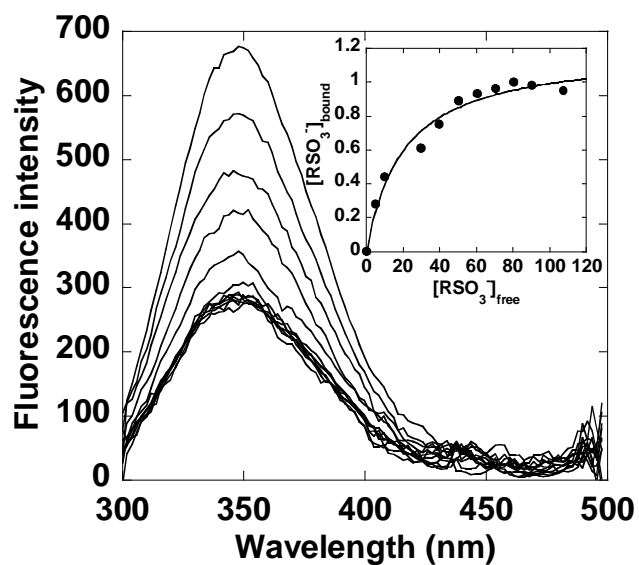
Figure 3.4 Fluorimetric titration of octanesulfonate to H228A SsuD complexed with octanesulfonate. Emission intensity measurements at 344 nm were measured using an excitation wavelength at 280 nm. The H228A SsuD variant (1 μM) was premixed with FMNH$_2$ (2 μM), and the complex was titrated with octanesulfonate (2.5-110 μM). Inset: Change in the emission intensity at 344 nm. The solid line represents the fit of the titration curve to Eq. 2. Each titration was performed in triplicate.

3.3.4 Steady-state kinetic parameters of the H228 SsuD variants

The kinetic parameters for wild-type SsuD with octanesulfonate as substrate were previous reported [*102*]. The kinetic parameters of the H228 SsuD variants with octanesulfonate as substrate were determined by an SsuE/SsuD coupled assay and compared to wild-type. When the kinetic parameters of H228A SsuD (Figure 3.5) was compared to the wild-type enzyme, a 50-fold decrease in the k_{cat}/K_m value for octanesulfonate was observed (Table 3.2). There was a 200-fold decrease in the k_{cat}/K_m value for H228D SsuD, and a 48-fold decreases in the k_{cat}/K_m value for H228K SsuD (Figure 3.5). H228A SsuD and H338K SsuD showed a similar decrease in the catalytic efficiency, while H228D SsuD showed a larger decrease in the k_{cat}/K_m value then the other variants. An aspartate residue would likely be unprotonated, and the negative charge may affect the electrostatic properties of the active site, or proper orientation of another catalytic residue. These results indicate that H228 plays a role in the oxidation of octanesulfonate; however, a more dramatic change in the kinetic parameters would be expected if His228 were acting as a general base in the desulfonation reaction.

3.3.5 Presteady-state kinetics

Stopped-flow kinetic studies were performed to probe the oxidation of flavin by H228A SsuD in the absence and presence of octanesulfonate substrate. In the absence of alkanesulfonate substrate, a C4a-(hydro)peroxyflavin intermediate has been identified in the wild-type SsuD reaction when SsuD are not preincubated with FMNH$_2$. Stopped-flow analyses were performed with varied substrate mixing to detect the formation and decay of this oxygenated-flavin intermediate by H228A SsuD in the absence of alkanesulfonate substrate. The FMNH$_2$ (15 μM) solution photoreduced in the presence of EDTA was
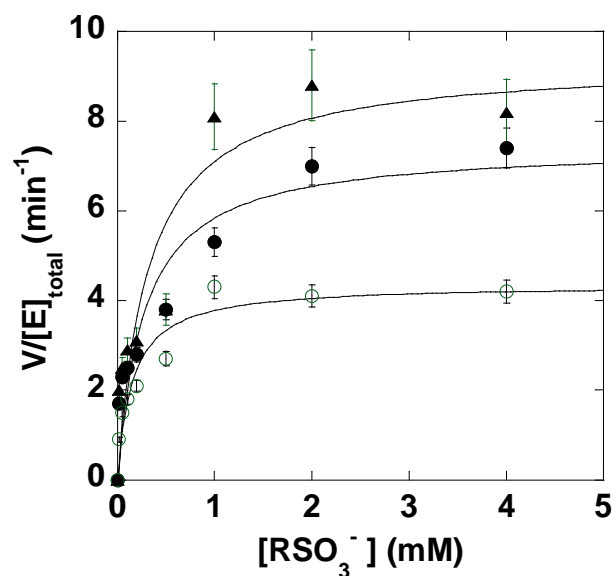
Figure 3.5 Initial velocities of H228A, H228D and H228K SsuD with octanesulfonate. The activity of H228 SsuD variants [H228A (●), H228D (○), and H228K (▲)] was measured by a modified SsuE-SsuD coupled enzyme assay at 25 ˚C. Each point represents the average of three to five measurements. The solid lines are the fits of the data to the Michaelis-Menten equation.

Table 3.2 Comparion of kinetic parameters and substrate binding afffinities for

wild-type and SsuD variants

	$K_{d,FMN}$	$K_{d,FMNH2}$	$K_{d,oct}$ [a]	k_{cat}	$K_{m,oct}$	k_{cat}/K_m
	(μM)	(μM)	(μM)	(min^{-1})	(μM)	($\mu M/min^{-1}$)
WT	15.5 ± 1.3	0.32 ± 0.15	17.5 ± 0.15	56.2 ± 6.4	38.4 ± 7.8	1.45 ± 0.45
H228A	18.3 ± 2.7	0.39 ± 0.09	22.8 ± 0.37	7.3 ± 1.4	256.1 ± 12.1	0.028 ± 0.07
H228D	16.5 ± 3.5	0.56 ± 0.24	19.9 ± 0.29	2.1 ± 0.7	278.2 ± 11.3	0.0075 ± 0.01
H228K	22.1 ± 4.4	0.41 ± 0.11	28.2 ± 0.46	9.2 ± 2.5	302.9 ± 22.5	0.030 ± 0.01

[a] Determined with the SsuD-FMNH$_2$ complex

mixed against H228A SsuD (45 μM) in air-saturated buffer. The kinetic traces were recorded at 370 nm and 450 nm (Figure 3.8). The kinetic trace at 370 nm was best fitted to a triple-exponential equation with rates of 19.2 s^{-1} (k_1), 1.88 s^{-1} (k_2),and 0.17 s^{-1} (k_3), while the kinetic trace at 450 nm was best fitted to a double exponential equation with rates of 2.5 s^{-1} (k_1), and 0.21 s^{-1} (k_2). A signal at 370 nm corresponding to the formation of the C4a-(hydro)peroxyflavin intermediate was observed in H228A SsuD reactions similar to wild-type SsuD. The rate of formation for the C4a-(hydro)peroxyflavin intermediate by H228A SsuD shows a 1.4-fold increase, while the rate of decay shows a 1.9 fold increase from wild-type.

Flavin oxidation by SsuD in the presence of octanesulfonate was investigated through stopped-flow kinetic analyses at 370 and 450 nm, mixing free FMNH$_2$ with H228A SsuD and octanesulfonate in air-saturated buffer (Figure 3.9). At low octanesulfonate concentrations (100 μM), the C4a-(hydro)peroxyflavin intermediate signal was observed; however, as the concentration of octanesulfonate increased the kinetic traces at both wavelengths increased at almost identical rates in two distinct phases at both 370 and 450 nm. All kinetic traces at 450 nm were best fitted to a double exponential equation. The k_{obs} for the fast phase showed a hyperbolic dependence on the octanesulfonate concentration that was best fitted to Eq. 2.4 to give a K_d of 74 μM and a limiting rate constant of 4.54 s^{-1} (Figure 3.10). The hyperbolic dependence of the fast phase on octanesulfonate cencentration is similar to wild-type SsuD, indicating a two-step binding of octanesulfonate. The K_d value is similar to wild-type SsuD (93 μM) obtained under similar conditions, while the limiting rate constant is 1.8-fold higher than wild-type (2.4 s^{-1}). The decay of the C4a-(hydro)peroxyflavin is 1.9-fold faster

124
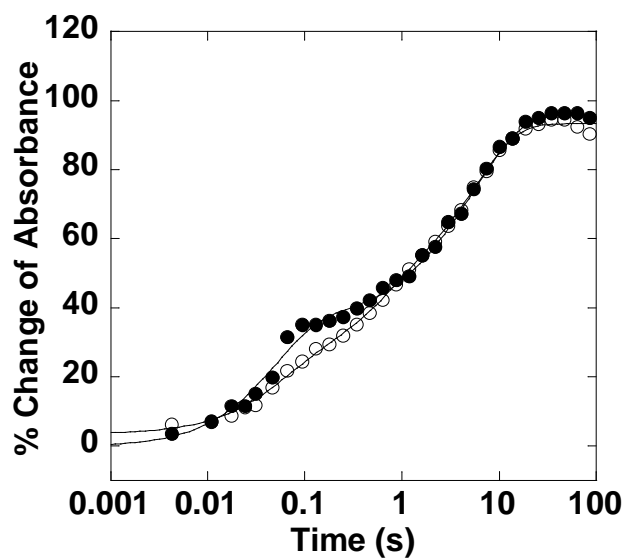
Figure 3.6 Kinetics of flavin oxidation by the H228A SsuD in the absence of octanesulfonate. Experiments were performed by stopped-flow kinetic analyses at 4 ˚C. Flavin oxidation of free $FMNH_2$ (15 μM) mixed with the H228A SsuD variant (45 μM) in air-saturated buffer monitored at 370 (●) and 450 (○) nm. The kinetic traces shown are the average of three separate experiments, and the solid lines are the fits of the kinetic traces to Eq. 2.3 or 2.4.
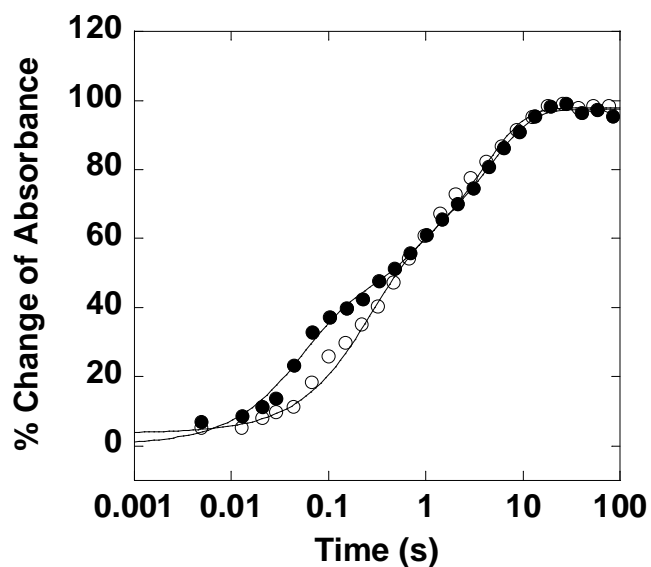
Figure 3.7 Kinetics of flavin oxidation by H228A SsuD variant at 100 μM octanesulfonate buffer. Experiments were performed by stopped-flow kinetic analyses at 4 ˚C. Flavin oxidation of free FMNH$_2$ (15 μM) mixed with H228A SsuD (45 μM), and octanesulfonate (100 μM) in air-saturated buffer monitored at 370 (●) and 450 (○) nm. The kinetic traces shown are the average of three separate experiments, The solid lines are the fits of the kinetic traces to Eq. 2.3 or 2.4.
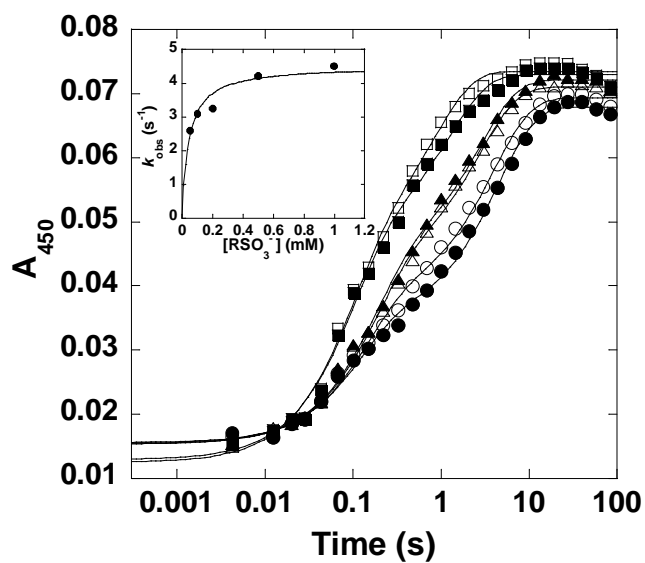
Figure 3.8 Kinetics of flavin oxidation by H228A SsuD in the presence of ocatanesulfonate. Experiments were performed by stopped-flow kinetic analyses at 4 ˚C. Flavin oxidation of free FMNH$_2$ (15 μM) mixed with H228A SsuD (45 μM) and various octanesulfonate concentrations [0 mM (●), 0.05 mM (○) 0.1 mM (▲) 0.2 mM (△) 0.5 mM(■) 1 mM (□)] in air-saturated buffer at 450 nm. Inset: octanesulfonate concentration dependence on the k_{obs} for the first phase at 450 nm.

than wild-type SsuD, so it is highly possible that this limiting rate change is caused by the instability of H228A-bound $FMNH_2$ in the presence of octanesulfonate.

Overall, the kinetics of flavin oxidation by H228A SsuD and wild-type SsuD enzyme are similar. The C4a-(hydro)peroxyflavin intermediate was observed with H228A SsuD in the absence of octanesulfonate or at low octanesulfonate concentrations. There is a hyperbolic dependence on the octanesulfonate concentration with H228A SsuD, which was also observed in wild-type SsuD under similar experimental conditions. These results indicate that His228 residue is not directly involved in the reaction between the C4a-(hydro)peroxyflavin and alkanesulfonate substrate

3.3.6 Chemical rescue of H228A SsuD

From a structural standpoint, the histidine to alanine mutation in the active site of SsuD is equivalent to the removal of an imidazole moiety from the side chain of the amino acid residue at position 228. The kinetic and biochemical properties that have been affected by such a mutation should be at least partially restored in the enzyme in the presence of exogenous imidazole. At pH values above 7.0, the activity of H228A SsuD increased with increasing amounts of exogenous imidazole in the assay reaction mixture (Figure 3.9), indicating that H228A SsuD activity can be rescued by imidazole. In contrast, no significant effect was observed with the wild-type enzyme under similar conditions. Interestingly, the rescue of activity by imidazole is pH dependent. The effect of imidazole on the turnover number of H228A SsuD was determined in the pH range of 5.5-9.0 (Figure 3.10). As summarized in table 3.3, no significant change was observed in the k_{cat} values in the presence of saturated imidazole (50 mM) at pH 5.5 and 6.0. In the pH range of 7.0-9.0, about 10-15% of the activity could be rescued by imidazole. The

results indicate that only the deprotonated form of imidazole is relevant to catalysis (pK_a of imidazole: 6.8-7.0 [66]).

3.3.7 pH dependence of wild-type and H228A SsuD

In order to further investigate the role of His228 as an active site base in the desulfonation reaction by SsuD, the pH profiles of the k_{cat} and k_{cat}/K_m values for wild-type SsuD were obtained from pH 5.8-9.5. The wild-type SsuD enzyme shows optimal catalysis between 7.0-8.5 (Figure 3.11 A and B). Controls with octanesulfonate substrate in the absence of SsuD or with SsuD in the absence of octanesulfonate gave no measurable activity. The pH dependence on the k_{cat} value for wild-type SsuD, an indicator of the enzyme-substrate complex, reveals two titratable residues with pK_a values of 6.61 ± 0.19 and 9.6 ± 0.10. The pH dependence on the k_{cat}/K_m value of SsuD, an indicator of free enzyme or substrate, reveals two titratable residues with pK_a values of 6.57 ± 0.32 and 9.54 ± 0.34.

To determine whether His228 is the catalytic base involved in desulfonation, the pH dependence on the k_{cat} and k_{cat}/K_m values for H228A SsuD were also evaluated from pH 5.8-9.5 (Figure 3.11 A and B). The pH profiles for the k_{cat} and k_{cat}/K_m values of H228A SsuD and wild-type SsuD were similar. For H228A SsuD, two titratable residues were also revealed in pH profiles of both k_{cat} and k_{cat}/K_m. The H228A SsuD variant gave pK_a values of 6.66 ± 0.18 and 9.77 ± 0.06 for the k_{cat} pH profile and 6.72 ± 0.26 and 9.89 ± 0.28 fot the k_{cat}/K_m pH profile. The pK_a values for both wild-type and H228A SsuD are summarized in table 3.3. The differences between the pK_a values between H228A SsuD and wild-type SsuD are modest and within the error range. If His228 is the catalytic base involved in the desulfonation reaction, pK_{a1} should be absent in the pH profiles of H228A

SsuD, or a more significant change should be observed. Results here suggest that the His228 residue is not an active site base in catalytic steps involving the octanesulfonate substrate.
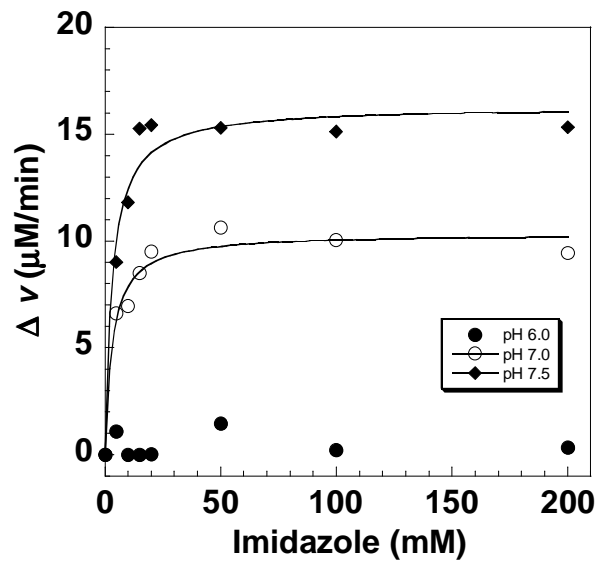
Figure 3.9 Initial velocities of H228A SsuD with imidazole at varying pH values. The activity of H228A SsuD was measured at saturating octanesulfonate concentration (1 mM) by varying imidazole concentrations at a range of pH values (pH 6.0-7.5). The points shown are the average of three separate experiments.
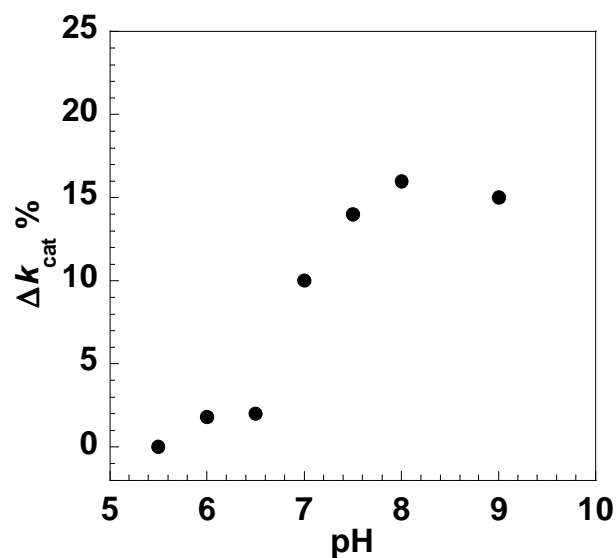
Figure 3.10 pH dependence of the imidazole-rescued activity of H228A SsuD. At each pH value, the activity of H228A was measured varying octanesulfonate concentrations (0.02-4 mM) in the presence of saturating imidazole (50 mM) and in the absence of imidazole. The k_{cat} values were determined by fitting the data to the Michaelis-Menten equation. The percentage increase in k_{cat} values of H228A SsuD as a function of pH, calculated from the ratio of the k_{cat} measured in the presence of saturating imidazole (50 mM) to the k_{cat} value measured in the absence of imidazole.

Table 3.3 The effect of imidazole on the turnover number of H228A SsuD at different pH values

pH	k_{cat}, min^{-1} [a]	$k_{cat(imidazole)}$, min^{-1} [b]	$K_{imidazole}$, mM [c]	R^2
5.5	5.13 ± 0.32	5.10 ± 0.17	ND	ND
6.0	5.21 ± 0.19	5.38 ± 0.25	ND	ND
7.0	6.37 ± 0.42	11.23 ± 2.32	3.2	0.982
7.5	6.91 ± 0.41	14.32 ± 3.11	4.9	0.984

[a]Turnover number in the absence of imidazole
[b]Turnover number in the presence of 50 mM imidazole
[c]The concentration of imidazole at which half the maximal initial velocity observed.
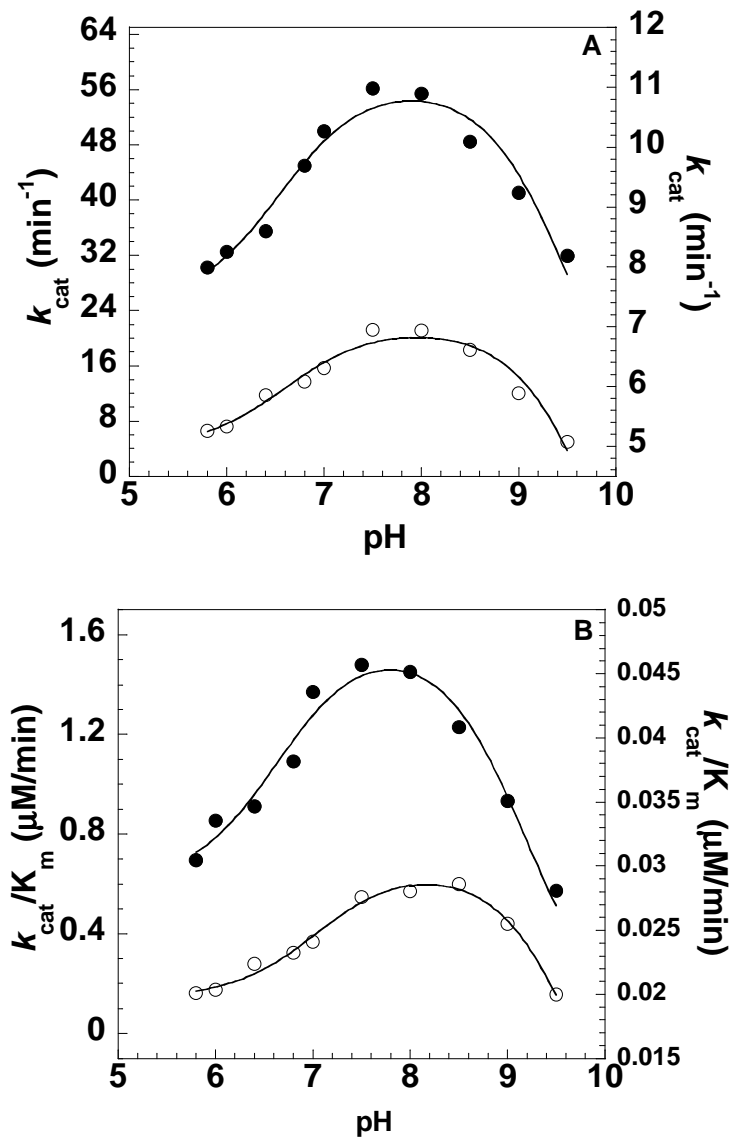
Figure 3.11 pH profiles of k_{cat}/K_m (A) and k_{cat} (B) of the wild-type SsuD (●, left *y*-axis) and H228A SsuD (○, right *y*-axis).

3.4 DISCUSSION

Although the amino acid sequence homology is low, SsuD is strikingly similar in overall structure to other flavin-dependent monooxygenases, bacterial luciferase [58, 87] and long-chain alkane monooxygenase (LadA) [59]. Several amino acids located in the putative acite site of SsuD are in a similar spatial arrangement as catalytically relevant amino acids from bacterial luciferase and LadA. A His residue is highly conserved in the active site of all three monooxygenases: His44 in the α-subunit of bacterial luciferase, His228 in SsuD, and His138 in LadA. The His44 residue has been reported to be the active site catalytic base involved in the reaction catalyzed by bacterial luciferase through mutagenesis and imidazole chemical rescue experiments [66]. Based on similar spatial orientations with bacterial luciferase, SsuD His228 and LadA His138 are both proposed to be the catalytic bases involved in proton abstraction from their corresponding substrates [59, 60]. To determine the catalytic role of His228 in the desulfonation reaction by SsuD, this putative active site residue was replaced by alanine, asparatate and lysine. The mechanistic and catalytic functions of this residue were elucidated by a combination of substrate binding, steady-state, and presteady-state kinetic analyses.

Steady-state kinetic assays were performed to determine the kinetic parameters of each His228 variant. The H228A and H228K SsuD enzymes showed similar decreases in k_{cat} values from wild-type at 7.3 ± 1.4 μM (8-fold) and 9.2 ± 2.5 μM (6-fold), respectively (Table 3.2). The H228D SsuD enzyme showed an almost 30-fold decrease in the k_{cat} value at 2.1 ± 0.7 μM. All of the SsuD variants gave similar 7-fold increases in the K_m values. While both the H228A and H228K SsuD enzymes showed an approximate

50-fold decrease in the k_{cat}/K_m value, the H228D SsuD variant decreased by nearly 200-fold. If this amino acid were acting as a general base as proposed then one would expect a more dramatic change in the kinetic parameters. It is interesting that H228D SsuD showed a larger decrease in the k_{cat}/K_m value than the other variants. An asparate residue would likely be unprotonated, and the negative charge may affect the electrostatic properties of the active site, or proper orientation of another catalytic residue. The putative active site residue His228 is not directly involved in the binding and orientation of $FMNH_2$ or alkanesulfonate substrate. Evidence to support this conclusion came from fluorimetric titration studies monitoring substrate binding. The K_d values for $FMNH_2$ and octanesulfonate binding to the H228 variants were similar as wild-type SsuD (Table 3.2). However, substrate induced conformational changes occur with both $FMNH_2$ and octanesulfonate, so it is not known how His228 affects substrate binding with both substrates present.

Stopped-flow kinetic analyses were performed with the H228A SsuD variant to determine the specific step affected in flavin oxidation by the replacement of histidine with alanine. In the absence of the alkanesulfonate substrate, the kinetic traces recorded at 450 nm and 370 nm in H228A SsuD reactions similar to wild-type with slight changes observed in the reaction rates (Figure 3.6). The rate of formation of the C4a-(hydro)peroxyflavin intermediate increased 1.4 fold (k_1 at 370), while the rate of decay increased 1.9 fold (both k_2 at 370 nm and k_1 at 450 nm). The C4a-(hydro)peroxyflavin intermediate was also observed in the H228A SsuD reaction at low octanesulfonate concentrations (100 μM), but was not detectable at higher octanesulfonate concentrations (Figure 3.7). The rate of the fast phase obtained from the

136

kinetic traces at 450 nm displayed a similar hyperbolic dependence on octanesulfonate concentration as wild-type (Figure 3.8). Therefore, there is no observable evidence showing any step was significantly changed by the replacement of His228 with alanine. If His228 were a catalytic base as proposed, this residue would directly uptake a proton from the alkane peroxyflavin intermediate based on the proposed mechanism (Scheme 3.1). One may expect to see a delay of the decay of this C4a-substituted intermediate in the presence of octanesulfonate substrate. Results herein imply that His228 is not directly involved in the reaction between C4a-(hydro)peroxyflavin with the alkanesulfonate substrate.

Chemical rescue experiments were performed with H228A SsuD to determine if the desulfonation activity could be enhanced by the addition of imidazole. On the basis of results of the rescue experiments with imidazole, the enzymatic activity of H228A SsuD can be partially rescued by imidazole. The k_{cat} values increased at pH values above 7 with maximum increases observed at pH 8 (figure 3.9). Even though a 15% increase in the k_{cat} value was observed with the addition of imidazole, the overall rescue of the enzymatic activity was limited compared to wild-type SsuD. The increase in activity at pH values greater than 7.0 suggest that the deprotonated form of His228 is important for catalysis; however, the modest increase in activity does not fully support this residue as the active site catalytic base in SsuD desulfonation reaction.

The pH dependence on the k_{cat} and k_{cat}/K_m values of wild-type and H228A SsuD enzymes was determined in the pH range of 5.8-9.5 (Figure 3.7). Wild-type SsuD pH profiles showed a bell shaped curve and were fitted to a two ionization equation to give two pK_a values of 6.61 ± 0.19 and 9.6 ± 0.10 from the pH profile of k_{cat}, and 6.57 ± 0.32

and 9.54 ± 0.34 from the pH profile of k_{cat}/K_m. The pK_a values from the pH profile of k_{cat} are almost identical to wild-type enzyme, while the pK_a values from the pH profile of k_{cat}/K_m are 6.72 ± 0.26 and 9.89 ± 0.28. These pK_a values are slightly shifted but still in the margin of error. The pH profiles of the SsuD enzyme were not dramatically perturbed by the replacement of histidine with alanine at position 228.

The overall results from these studies suggest that His228 plays a role in the desulfonation reaction by SsuD, but is not directly involved in catalysis. His228 was proposed as a catalytic base on the basis of structural comparisons with bacterial luciferase and LadA and kinetic studies on the putative active site base from bacterial luciferase. Even though imidazole could rescue H228A SsuD activity at pH values higher than 7.0, this only indicates that the deprotonated form of His228 is the active form during catalysis. If His228 was the catalytic base, one would expect that pH profiles of H228 variant would be altered; however, the pH profiles for the k_{cat} and k_{cat}/K_m values of wild-type and H228A SsuD enzymes are similar. Results here suggest that His228 is not an active site base in catalytic steps involving the octanesulfonate substrate. Unless an an alternative base is utilized when His228 is substituted with Ala. However, it seems more plausible that histidine in the depronated form is needed either for a catalytic step following the release of sulfite and the corresponding aldehyde, or is required for the stabilization and proper orientation of an amino acid residue important in catalysis.

Based on chemical rescue experiments by imidazole, His44 was identified as the catalytic base in bacterial luciferase. Because this histidine is a highly conserved active

138

site residue among some flavin-dependent monooxygenases, the corresponding conserved histidine residues located in the active sites of other monooxygenases were proposed as the catalytic base as well. Our results also demonstrate a pH dependent imidazole rescue of the His228A SsuD variant; however, His228 is not the catalytic base as proposed based on further kinetic and biochemical analyses. Since there were no reported pH profiles of bacterial luciferase, it is not clear if the pH profiles would be perturbed by the replacement of His44 with other amino acids. Based on the results reported here, the evidence from imidazole rescue experiments is not enough to identify the His228 residue as a catalytic base.

On the basis of the proposed mechanism of SsuD (Scheme 3.1) and the data reported here, there are two possibilities on the catalytic role of His228: a) the stabilization and proper orientation of an amino acid residue important in catalysis, or b) involvement in a step following the C4a-(hydro)peroxyflavin reaction with alkanesulfonate. The proposed proton transfer events are shown in Scheme 3.2. After the release of sulfite and aldehyde products, an active site residue (HA) is proposed as a general acid to provide a proton to form a hydroxyflavin (FMNOH), which decays to oxidized flavin. Chemical rescue experiments with imidazole showed that it is the deprotonated state of His228 that directly participates in the desulfonation reaction by SsuD, which implies His228 is unable to work as a general acid. Therefore, the most likely catalytic role of His228 is in the stabilization and proper orientation of an amino acid residue important in catalysis.
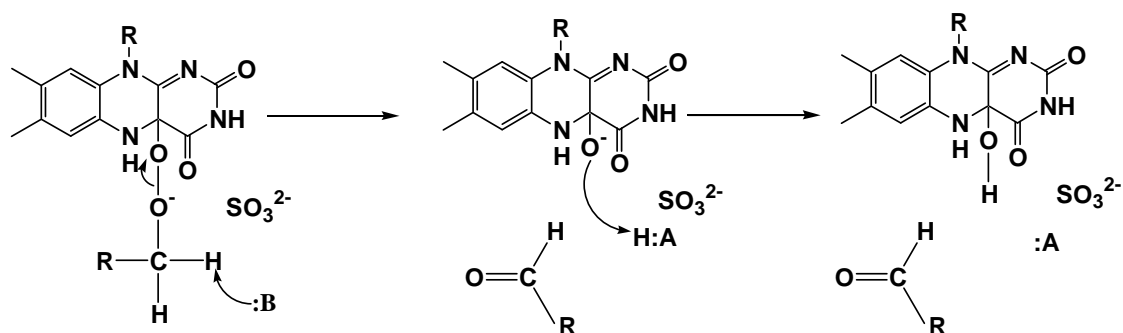
Scheme 3.2 Proton-transfer events involved in SsuD desulfonation reactions

Based on three-dimensional structural information, Tyr331 or His333 could be the catalytic base in the SsuD reaction. Both of these residues are within hydrogen-bonding distance with the His228 residue (Figure 3.12). Tyr331 is another conserved amino acid located in a similar spatial position in the active site of SsuD whose catalytic relevance has not been explored. The pK_a of Tyr is about 10.1, which is somewhat higher than the pK_{a2} of the active site base (pK_{a2}=9.7) obtained from the pH profiles of wild-type SsuD. The pK_a of an amino acid residue can be altered in the microenviroment of the active site. If Tyr331 is the catalytic base in the SsuD reaction, it is highly possible that the SsuD desulfonation reaction undergoes a reverse deprotonation mechanism [105]. In this case, a His residue may help to bind and orientate Tyr110. Another potential catalytic base is His333. The pK_{a1} is about 6.6, which is close to the pK_a of histidine, suggesting that the proposed catalytic base could be a histidine residue in the putative active site. It is possible that His333 is the active site catalytic base, while His228 is required for the stabilization and proper orientation of His333. Current studies are aimed at the identification of the catalytic base.

140
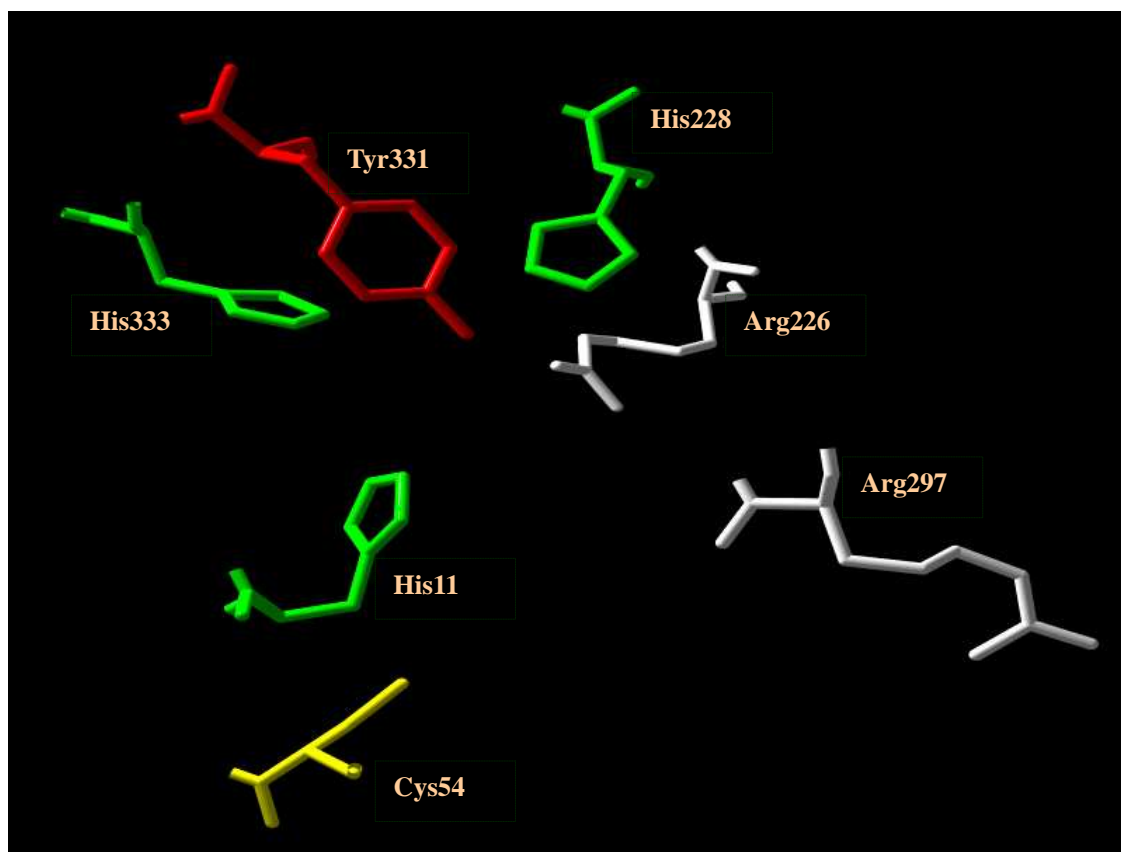
Figure 3.12 Putative active site of SsuD

In summary, the results presented herein use a combination of biochemical and mechanistic approaches to probe the catalytic role of His228, a conserved residue in the putative active site of SsuD. His228 plays a role in the desulfonation reaction by SsuD; however, it is not the catalytic base proposed in previous studies. Further kinetic analyses indicates that this residue is more likely indirectly participating in catalysis by stabilizing and properly orientating another amino acid, which is directly involved in the desulfonation reaction by SsuD.

CHAPTER FOUR

SUMMARY

The alkanesulfonate monooxygenase system from *E.coli*, which is composed of a NAD(P)H-dependent flavin reductase (SsuE) and a flavin-dependent monooxygenase (SsuD), is capable of desulfonating a wide range of alkanesulfonate substrates in the presence of FMN, NAD(P)H, and dioxygen to form a corresponding aldehyde, sulfite and NAD(P)$^+$ [73]. This enzymatic system is induced under sulfur starvation conditions and expressed on a single operon along with an ABC-type transporter which transfers alkanesulfonate substrates into cells for desulfonation. The flavin reductase supplies FMNH$_2$ to the flavin-dependent monooxygenase to activate dioxygen for C-S bound cleavage. Alkanesulfonates are considered natural stable compounds, which are difficult to eliminate from the environment. The two-component alkanesulfonate monooxygenase system has potential applications for the biodegradation of these stable organosulfur compounds [74]. From a mechanistic view, the chemistry of C-S bond cleavage and flavin transfer between the two components are both novel in these enzymes.

While the flavin reductase of the alkanesulfonate monooxygenase system has been well characterized and the flavin transfer mechanism has been extensively explored [79,

80, 86], much less is known about the catalytic mechanism of the monooxygenase component. In this research, the catalytic mechanism of the alkanesulfonate monooxygenase enzyme has been extensively probed through a combination of biochemical and mechanistic approaches.

4.1 Flavin binding and flavin transfer mechanism of the alkanesulfonate monooxygenase system.

Based on the overall mechanism of this two-component monooxygenase system, SsuE reduces FMN in the presence of NAD(P)H, then the reduced flavin is further transferred to SsuD for the oxygenation of alkanesulfonate substrates. The information on flavin binding and transfer within the two-component system is important in understanding the overall catalytic mechanism of this alkanesulfonate monooxygenase system.

The dissociation constants of oxidized FMN for both SsuE and SsuD proteins were previously reported. The SsuE enzyme had a 1000-fold lower K_d value than the SsuD enzyme for the oxidized flavin. Due to the instability of reduced flavin in the presence of dioxygen, the reduced flavin binding affinities can provide valuable information regarding the mechanism of flavin transfer between the reductase and monooxygenase components. A fluorimetric titration method was developed to determine the dissociation constants of reduced FMN binding to SsuE and SsuD under anaerobic conditions. SsuD had a 40-fold lower K_d value than SsuE for the reduced flavin, which indicates that SsuE has a preference for oxidized FMN, while SsuD has a higher affinity for reduced flavin.

The preference of the flavin reductase for FMN and the monooxygenase for $FMNH_2$

is a commonly observed feature in the flavin-dependent two-component monooxygenase family. The reductase and monooxygenase dissociation constants for the reduced and oxidized flavin are summarized in Table 4.1 for several two-component systems. The dissociation constants for both oxidized and reduced flavin binding to the reductase and monooxygenase enzymes were only determined in the alkanesulfonate sulfonate system from *E.coli* and the ActVA-ActVB system involved in actinorhodin biosynthesis from *Streptomyces coelicolor* [*90*]. In both systems, the monooxygenase enzymes were able to bind reduced flavin with high affinity, while the reductase components had a higher binding affinity for oxidized flavin. In HPA hydroxylase and styrene monooxygenase, the monooxygenase component had a several hundred fold lower K_d value for reduced flavin than oxidized flavin, [48, *106*]. The preference of the flavin reductase and monooxygenase for different redox forms of the flavin appears to play an essential role in flavin transfer between these two components.

Table 4.1 Dissociation constants for oxidized and reduced flavin binding in

flavin-dependent two-component systems

System	*Component*	*Oxidized flavin*	*Reduced flavin*
Alkanesulfonate	*Reductases*	0.015 ± 0.004 μM	10.2 ± 0.4 μM
monooxygenase	*Monooxygenases*	15.5 ± 1.3 μM	0.32 ± 0.15 μM
The ActVA-ActVB system	*Reductases*	4.4 ± 0.6 μM	6.6 ± 0.6 μM
	Monooxygenases	26.3 ± 6.2 μM	0.30 ± 0.04 μM
Styrene monooxygenase	*Reductases*	ND	ND
	Monooxygenases	68.5 μM	0.5 μM
p-Hydroxyphenylacetate	*Reductases*	ND	ND
hydroxylase (HPAH)	*Monooxygenases*	250 ±50 μM	1.2 ± 0.2 μM

To elucidate the flavin transfer mechanism between SsuE and SsuD, a combination of kinetic analyses and biochemical approaches were performed. Results from steady-state kinetic analyses indicated that SsuE follows an ordered sequential mechanism, with NADPH as the first substrate to bind and NADP$^+$ as the last product to dissociate. Interestingly, the kinetic mechanism of SsuE is altered to a rapid equilibrium ordered mechanism in the presence of SsuD and octanesulfonate, even though the steady-state kinetic parameters of the system were not significantly altered [79]. More recently, stable protein-protein interactions were detected between SsuE and SsuD through affinity chromatography and spectroscopic analyses. Based on information from kinetic studies, biophysical analyses, and binding affinities of flavin substrates, our studies support a model involving direct flavin transfer from the reductase to the monooxygenase enzyme.

4.2 Ordered substrate binding mechanism and protein dynamics

Flavoprotein monooxygenases are capable of catalyzing various reactions involving oxygen activation and transfer. Reactions by flavoprotein monooxygenases include three steps: a) flavin reduction by NAD(P)H; b) activation of dioxygen to form a enzyme-stabilizing C4a-(hydro)peroxyflavin intermediate; c) the oxygenation of the substrate. Two different strategies have been adopted by flavoenzymes to accomplish the oxidation of substrate [7]. In single-component monooxygenases, flavin is tightly bound to protein as a prosthetic group and complicated protein dynamics occurs during catalysis to modify the different mechanistic steps. In two-component monooxygenase systems, the reductive and oxidative reactions are performed by two separate enzymes and the flavin is present as a cosubstrate rather than a prosthetic group.

The results from fluorimetric titrations revealed that octanesulfonate is not able to bind to SsuD enzyme unless $FMNH_2$ is first bound. A $FMNH_2$ induced conformational change is important for the alkanesulfonate substrate to access the active site. These results further support the presence of an inactive complex between SsuD and $FMNH_2$. An isomerization followed by the binding of octanesulfonate was observed in stopped-flow kinetic analyses. This isomerization is a rate-limiting step based on alternate mixing experiments in the presence of octanesulfonate. The oxidation of reduced flavin was 2-fold faster in the reaction of premixed SsuD-$FMNH_2$-octanesulfonate with oxygenated buffer than the reaction of the SsuD-$FMNH_2$ complex with octanesulfonate in oxygenated buffer. If the initially formed SsuD-$FMNH_2$-octanesulfonate complex directly reacts with O_2, then the rates of these two alternate mixing reactions should be similar. This situation was not experimentally observed, thus the results shows the ternary complex does not react with O_2 until a rate-limiting unimolecular isomerization occurs. Protein dynamics has been shown to be critical in catalysis by flavin monooxygenases. These multiple substrate induced conformational changes have been observed in several well-characterized flavin-dependent monooxygenase systems. In bacterial luciferase, the enzyme-$FMNH_2$ complex has to convert to an active enzyme-$FMNH_2$ complex by a unimolecular conversion before reaction with O_2 to form C4a-(hydro)peroxyflavin occurs [*78*]. The reaction kinetics for the flavin-dependent halogenase (RebH) indicated there are significant protein dynamics prior to the formation of the FADOOH intermediate. This complicated protein dynamics process includes three forms of the RebH-$FADH_2$ complex [*57*]. These dynamic properties afford multiple conformations in catalysis, so enzymes

are able to utilize the shielded conformation to prevent access of the solvent to the reactive flavin intermediate.

In summary, an ordered substrate binding mechanism has been proposed in SsuD catalysis based on the reaction kinetics and substrate binding studies. Multiple conformational changes were observed during the SsuD catalytic reaction to control the binding order of substrates and protect the reactive intermediates from solvent. Therefore, ordered substrate binding and protein dynamics is a general property of the alkanesulfonate monooxygenase.

4.3 C4a-(hydro)peroxyflavin intermediate

One of the general properties of flavoprotein monooxygenases is their ability to stabilize a C4a-(hydro)peroxyflavin intermediate generated by flavin activation of dioxygen. This flavin intermediate is usually the oxygenating agent involved in substrate oxygenation. Therefore, identification and characterization of a C4a-(hydro)peroxyflavin intermediate is essential to elucidate the catalytic mechanism of flavoprotein monooxygenases. The C4a-(hydro)peroxyflavin intermediate has a distinguished UV-vis spectrum from oxidized and reduced flavins with an absorbance peak between 350-400 nm. Rapid reaction kinetics on the formation and decay of this C4a-(hydro)peroxyflavin intermediate provides valuable information about the catalytic mechanism of flavoprotein monooxygenases.

The C4a-(hydro)peroxyflavin has been identified in the SsuD reaction by stopped-flow analyses in the absence of or at low concentrations of alkanesulfonate substrate. Interestingly, the order of addition of $FMNH_2$ and O_2 determines whether the formation of the C4a-(hydro)peroxyflavin intermediate is observed in stopped-flow

kinetic traces. The oxidation of pre-mixed $FMNH_2$-SsuD is significantly slower than that of free flavin, and the kinetic traces obtained at 370 nm and 450 nm increased at identical rates in a two step model, indicating that flavin oxidation was an enzyme-mediated reaction. However, when free flavin was mixed with SsuD in oxygenated buffer, the kinetic trace obtained at 370 nm increased at a faster rate than the kinetic trace at 450 nm with a new fast phase (12 s^{-1}) observed. These results suggested that a C4a-(hydro)peroxyflavin was likely generated in the desulfonation reaction catalyzed by SsuD. Under anaerobic conditions, the initially formed SsuD-$FMNH_2$ complex will undergo a unimolecular reaction to convert to a inactive SsuD-$FMNH_2$ complex which is unable to stabilize the C4a-(hydro)peroxyflavin intermediate. This unique dependence on the enzyme and substrate mixing order for the observed formation of the C4a-(hydro)peroxyflavin was also reported for the flavin-dependent halogenase RebH. Three forms of the Reb-$FADH_2$ complex have been proposed in this enzymatic reaction. The initial binding of $FADH_2$ by RebH yields an enzyme complex (complex A) which readily reacts with dioxygen to form FADOOH. However, under anaerobic conditions, the active complex converts to complex B and C. Complex B does not readily react with O_2 and undergoes a slow conversion back to complex A. Complex C is an inactive complex, which reacts with O_2 to form FAD and H_2O_2 with no significant accumulation of FADOOH observed. These complicated conformational changes during the formation of C4a-(hydro)peroxyflavin in SsuD and RebH demonstrate the ability of enzyme to adjust to the availability of O_2 [57].

The stability of the C4a-(hydro)peroxyflavin intermediates formed in two-component monooxygenase reactions are quite variable depending on the enzyme under investigation.

This intermediate in the SsuD reaction is weak compared to other extensively-characterized enzymes from this family. One possible reason for the decrease stability may be a more polor enviroment, or the complicated conformational changes that occur during the binding of $FMNH_2$.

4.4 Putative active site of SsuD and the catalytic role of His228

Most structures reported for monooxygenases from the flavin-dependent two-component monooxygenase shows a dimeric oligomerization state of the enzyme, while SsuD is an unusual homotetramer which comprises of two homodimers. Although the amino acid sequence homology is low, SsuD is similar in overall structure to other flavin-dependent monooxygenases, bacterial luciferase and long-chain alkane monooxygenase (LadA). More interestingly, several amino acids located in the putative active site of SsuD (His228, Tyr331, Arg297 and Cys54) are in a similar spatial arrangement as catalytically relevant amino acids from bacterial luciferase and LadA. Amino acid residue His44 in the α-subunit of bacterial luciferase has been reported to be a catalytic base in the bioluminescence reaction. The H228 residue, which corresponds to His44 in the α-subunit of bacterial luciferase, has been reported to be the catalytic base in the desulfonation reaction.

Several His228 variants (H228A, H228K and H228D) were generated in order to determine the catalytic role of this residue. Results from substrate titrations indicated that His228 is not directly involved in $FMNH_2$ or alkanesulfonate binding. Stopped flow kinetic analyses showed that the replacement of His228 with alanine did not generate any significant changes in flavin oxidation in the absence and presence of alkanesulfonate substrate, which implies that His228 is not directly involved in the reaction between the

149

C4a-(hydro)peroxyflavin intermediate and alkanesulfonate substrate. There was not a dramatic reduction in the k_{cat}/K_m values (50 fold in H228A and H228K, 200-fold in H228D), as would be expected for a catalytic base. Chemical rescue was performed with the His228A SsuD variant to determine if the activity could be enhanced by the addition of imidazole. Even though a 10-15 % increase in the k_{cat} value was observed at pH values above 7, the overall rescue of the enzymatic activity was limited compared to wild-type SsuD. The increase in activity at pH values greater than 7 suggest that the deprotonated form of the His is important for catalysis, however the modest increase in activity does not fully support this enzyme as the active site base important in catalysis. The pH dependence on the k_{cat}/K_m and k_{cat} values of H228A and wild-type SsuD are also similar, further suggesting that the His228 is not an active site base in catalytic steps involving the octanesulfonate substrate. While these results could suggest that an alternative base is utilized when His228 is substituted with Ala, it seems more plausible that His228 in the deprotonated form is either needed for a catalytic step following the release of sulfite and the corresponding aldehyde, or is required for the stabilization and proper orientation of an amino acid residue important in catalysis.

The catalytic functions of other conserved residues in the putative active site were explored in our current studies. Results from kinetic analyses suggest that the C54 variant plays a role in the stabilization of the C4a-(hydro)peroxyflavin similar to Cys106 in bacterial luciferase (unpublished data). It was previously reported that the activity of an abherrent R297C SsuD variant was totally abolished [73]. Arg 297 is located in a flexible loop, which may play essential roles in protein dynamics and protein-protein interactions. SsuD was shown to be more susceptible to proteolysis in the absence of reduced flavin,

while SsuD was cleaved more slowly in the presence of $FMNH_2$. These results indicate that the binding of $FMNH_2$ induces a conformational change that protects the SsuD enzyme from proteolysis, and the flexible loop is likely involved in this conformational change. There is no activity detected in the steady-state kinetics for R297A and R297K SsuD. Results from fluorescence titrations showed that a slight decrease in the binding affinity $FMNH_2$ was observed in R297A and R297K SsuD, suggesting that the Arg297 residue is not essential for flavin binding. In stopped-flow studies, flavin oxidation by R297A or R297K SsuD occurs at a faster rate following reduction by SsuE than wild-type SsuD. Since the Arg297 residue is located on the flexible loop, there are two possible explainations for this faster oxidation: 1) the flexible loop is essential to protect reduced flavin and C4a-(hydro)peroxyflavin intermediate; 2) Arg297 play an essential role in the acquisition of flavin by SsuD from SsuE. The lag phase present in kinetic traces of wild-type SsuD at 450 nm, but not in the traces of R297A or R297K SsuD, could represent the transfer of $FMNH_2$ to SsuD. (unpublished data). Therefore, these results provided evidence for the Arg297 residue facilitating the transfer to the $FMNH_2$ to SsuD or protecting the $FMNH_2$ in the active site of SsuD.

In summary, the catalytic mechanism of the alkanesulfonate monooxygenase enzyme, SsuD, has been extensively explored. The overall mechanism of SsuD shows some common properties with other flavin-dependent monooxygenases with a ordered substrate binding mechanism and a C4a-(hydro)peroxyflavin intermediate generated in catalysis. Multiple conformational changes are involved in catalysis and play important roles in protecting the reactive intermediates and controling the substrate binding order. Catalytic roles of His228 have been probed by kinetic analyses, chemical rescue, pH

profile evaluation, and substrate binding studies. The His228 residue is not a catalytic base as previous proposed, but is more likely required for the stabilization and proper orientation of an amino acid important in catalysis. Determinating the catalytic roles of additional conserved residues in the putative active site will lead to information on the desulfonation reaction catalyzed by SsuD.

REFERENCES

1. Massey V. (2000) The chemical and biological versatility of riboflavin. *Biochem Soc Trans.* 28, 283-296.

2. Massey, V. (1994) Activation of molecular oxygen by flavins and flavoproteins, *J. Biol. Chem. 269,* 22459-22462.

3 Müller F. (1987) Flavin radicals: chemistry and biochemistry, *Free Radic Biol Med.* 3, 215-230.

4 Mewies M., Mcintire W.S., and Scrutton N.S. (1998) Covalent attachment of flavin adenine dinucleotide (FAD) and flavin mononucleotide (FMN) to enzymes: The current state of affairs, *Protein Sci.* 7, 7-20.

5 Wellner D. (1967) Flavoproteins, *Annu. Rev. Biochem.*, 36, 669-690.

6 Tu S-C. (2001) Reduced flavin: donor and acceptor enzymes and mechanisms of channeling, *Antioxid Redox Signal.* 3, 881-897.

7 Ballou D. P., Entsch, B., and Cole L. J. (2005) Dynamics involved in catalysis by single-component and two-component flavin-dependent aromatic hydroxylases, *Biochem. Biophy. Res. Comm.* 338, 590-598.

8 Bruice T. C. (1984) Oxygen-flavin chemistry, *Isr. J. Chem.* 24, 54-61.

9 Strittmatter P. (1966) Dehydrogenases and flavoproteins, *Annu. Rev. Biochem.*, 35, 125-156.Thorpe C., and Kim J. J., (1995) Structure and mechanism of the action of

the Acyl-CoA dehydrogenase. *FASEB J.*, 9, 718-725.

10 Deistung J., and Thorneley R. N. (1986) Electron transfer to nitrogenase. Characterization of flavodoxin from *Azotobacter chroococcum* and comparison of its redox potentials with those of flavodoxins from *Azotobacter vinelandii* and *Klebsiella pneumoniae*, *Biochem J.*, 239, 69–75.

11 Nakamura S., and Ogura Y. (1968) Action Mechanism of Glucose Oxidase of *Aspergillus niger, Biochem J.,* 308-316.

12 Ziegler D. M. (1993) Recent studies on the structure and function of multisubstrate flavin-containing monooxygenases, *Annu. Rev. Biochem.,* 33, 179-199.

13 Cashman J. R., and Zhang J. (2006) Human flavin containing monooxygenases, *Annu. Rev. Biochem.* 46, 65-100.

14 Schlaich N. L. (2006) Flavin-containing monooxygenases inplants: looking beyond detox *Trend. Plant. Sci.,* 12, 412-18.

16 Poulsen, L. L., and Ziegler, D. M. (1979) The liver microsomal FAD-containing monooxygenasesS. pectral characterization and kinetic studies. *J. Biol. Chem.* 254, 6449-55.

17 Beaty, N. B., and Ballou, D. P. (1981) The reductive half-reaction of liver microsomal FAD-containing monooxygenases. *J. Biol. Chem.* 256, 4611-18.

18 Beaty, M. B., and Ballou, D. P. (1981) The oxidative half-reaction of liver microsomal FAD-containing monooxygenase. *J. Biol. Chem.* 256, 4619-25.

19 Jones, K. C., and Ballou, D. P. (1986) Reactions of the 4a-bydroperoxide of liver microsomal flavin-containing monooxygenase with nucleophilic and electrophilic substrates. *J. Biol. Chem,.*261, 2553-59.

20 Smyser, B. P., and Hodgson, E. (1985) Metabolism of phosphorous-containing compounds by pig liver microsomal FAD-containing monooxygenase. *Biochem. Pharmacol.* 34:1145-50.

21 Prough, R. A., Freeman, P. C., and Hines, R. N. (1981) The oxidation of hydrazine derivatives catalyzed by the purified microsomal FAD-containing monooxygenase. *J. Biol. Chem.* 256, 4178-84.

22 Ziegler, D. M. (1988) Flavin-containing monooxygenases: catalytic mechanism and substrate specificities. *Drug Metab. Rev.* 19, 1-32.

23 Ryerson, C. C., Ballou, D. P., and Walsh, C. Z. (1982) Mechanistic studies on cyclohexanone oxygenase. *Biochemistry* 21, 2644-55.

24 Taylor, K. H., and Ziegler, D. M. (1987) Studies on substrate specificity of the hog liver flavin-containing monooxygenase: anionic organic sulfur compounds. *Biochem. Pharmacol.* 36, 141~46.

25 Sheng D., Ballou D., and Massey V. (2001) Mechanistic studies of cyclohexanone monooxygenase: chemical properties of intermediates involved in catalysis. *Biochemistry* 40, 11156-67.

26 Entsch B., Palfey B. A., Ballou D. P., and Massey V. (1991) Catalytic function of tyrosine residues in *para*-hydroxybenzoate hydroxylase as determined by the study of site-directed mutants. *J. Biol. Chem.* 266, 17341-49.

27 Palfey B. A., Entsch B., Ballou D. P., and Massey V. (1994) Changes in the catalytic properties of p-hydroxybenzoate hydroxylase caused by the mutation Asn300Asp, *Biochemistry* 33, 1545-54.

28 Entsch, B., Ballou D. P., and Massey V. (1976) Flavin-oxygen derivatives involved in

hydroxylation by p-hydroxybenzoate hydroxylase, *J. Biol. Chem.*, 251, 2550-63.

29 Ziegler D. M. (1990) Enzymes adapted for multisubstrate specificity trends. *Pharmacol.Sci.* 11, 321–34.

30 Lang D. H, Yeung C. K., Peter R. M., Ibarra C, Gasser R, et al. (1998) Isoform specificity of trimethylamine N-oxygenation by human flavin-containing monooxygenase (FMO) and P450 enzymes: selective catalysis by FMO3. *Biochem. Pharmacol.* 56, 1005–12.

31 Cashman JR, Camp K, Fakharzadeh SS, Fennessey PV, Hines RN, et al. (2003) Biochemical and clinical aspects of the human flavin-containing monooxygenase form 3 (FMO3) related to trimethylaminuria. *Curr. Drug Metabol.* 4, 151–70.

32 Poulsen L. L. (1981). Organic sulfur substrates for the microsomal flavincontaining monooxygenase. In *Reviewsin Biochemical Toxicology*, ed. E Hodgson, JR Bend, RM Philpot, pp. 33–49.

33 Decker C. J., Doerge D. R., and Cashman J. R. (1992). Metabolism of benzimidazoline-2-thiones by rat hepatic microsomes and hog liver flavin-containing monooxygenase. *Chem. Res. Toxciol*. 5, 726–33.

34 Henderson M. C., Krueger S. K., Stevens J. F., Williams D. E. (2004). Human flavincontaining monooxygenase form 2 Soxygenation: sulfenic acid formation from thioureas and oxidation of glutathione. *Chem. Res. Toxicol.* 17:633–40.

35 Hernandez, D., Janmohamed, A., Chandan, P., Phillips, I. R., and Shephard EA. (2004). Organization and evolution of the flavincontaining monooxygenase genes of human and mouse; identification of novel gene and pseudogene clusters. *Pharmacogenetics,* 14, 117–30.

156

36 Swarup, R., Kargul, J., Marchant A., and Zadik D., *et al, (2004)* Structure-Function Analysis of the Presumptive *Arabidopsis* Auxin Permease AUX1, *The Plant Cell* 16, 3069-3083.

37 Mou, Z. Fan, W., and Dong, X., (2003) Inducers of plant systemic acquired resistance regulate NPR1 function through redox changes, *Cell* 113, 935-44.

38 Jones, D.A. and Takemoto, D. (2004) Plant innate immunity – direct and indirect recognition of general and specific pathogen-associated molecules, *Curr. Opin. Immunol.* 16, 48-62.

39 van Berkel, W. J. H., Kamerbeek, N.M., and Fraaije, M.W., (2006) Flavoprotein monooxygenases, a diverse class of oxidative biocatalysts, *J. Biotech.* 124, 670-89.

40 Eppink, M. H. M., Overkamp, K. M., Schneider, H. A., and van Berkel, W. J. H., (1999) Switch of coenzyme specificity of *p*-hydroxybenzoate hydroxylase. *J. Mol. Biol.* 292, 87-96.

41 Wang, J., Oritiz-Maldonado, M., Entsch, B., Massey V., Ballou, D., and Gatti, D. L., (2002) Protein and ligand dynamics in 4-hydroxybenzoate hydroxylase. *Proc. Natl. Acad. Sc. U. S. A.* 99, 608-13.

42 Entsch, B., van Berkel, W. J. H. (1995) Structure and mechanism of *para*-hydroxybenzoate hydroxylase. *FASEB J.* 9, 476-483.

43 Entsch, B., Cole, L. J., Ballou, and D., P., (2005) Protein dynamics and electrostatics in the function of *p*-hydroxybenzoate hydroxylase. *Arch. Biochem. Biopys.* 433, 297-311.

44 Prado, L., Fernandez, E., Weissbach, U., and Blanco, G., *et al* (1999) Oxidative cleavage of premithramycin B is one of the last steps in the biosynthesis of the

antitumor drup mithrmycin. *Chem. Biol.* 6, 19-30.

45 Gibson, M., Nur-e-alam, M., Lipata, F., Oliveira, M. A., and Rohr, J., (2005) Characterization of kinetic and products of the Baeyer-Villger oxygenase MtmOIV, the key enzyme of the biosynthesis patheay toward the natural product anticancer drup mithramycin from Streptomyces argillaceus. *J. Am. Chem. Soc.* 127, 17594-95.

46 Malito, E., Alfieri, A., Fraaije, M. W., and Mattevi, A., (2004) Crystal structure of a Baeyer-Villiger monooxygenase. Proc. *Natl. Acad. Sci. U. S. A.* 101, 13157-62.

47 Palfey, B. A., Moran, G. R., Entsch, B., Ballou, D. P., and Massey,V. (1999) Substrate recognition by "password" in p-hydroxybenzoate hydroxylase, *Biochemistry 38*, 1153-1158.

48 Palfey, B. A., Ballou, D. P., and Massey, V. (1997) Flavin conformational changes in the catalytic cycle of p-hydroxybenzoate hydroxylase substituted with 6-azido- and 6-aminoflavin adenine dinucleotide, *Biochemistry 36*, 15713-15723.

49 Gatti, D. L., Palfey, B. A., Lah, M. S., Entsch, B., Massey, V.,Ballou, D. P., and Ludwig, M. L. (1994) The mobile flavin of 4-OH benzoate hydroxylase, *Science 266*, 110-114.

50 Coves J., Delon B., Climent I., Sjoberg B. M., and Fontecave M. (1995) Enzymatic and chemical reduction of the iron center of the *Escherichia coli. Eur. J. Biochem.* 260, 635-641.

51 Coves J., and Fontecave M. (1993) Reduction and mobilization of iron by a NADPH:flavin oxidorreductase from *Escherichia coli. Eur. J. Biochem.* 211, 635-641.

52 Gerlo, E., and Charlier, J. (1975) Identification of NADH-specific and

NADPH-specific FMN reductase in *beneckea harveyi. Eur. J. Biochem.* 57, 461-67.

53 Wang, H., Lei, B., and Tu, S-C. (2000) *Vibrio harveyi* NADPH-FMN oxidoreductase Arg203 as a critical residue for NADPH recognition and binding. *Biochemistry* 39, 7813-19.

54 Tanner, J. J., and Tu, S-C., Barbour, L. J., Barnes, C. L., Krause, K. L., (1999) Unusual folded conformation of nicotinamide adenine dinucleotide bound to flavin reductase P, *Protein Sci.* 8, 1725-32.

55 Lei, B., and Tu, S-C., (1998) Mechanism of reduced flavin transfer from *Vibrio harveyi* NADPH-FMN oxidoreductase to luciferase, *Biochemistry* 37, 14623-14629.

56 Hastings, J. W., and Nealson, H. K., (1977) Bacterial bioluminescence, *Ann. Rev. Microbiol.* 31, 549-95.

57 Yeh, E., Cole, L. J., Barr, E. W., Bollinger, J. M., Ballou, D. P., and Walsh, C. T. (2006) Flavin redox chemistry precedes substrate chlorination during the reaction of the flavin-dependent halogenase RebH, *Biochemistry 45*, 7904-7912.

58 Fisher, A. J., Raushel, F. M., Baldwin, T., and Rayment, I., (1995) Three-dimensional structure of bacterial luciferase from *Vibrio haweyi* at 2.4 A resolution, Biochemistry 34, 6581-86.

59 Li, L., Liu, X., Yang, W., and Xu, F., *et al* (2008) Crystal structure of long-chain alkane monooxygenase (LadA) in complex with coenzyme FMN: unveiling the long-chain alkane hydroxylase. *J. Mol. Biol.* 376, 453-65.

60 Eichhorn, E., Davey, C. A., Sargent, D. F., Leisinger, T., and Richmond, T. J. (2002) Crystal structure of *Escherichia coli* alkanesulfonate monooxygenase SsuD, *J. Mol. Biol. 324*, 457-468.

61 Hasting, J. W., Balny, C., Christian Le. P., and Pierre, D. (1973) Spectral properties of an oxygenated luciferase-flavin intermediate isolated by low-temperature chromatography, *Proc. Natl. Acad. Sci.* 70, 3468-72.

62 Alfieri, A., Fersini, F., Ruangchan, N., and Prongjit, M., *et al* (2007) Structure of the monooxygenase component of a two-component flavoprotein monooxygenase, *Proc. Natl. Acad. Sci. U. S. A.* 104, 1177-82.

63 Tu, S-C. (1979) Isolation and properties of bacterial luciferase-oxygenated flavin intermediate complexed with long-chain alcohols, Biochemistry 18, 5940-45.

64 Baldwin, T. O., Chen, L. H., Chlumsky, L. J., Devine, J. H., and Ziegler, M. M. (1989) Site-directed mutagenesis of bacterial luciferase: analysis of the 'essential' thiol, *J. Biolumin. Chemilumin. 4*, 40-48.

65 Li, H., Ortego, B. C., Maillard, K. I., Willson, R. C., and Tu, S.-C. (1999) Effects of mutations of the alpha His45 residue of *Vibrio harveyi* luciferase on the yield and reactivity of the flavin peroxide intermediate, *Biochemistry 38*, 4405-4415.

66 Huang S., and Tu, S.-C. (1997) Identification and characterization of a catalytic base in bacterial luciferase by chemical rescue of a dark mutant, *Biochemistry 36*, 14609-14615.

67 Xin, X., Xi, L., and Tu, S-C., (1994) Probing the Vibrio harveyi luciferase beta subunit functionality and the intersubunit domain by site-directed mutagenesis. *Biochemistry* 33, 12194-201.

68 Lin L. Y., Sulea, T., Szittner, R., and Vassilyev, V., *et al* (2001) Modeling of the bacterial luciferase-flavin mononucleotide complex combining flexible docking with structure-activity data, *protein Sci.* 10, 1563-71.

69 Li, C., and Tu, S-C., (2005) Active site hydrophobicity is critical to the bioluminescence activity of *Vibrio harveyi* luciferase, *Biochemistry* 44, 12970-77.

70 Abu-Soud, H. M., Clark, A. C., Francisco, W. A., Baldwin, T. O., and Raushel, F. M., (1993) Kinetic destabilization of the hydroperoxy flavin intermediate by site-directed modification of the reactive thiol in bacterial luciferase, *J. Biol. Chem.* 268, 7699-7706.

71 Sucharitakul, J., Chaiyen, P., Entsch, B., and Ballou, D. P. (2006) Kinetic mechanisms of the oxygenase from a two-component enzyme, *p*-hydroxyphenylacetate 3-hydroxylase from *Acinetobacter baumannii*, *J. Biol. Chem. 281*, 17044-17053.

72 Li, X., and Tu, S-C. (2006) Activity coupling of *Vibrio harveyi* luciferase and flavin reductase (FRP): Oxygen as a probe, *Arch. Biochem. Biophy.* 454, 26-31.

73 Eichhorn, E., Van der Ploeg, J. R., and Leisinger, T. (1999) Characterization of a two-component alkanesulfonate monooxygenase from *Escherichia coli, J. Biol. Chem. 274*, 26639–26646.

74 Van der Ploeg, J. R., Eichhorn, E., and Leisinger, T. (2001) Sulfonate-sulfur metabolism and its regulation in *Escherichia coli, Arch Microbiol.* 176, 1–8.

75 Van der Ploeg, J. R., Weiss, M. A., Saller, E., Nashimoto, H., Saito, N., Kertesz, M. A., and Leisinger, T. (1996) Identification of sulfate starvation-regulated genes in *Escherichia coli*. A gene cluster involved in the utilization of taurine as a sulfur source, *J. Bacteriol.* 178, 5438-5446.

76 Van der Ploeg, J. R., Nowicka, R., Kertesz, M. A., Leisinger, T., and Hryniewicz, M. M. (1997) Involvement of CysB and Cbl regulatory proteins in expression of the

tauABCD operon and other sulfate starvation-inducible genes in *Escherichia coli*. *J. Bacteriol.* 179, 7671–7678

77 Eichhorn, E., van der Ploeg, J. R., Kertesz, M. A., and Leisinger, T. (1997) Characterization of α-ketoglutarate-dependent taurine dioxygenase from *Escherichia coli*. *J. Biol. Chem.* 272, 23031–36.

78 Ryle, M. J., Padmakumar, R., and Hausinger, R. P. (1999) Stopped-flow kinetic analysis of *Escherichia coli* taurine/α-ketoglutarate dioxygenase: interactions with α-ketoglutarate, taurine, and oxygen. *Biochemistry* 38:15278–15286.

79 Gao, B., and Ellis, H. R. (2005) Altered mechanism of the alkanesulfonate FMN reductase with the monooxygenase enzyme, *Biochem. Biophy. Res. Comm. 331*, 1137–1145.

80 Gao, B., and Ellis, H. R. (2007) Mechanism of flavin reduction in the alkanesulfonate monooxygenase system, *Biochim.Biophys.Acta.1774*, 359-367.

81 Quadroni, M., Staudenmann, and W., James, P. (1996) Analysis of global responses by protein and peptide fingerprinting of proteins isolated by two-dimensional gel electrophoresis. Application to the sulfate starvation response of *Escherichia coli*, *Eur. J. Biochem. 239*, 773-781.

82 Xi, L., Squires, C. H., Monticello, D. J., and Childs, J. D. (1997) A flavin reductase stimulates DszA and DszC proteins of Rhodococcus erythropolis IGTS8 *in vitro*, *Biochem. Biophy. Res. Comm. 230*, 73-75.

83 ontecave, M., Eliasson, R., and Reichard, P. (1987) NAD(P)H:Flavin oxidoreductase of *Escherichia coli*, *J. Biol. Chem. 262*, 12325-12331.

84 Valton J., Filisetti L., Fontecave M., and Nivière, V. (2004) A two-component flavin

dependent monooxygenase involved in actinorhodin biosynthesis in *Streptomyces coelicolor*, *J. Biol. Chem. 279,* 44362–44369.

85 Parry, R. J., and Li, W. (1997) Purification and characterization of isobutylamine N-hydroxylase from the valanimycin producer *Streptomyces viridifaciens* MG456-hF10, *Arch. Biochem. Biophys. 339,* 47–54.

86 Abdurachim, K., and Ellis, H. R. (2006) Detection of protein-protein interactions in the alkanesulfonate monooxygenase system from *Escherichia coli*, *J. Bacteriol. 188*, 8153-8159.

87 Fisher, A. J., Thompson, T. B., Thoden, J. B., Baldwin, T. O., and Rayment, I. (1996) The 1.5-Å resolution crystal structure of bacterial luciferase in low salt conditions, *J. Biol. Chem. 271*, 21956-21968.

88 Paquatte, O., and Tu, S-C. (1989) Chemical modification and characterization of the alpha cysteine 106 at the *Vibrio harveyi* luciferase active center, *Photochem. Photobiol. 50,* 817-825.

89 Hosseinkhani, S., Szittner, R., and Meighen, E. A. (2005) Random mutagenesis of bacterial luciferase: critical role of Glu175 in the control of luminescence decay, *Biochem. J. 385*, 575-580.

90 Valton, J., Fontecave, M., Douki, T., Kendrew, S. G., and Niviere, V. (2006) An aromatic hydroxylation reaction catalyzed by a two-component FMN-dependent monooxygenase. The ActVA-ActVB system from *Streptomyces coelicolor, J. Biol. Chem. 281*, 27-35.

91 Sucharitakul, J., Chaiyen, P., Entsch, B., and Ballou, D. P. (2005) The reductase of *p*-hydroxyphenylacetate 3-hydroxylase from *Acinetobacter baumannii* requires

p-hydroxyphenylacetate for effective catalysis, *Biochemistry 44*, 10434-10442.

92 Sucharitakul, J., Phongsak, T., Entsch, B., Svasti, J., Chaiyen, P., and Ballou, D. P. (2007) Kinetics of a two-component *p*-hydroxyphenylacetate hydroxylase explain how reduced flavin is transferred from the reductase to the oxygenase, *Biochemistry 46*, 8611-8623.

93 Louie, T. M., Xie, X. S., and Xun, L. (2003) Coordinated production and utilization of $FADH_2$ by NAD(P)H-flavin oxidoreductase and 4-hydroxyphenylacetate 3-monooxygenase, *Biochemistry 42*, 7509-7517.

94 Francisco, W. A., Abu-Soud, H. M., Topgi, R., Baldwin, T. O., and Raushel, F. M. (1996) Interaction of bacterial luciferase with 8-substituted flavin mononucleotide derivatives, *J. Biol. Chem. 271*, 104-110.

95 Francisco, W. A., Abu-Soud, H. M., Baldwin, T. O., and Raushel, F. M. (1993) Interaction of bacterial luciferase with aldehyde substrates and inhibitors, *J. Biol. Chem. 268*, 24734-24741.

96 Francisco, W. A., Abu-Soud, H. M., DelMonte, A. J., Singleton, D. A., Baldwin, T. O., and Raushel, F. M. (1998) Deuterium kinetic isotope effects and the mechanism of the bacterial luciferase reaction, *Biochemistry 37*, 2596-2606.

97 Otto, K., Hofstetter, K., Rothlisberger, M., Witholt, B., and Schmid, A. (2004) Biochemical characterization of StyAB from *Pseudomonas* sp. strain VLB120 as a two-component flavin-diffusible monooxygenase, *J. Bacteriol. 186*, 5292–5302.

98 Maeda-Yorita, K., and Massey, V. (1993) On the reaction mechanism of phenol hydroxylase. New information obatained by correlation of fluorescence and absorbance stopped flow studies, *J. Biol. Chem. 268*, 4134-4144.

99 Chaiyen, P., Brissette, P., Ballou, D. P., and Massey, V. (1997) Unusual mechanism of oxygen atom transfer and product rearrangement in the catalytic reaction of 2-methyl-3-hydroxypyridine-5-carboxylic acid oxygenase, *Biochemistry 36*, 8060-8070.

100 Hummel, J. P. and Dreyer, W. J. (1962) Measurement of protein-binding phenomena by gel filtration. *Biochim. Biophys. Acta.* 63, 530-532.

101 Berger, G., and Girault, G. (2003) Macromolecule-ligand binding studied by the Hummel and Dreyer method: current state of the methodology, *J Chromatogr B Analyt Technol Biomed Life Sci.* 797, 51-61.

102 Zhan, X., Carpenter, R. A., and Ellis, H. R. (2008) Catalytic Importance of the Substrate Binding Order for the $FMNH_2$-Dependent Alkanesulfonate Monooxygenase Enzyme, *Biochemistry* 47, 2221-30.

103 Stefanova, M. E., Davies, C., Nicholas, R. A., and Gutheil, W. G. (2002) pH, inhibitor, and substrate specificity studies on Escherichia coli penicillin-binding protein 5, *Biochim. Biophy. Acta.* 1597, 292-300.

104 Zhang, W., Shi, Q., Meroueh, S. O., Vakulenko, S. B., and Mobashery, S., (2007) Catalytic mechanism of penicilline-binding protein 5 of *Escherichia coli*, 46, 10113-21.

105 Sims, P. A., Larsen, T. M., Poyner, R. R., Cleland, W. W., and Reed, G. H. (2003) Reverse protonation is the key to general acid-base catalysis in enolase, *Biochemistry* 42, 8298-306.

106 Kantz, A., Chin, F., Nallamothu, N., Nguyen, T., and Gassner, G. T. (2005)

Mechanism of flavin transfer and oxygen activation by the two-component flavoenzyme styrene monooxygenase, *Arch Biochem Biophys.* 442, 102-16.

107 Poulsen, L. L., and Ziegler, D. M. (1979) The liver microsomal FAD-containing monooxygenase. Spectral characterization and kinetic studies, *J. Biol. Chem.* 254, 6449-55.